University Transportation Center Research Project

Final Report

REAL TIME ESTIMATION OF ARTERIAL TRAVEL TIME AND OPERATIONAL MEASURES THROUGH INTEGRATION OF REAL TIME FIXED SENSOR DATA AND SIMULATION

By

Michael Hunter, Ph.D. (P.I.)

Richard Fujimoto, Ph.D., Angshuman Guin, Ph.D, and Jorge Laval, Ph.D. (Co-PI)

Dwayne Henclewood, Wonho Suh, Ya-Lin Huang, Ying Li,

Brian Stebar, and Prashant Chari (Graduate Research Assistants)

Contract with

Research and Innovative Technology Administration (RITA)

In cooperation with

Georgia Transportation Institute / University Transportation Center

GDOT Research Project No. RP 09-01

Final Report (Draft)

REAL TIME ESTIMATION OF ARTERIAL TRAVEL TIME AND OPERATIONAL MEASURES THROUGH INTEGRATION OF REAL TIME FIXED SENSOR DATA AND SIMULATION

By:

Michael Hunter, Ph.D. (P.I.)

Richard Fujimoto, Ph.D., Angshuman Guin, Ph.D, and Jorge Laval, Ph.D. (Co-PI)

Dwayne Henclewood, Wonho Suh, Ya-Lin Huang, Ying Li,
Brian Stebar, and Prashant Chari (Graduate Research Assistants)

School of Civil and Environmental Engineering and
Computer Science and Engineering Division
Georgia Institute of Technology

Contract with

Georgia Department of Transportation

In cooperation with

U.S. Department of Transportation
Federal Highway Administration

February 2012

ACKNOWLEDGMENTS

The authors of this report wish to thank the Georgia Department of Transportation for its support and assistance throughout this effort, in particular the efforts of Supriya Kamatkar and Mark Demidovich. In addition the authors wish to thank the National Science Foundation for the support from a companion project, provided through EFRI ARES-CI Project Award Number 0735991.

EXECUTIVE SUMMARY

A wide variety of advanced technological tools have been implemented throughout Georgia's transportation network to increase its efficiency. These systems are credited with reducing or maintaining freeway congestion levels in light of increasing travel demands. In Georgia these benefits are primarily gained through the Traffic Management Center's freeway monitoring and quick response in ridding the roadway of any obstacles that may reduce freeway service levels. There have been a number of efforts to leverage the work done by TMCs to provide travelers with more current traffic information such as Georgia 511 and Navigator. In addition, private efforts and partnerships have made the TMC's information more accessible to travelers, aiding their traveler decisions. The effort presented in this report aims to compliment real-time freeway information by addressing the more limited availability of real-time arterial performance measures.

This research project explores the feasibility of integrating real-time data streams with an arterial simulation to support an arterial performance monitoring system. Such information will facilitate increased efficiency in facility utilization by enabling more informed decisions in the use and management of Georgia's transportation facilities. This objective was accomplished by undertaking the following tasks:

1. Describe the current state of practice concerning the estimation of real-time arterial performance measures.
2. Develop a federated (integrated) simulation test-bed for testing procedures and algorithms.

3. Determine the feasibility of integrating point sensor data with simulation to create a data-driven, on-line simulation tool.
4. Develop procedures and algorithms to calibrate an on-line simulation tool that estimates of travel time and other performance measures in real-time.
5. Determine any potential improvements in travel time estimation resulting from sensors placed in atypical locations, such immediately downstream of an intersection.
6. Field-test the data-driven, on-line arterial simulation tool on a target corridor.
7. Devise method(s) to deliver travel time and other operational characteristics to GDOT and the general public. .

These tasks lead to the following findings.

Description of the Current State of Practice

Efforts related to estimating performance measures along freeways and arterial are presented as lessons from those experiences inform the development of the methodology used to accomplish the research objective. A series of mathematical techniques is also be explored as previous researchers have developed performance measure estimation techniques based on vehicular input onto roadways. In addition to these techniques and methodologies, efforts that involve real-time, data-driven simulations, outside the transportation industry are explored.

Simulated Test Bed Environment

The first step in developing the real-time, data-driven microscopic simulation tool was the construction of such a framework in a laboratory environment (Task 2). To achieve this, the team federated (integrated) two simulation instances to be used as a test bed. VISSIM is employed to represent the two simulation instances. These two simulation instances, referred to as the "reference world" and "modeled-world" have the same roadway and signal timing configuration. The primary aim of this test bed was to determine if the modeled-world reflects the reference-world performance measures when driven by point sensor data from the reference-world, i.e. data similar to that streamed by field detectors. For the simulated test-bed, point sensor data included time, vehicle speed, and location. It was seen using this test bed that the underlying real time approach could be successful in a simulated environment. In addition, the simulated test bed enabled subsequent tasks through the development of the ability to utilize data streams to successfully drive a VISSIM simulation during runtime.

Federation of Real-Time Detector Stream with Simulation

A "hardware-in-the-loop" framework was developed that directly inputs detector data into a simulation model during runtime (task 3). Successful integration of the data stream with VISSIM enabled a field evaluation of the framework on an arterial using streaming point sensor data. A key attribute of the federation is the ability for the simulation to receive a PVR (per vehicle record) detector data stream in a real-time, allowing for the use of multiple detector technologies.

Real-Time, Data-Driven Arterial Simulation Algorithms

The arterial simulation algorithms provide the proposed framework with the necessary mechanisms to ensure that simulated performance measures reflect those of the field (Task 4). It is anticipated that a number of assumptions about the field traffic system parameters (e.g. turning movement percentages) will change as time progresses. For the performance measures from the simulated environment to remain aligned with those of the field, a series of algorithms and techniques are developed to as part of the real time platform. Two primary areas in which significant advances were made are in the placement and integration of point sensor data and model calibration.

The point sensor technology implemented throughout the test bed is capable of extracting and streaming a number of different traffic related data. Therefore, it was necessary to identify which data combination is best suited to aid in the accurate estimation of current performance measures (Task 2 and Task 4). In addition, the most suitable location for each point sensor is also explored (Task 5). The location of each detector is important as it dictates the type of data extracted from the roadway. For example, a mid-block detection is more suitable for speed detection while stop-bar detection is suited for vehicle presence detection. It was seen in this effort that simulation boundary detectors (i.e. detectors in the field placed at the boundary of the simulated area) are critical to the success of the simulation. It was also noted where advances in intersection detection are needed to allow for a better pairing of simulated vehicle travel paths with vehicles in the field.

It was shown that a number of parameters will need adjustments to ensure that the estimated performance measures alignment with those of the field (Task 4 and Task 6). It is anticipated that real time adjustments will be indicated by the differences in performance measures that will be collected from the real world and the simulated environment. A calibration process is presented for adjusting VISSIM's calibration parameters in which the underlying performance measure distribution is considered rather than a simple mean of the performance measure. This more robust calibration procedure enables a more accurate real-time simulation environment. The significant role played my pedestrians and the need for a model to accurately account for pedestrian activity is investigated and discussed. It is seen that relying on default simulation parameters to model pedestrian behavior can result in simulated pedestrian behavior significantly different from that of pedestrians in the field.

Real-World Test-Bed and Field Test

Integral to the creation of a test bed (Task 6) are detectors that are capable of streaming traffic data in real-time to a central server. The developed test bed utilized video detection systems capable of streaming per vehicle records. The primary data transmitted included detection timestamp, presence, speed, location, and lane number. This data was sent to a central server responsible for data processing and transmitting the data to the VISSIM client. Utilizing this test bed several real time simulation experiments were undertaken. These experiments demonstrated the ability of the real time simulation, for the given system, to provide reasonable estimates of travel time. However, in several instances difference were noted. These difference where attributed to

several causes: detector errors at simulation boundary detectors resulting in volume discrepancies between the simulation and field, differences between individual vehicle turning movements in the field and simulated environment, challenges in the synchronization of field and simulated signal indications, model calibration, and downstream congestion influencing simulations boundary conditions. Future efforts will seek to continue to improvement the real time environment in each of these areas.

To test the proposed real-time approach in an environment that allowed for eliminating or significantly reducing the errors resulting from the proceeding issues a “pseudo” real time field test was undertaking using the FHWA Next Generation Simulation (NGSIM) program. The NGSIM program created high fidelity data sets intended for use in the study of traffic behavior and the development of the next generation of traffic simulation tools and algorithms. Utilizing this data set to create a pseudo real time data stream it is seen that the real time approach is capable of providing accurate performance measures given high quality data inputs. Future efforts will seek to explore the relationship between degradations in data accuracy and performance measure estimates.

Real-Time Presentation of Arterial Performance Measures

Finally, a web-based interface was developed presenting the arterial performance measures in real time. The data generated by the simulation is polled in real-time to generate time space diagrams and summary charts and statistics of the various performance measures. An animated representation of traffic moving through the study corridor is also provided

TABLE OF CONTENTS

LIST OF TABLES

LIST OF FIGURES

1 INTRODUCTION

1.1 Background and Motivation

Traffic congestion is a one hundred billion dollar problem in the US. In 2010, Americans spent approximately five billion additional hours and purchased an estimated two billion gallons of additional gas due to congestion. The State of Georgia has shared in these congestion challenges. For example, in Atlanta, 116 million hours was spent in congestion, which resulted in the purchase of approximately 53 million gallons of excess fuel. In total, the cost of congestion to Atlanta's traveling population was approximately two and half billion dollars in 2010. [1]

Like the United States, Atlanta's cost of congestion has been trending upwards over the last few decades, Figure 1. Also like the United States, Georgia has been taking strides to reduce congestion levels.

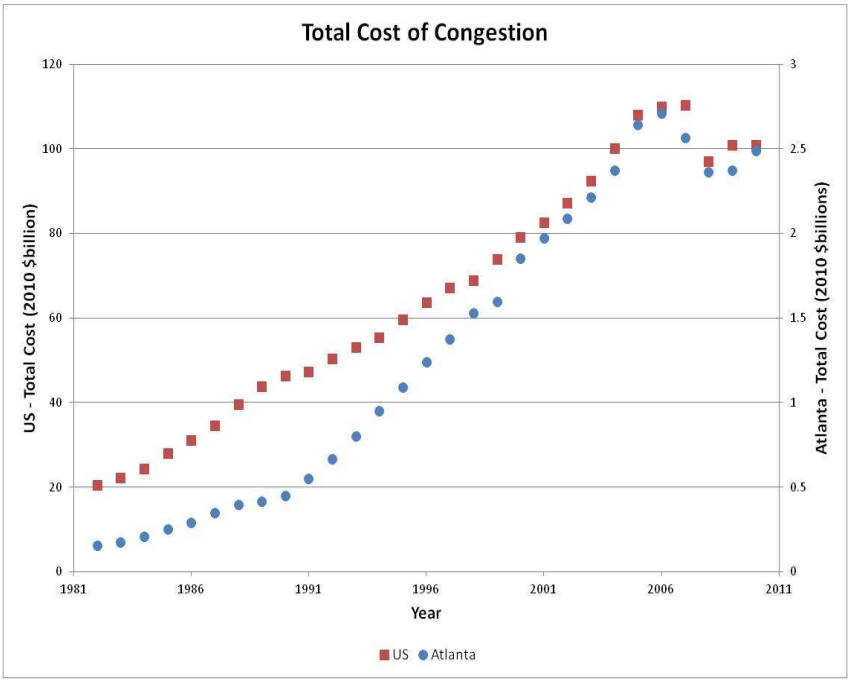

Figure 1 Total Cost of Congestion in the United States and Atlanta, GA [1]

This research project explores the feasibility of integrating real-time data streams with an arterial simulation. Such an integration is geared towards providing the Georgia Department of Transportation (GDOT) and the public with current estimates of arterial performance measures. This additional information will facilitate increased efficiency in facility utilization by enabling more informed decisions in the use and management of Georgia's transportation facilities. To accomplish this, the research team utilizes fixed sensors in the development of an online, data-driven, microscopic traffic simulation tool to determine and provide arterial performance measures.

1.2 Problem Statement

A wide variety of advanced technological tools have been implemented throughout Georgia's transportation network to increase the efficiency. Some of these tools include Advance Traffic Control System (ATCS), Advance Traffic Management Systems (ATMS), Advanced Traveler information System (ATIS), and Ramp Metering and Managed Lane Strategies. Currently, these systems are credited with reducing or maintaining freeway congestion levels in light of increasing travel demands. In Georgia these benefits are primarily gained through the Traffic Management Center's freeway monitoring and quick response in ridding the roadway of any obstacles that may reduce freeway service levels. There have been a number of efforts to leverage the work done by TMCs to provide travelers with more current traffic information such as Georgia 511 / Navigator [2]. In addition, private efforts and partnerships with companies such as Google, NAVTEQ, and INRIX have made the TMC's information more accessible to travelers, aiding their traveler decisions [3–6]. This effort aims to compliment real-time freeway information by addressing the lack of available real-time arterial performance measures.

In comparison to the vast investments in equipping freeways with advance technology to improve mobility widespread outfitting of arterials with similar technologies in its early stages. Successful ITS arterial deployments include both advance and adaptive traffic signal control systems and various surveillance efforts. The benefits of these limited deployments range from a reduction in the number of stops along an arterial segment to increases in traveler satisfaction [2]. Also, more recently, real-time traffic information providers have been supplying information regarding traffic condition along arterials, the accuracy of which is still being improved.

Table 1 and Table 2 highlight the current differences in the ITS related benefits experienced by travelers on arterials and freeways, respectively. The difference in disseminating ITS information to the traveling public is noticeable. Table 2, referring to freeways, demonstrates that presenting traffic information to the travelling public has positive impacts on safety, mobility, and customer satisfaction. From Table 1 (referring to arterials) one notices that there is insufficient data to support a conclusion regarding the benefits of disseminating traffic information to the travelling public along arterials. One of the reasons for this lack of conclusion is that information disseminated is very limited. Of the arterial streets network in the nation's largest 108 metropolitan areas, arterial traffic information is only available for approximately two percent of the network miles [2]. This effort seeks to address this lack of available real-time arterial traffic information and aid in the realization of all possible benefits that may be experienced by potential travelers, drivers and transportation facility managers.

Table 1 ITS Arterial Management Benefits Summary [2]

	Safety	Mobility	Efficiency	Productivity	Energy and Environment	Customer Satisfaction
Surveillance						
Traffic Control	✚	●	●		●	
Lane Management						
Parking Management		●	✚			●
Information Dissemination						
Enforcement	●					●

● Substantial positive impacts
✚ Positive impacts
○ Negligible impacts
✱ Mixed results
✖ Negative impacts
blank Not enough data

Table 2 ITS Freeway Management Benefits Summary [2]

	Safety	Mobility	Efficiency	Productivity	Energy and Environment	Customer Satisfaction
Surveillance	**Enabling technology**					
Ramp Control	✚	●	●			●
Lane Management	✚					
Special Event Transportation Management						
Information Dissemination	✚	✚				✚
Enforcement	●					●

● Substantial positive impacts ✚ Positive impacts
○ Negligible impacts ✱ Mixed results
✖ Negative impacts **blank** Not enough data

1.3 Research Objective

As stated the overall objective of this research is to determine the feasibility of integrating real-time data with an arterial simulation to estimate performance measures in real-time and provide such information to facility managers and travelers. This objective was accomplished by undertaking the following tasks:

1. Describe the current state of practice concerning the estimation of real-time arterial performance measures.
2. Develop a federated (integrated) simulation test-bed for testing procedures and algorithms.

3. Determine the feasibility of integrating point sensor data with simulation to create a data-driven, on-line simulation tool.
4. Develop procedures and algorithms to calibrate an on-line simulation tool that estimates of travel time and other performance measures in real-time.
5. Determine any potential improvements in travel time estimation resulting from sensors placed in atypical locations, such immediately downstream of an intersection.
6. Field-test the data-driven, on-line arterial simulation tool on a target corridor.
7. Devise method(s) to deliver travel time and other operational characteristics to GDOT and the general public. .

1.4 Organization of Report

The organization of the remaining report is as follows. Chapter 2, Literature Review, provides a comprehensive review of previous work that made strides towards estimating arterial performance measures and highlights how this effort will build upon these previous efforts. Chapter 3, Methodology, presents the methodology that has been developed to achieve the objectives of this research project. Chapter 4, TRTI Transportation Run-Time Infrastructure, highlights the details of the integral communication mechanism developed for the project to manage data transmission amongst the various components of the system. Chapter 5, Experimentation and Evaluation, details the execution and results of number field experiments that were used to validate the developed methodology. Chapter 6, Advanced Model Calibration Procedure, summarizes a procedure

that was developed to calibrate a VISSIM simulation model. Chapter 7, Modeling Pedestrian Behavior, gives insight into how to address the issue of pedestrian-vehicle interaction in a simulation environment. Chapter 8, visualization of arterial performance, provides means of visualizing and presenting performance measures to users and facility managers. Chapter 9, future research, offers readers a few tasks that will be tackled in the future to increase the robustness of this method. Chapter 10, Implementation Plan, directs readers to requirements and challenges that will have to be addressed in order for proper implementation and the fulfillment of the goals that the system is intended to accomplish. Finally, Chapter 11, Closing Remarks, concludes this report by highlighting the objectives of this task and the manner in which they were accomplished and the anticipated impact to transportation in Georgia as well as possible impacts on the state of the practice.

2 LITERATURE REVIEW

The following chapter provides a comprehensive review of previous efforts in estimating and predicting performance measures along signalized arterial streets. A number of estimation models, along with their successes and contributions to the field of estimating performance measures will be presented. Models that have been developed to predict performances measures along arterial will also be reviewed.

2.1 Estimating Arterial Performance Measures

Estimating performances measures along arterials is often more challenging than for freeways. The primary reason for this is that freeways are controlled access facilities with limited mainline traffic control (i.e. no signals, stop signs, etc.) while arterials are often uncontrolled (or limited control) access facilities. That is, vehicles may turn on and off the facility at multiple locations, interaction with potentially numerous crossing arterials may be significant, and control devices (e.g. traffic signals) can significantly influence vehicle movements. As a result of such interruptions volume and speed are extremely varied. Given the large variations in speed and volume along arterials, the ability to determine performance measures can be dependent on significant data needs and more advance mathematical techniques than those employed to extract performance measures from freeways.

2.1.1 The Early Models

In 1977 P.G. Gipps provided one of the earliest models for estimating performance measures along arterials. Gipps developed a regression model that employed occupancy measurements and vehicle arrival times, from loop detectors, to estimate arterial link travel times. The model was then validated using simulated data. Despite several model adjustments and the relative success of the model, Gipps noted that in order to improve the accuracy of his model, incorporating other parameters such as signal timing plans, number of lanes, and link length was needed. In building on the accomplishments of Gipps' 1977 model, a number of researchers used his model as a foundation for their own model to improve the estimation of arterial performance measures. Gault and Taylor sought to improve Gipps' 1977 model by calibrating it to a two lane roadway and eliminating a few of the parameters that they deem to have minimal impact on the relevant performances measures. [7–9]

A review of a number of the earlier works, including the two previously mentioned models, was conducted by Sisiopiku and Pouphail [8]. The limitations presented ranged from the lack real-world validation results to use of assumptions that may prevent the respective model from being implemented in the real-world. Table 3 presents a number of early models and their associated limitations and validations results [8].

Table 3 Limitation and Validation Results for the "Early" Models [8]

Model	Limitations	Validation
Gipps	- Lack of empirical validation - Signal settings/geometry not considered - Correlation of the parameters exists	With simulated data only; MSE[a]= 10-15%
Gault et al[b]	- Underestimates travel time for occ.>50% - Lack of empirical validation	With simulated data only; Within 10% of the mean
Gault[c]	- Bounded (occ. should be $\leq$ 70%) - Not appropriate for oversaturation	With video tape data; Within 10% (rarely up to 50%)
Abours	- Signal settings are ignored - Formulation not reported	With floating car data; RMSE[d]= 13%
Luk et al Usami	- Requirement of stop-line detectors - Applicable for oversaturation only	Not reported With simulation & field data RMSE = 10-19%
Luk	- Flow conservation assumption - More suitable for freeway environment - Requirement of stop-line detectors	With wheelbase data Within 10% of the mean
Takaba	- Linearity assumption between travel time & flow in congestion - Neglect of dependency between links	Error ratio = 12-24%

[a]MSE: Mean Square Error
[b]Arrival Type Model
[c]Occupancy Model
[d]RMSE: Relative Mean Square Error

Zhang and Kwon also presented an overview of a few of the earlier models that were used to estimate arterial performance measures. In this report, the authors grouped the models being studied into five (5) categories. These model categories are regression, dynamic input-output, pattern matching, sandglass, and models developed by the Bureau of Public Roads

(BPR). The following will sections will briefly highlight the characteristics of these categories as well as their limitation as it pertains to estimating performance measures along arterial. [10]

2.1.1.1 Regression Travel Time Estimation Models

Regression models attempt to use data that is currently available via today's surveillance and control systems. These models are capable of accounting for the various different factors that may affect arterial travel time, however, the models often become location specific and difficult to transfer to other arterials. One of the main similarities among the different regression models is required input data. The input data needed for these may include time registered by a vehicle on a loop detector, occupancy (derived from a loop detectors), offsets, and other signal parameters. Despite the applicability of these models, their estimation of travel times, when compared to those from the field, are often less than satisfactory and therefore in need of further improvements. [7], [9], [10]

2.1.1.2 Dynamic Input-Output Link Travel Time Models

Generally these models use input-output traffic flow relationships, measured at upstream and downstream detectors, along with assumptions describing the change in flow characteristics between the detectors. This class of models is able to estimate both link and route travel times using minimal site specific data. However, a disadvantage of these models can be an inability to predict travel times (as opposed to estimating current travel times) and they require a greater data

sampling rate than what is currently available with the use of today surveillance equipment. [10], [11]

2.1.1.3 Pattern Matching Models

In pattern matching the upstream loop detectors record a sequence of voltage signatures from various vehicle types. This sequence of voltage signatures is then compared to those collected from a downstream loop detector. The time between upstream and downstream matching sequences is the average travel time. This approach can also be used to estimate other performance measures such as traffic density and space mean speed. A challenge to pattern matching approaches is that they often require a data sampling rate and accuracy that is higher than that which is obtainable from today's field detectors. [10], [12] A more recent example of a technology that has demonstrated success using pattern matching is the wireless traffic detection and integrated traffic data systems offered by Sensys Networks [13].

2.1.1.4 Sandglass Link Travel Time Models

These model use the concept that travel-time can be estimated as the sum of time spent on two segments of a link – a congested segment and an uncongested segment. On the congested segment of the link there is no inflow of vehicles from external sources nor is there outflow to other roads, thus travel times are essentially deterministic queuing delays. For the uncongested segment travel time is determined by using a constant speed relationship. One with a challenge of these models is that the required input is queue lengths which may only be indirectly obtained

from the field data. Therefore any error in estimating queue lengths from the loop detectors will be propagated throughout travel time estimation. Furthermore, the accuracy of these models is unsatisfactory especially for dynamic short-term traffic management applications. [10], [14]

2.1.1.5 Bureau of Public Roads (BPR) Models

The models developed by the BPR to estimate performance measure along arterial have primarily been used in transportation planning and intersection studies. Like sandglass models, travel-times are computed as the sum of time spent on two segments in a link, the free-flow travel time and intersection delay. The input required for these models is traffic volume data which is obtained directly from loop and video detectors. However, despite the anticipated accuracy of these model, when tested the result tended to be unsatisfactory. [10], [15]

2.1.2 Developments in Estimation Models

Building on the successes and lessons learned from earlier models, a number of recent efforts have been devoted to addressing the limitations and refocusing the assumptions of earlier models. One of the first significant attempts to build on earlier models was presented by H. M. Zhang in 1998. Zhang developed the Link-Journey-Speed (LJS) model which estimates the speed, and subsequently the travel time, along signalized arterials. The LJS model combines the speeds estimated from the roadway's critical volume to capacity ratio and the one calculated from the volume and occupancy measurements from loop detectors. The model has been demonstrated to work well in under capacity conditions although may break down under congestion conditions -

particularly when the built up queues are not long enough to be detected by upstream detectors. [16]

In 2007, Liu and Ma presented a time-dependent model to estimate travel time along arterials. In this paper the authors developed a model that used loop detector and signal status data to calculate travel time along an arterial corridor. When calculating travel time the model decomposes travel time into two components; free flow travel time and intersection delay. Although the presented model estimates travel time along arterials fairly accurately its validation was completed in a simulated environment. Additionally, given that the model greatly relies on loop detector and signal status data, a real-world implementation of this model may be met with a number of challenges relating to data accuracy and transmitting the data from the field to a remote location to be implemented in the model. [17]

Wang and Hobeika present a modified HCM2000 model to estimate travel time along arterials. Similar to previous models, this model estimates travel times as a sum of free flow link travel time and delay experienced at an intersection. Essential to this model is the speed and volume data collected by upstream loop detectors. Based on these data free flow travel time is a simple calculation involving travel speed and link length while intersection delay is calculated by grouping vehicles together and using the relationship between average intersection delay and number of vehicles per cycle length as a well as average intersection delay and the delay of the first vehicle in a group of vehicles. The proposed model was validated using average intersection delay from a single intersection in the field and delay computed using the HCM 2000 method. Despite the accuracy with which this model estimates intersection delay for a single intersection

along an arterial, the authors acknowledge that extending the model to involve a number of intersections will further demonstrate the feasibility of employing this model to estimate arterial travel time. Additionally, a potential limitation of this model is that it requires upstream loop detectors, which are not often times available in the real-world. [18]

2.1.3 Automatic Vehicle Location and Identification Estimation Methods

As technological advancements have been made in the fields of global position systems and various vehicle identification technologies, a number of researchers have employed the use of such technologies to better estimate transportation network performance measures, particularly travel time. Although the usage of these technologies has been largely geared toward freeway implementation there are a number of efforts that are aimed at extracting performance measures along arterial streets. Dailey and Cathey, in 2002 developed a estimation methodology that used transit vehicles that were equipped with advance vehicle location (AVL) technology, with the aid of Kalman filtering to estimate speeds and travel times along freeway and principal arterials [19]. Li and McDonald in 2002 presented a link travel time estimation model that used GPS data from a single probe vehicle. This model uses the time-speed profile of the probe vehicle to produce a maximum continuous acceleration and an average speed value to be inputted into fuzzy set. Once these values enter the sets they will be analyzed with historical traffic data to derive travel time along the link being studied. Despite the promising results from this research effort the model's use of a single (or a few probe vehicles) to represent the traffic in its entirety along a particular arterial may provide erroneous data as a particular driver's behavior may not be repre-

sentative of the traffic's current condition. Furthermore building fuzzy sets of driving patterns for a large arterial network may be a tedious and labor intensive process. [20]

Choi and Chung in 2003 presented an algorithm the fused data from GPS equipped vehicles and loop detectors to estimate link travel times along arterials. This algorithm also employed the use of a voting technique, fuzzy regression, and Bayesian pooling to aid in the estimation of arterial travel time. The base of this proposed algorithm is a double fusion data process while incorporating the historical traffic data of the link being studied to estimate link travel time. The results from the model indicate that this algorithm does accurately estimated the travel time for the arterial links understudy. However, possible limitations include lack of feasibility in, near-term, real-world implementation of the algorithm given its dependency on GPS and transmitted loop detector data. Also the authors indicate that further tests need to be done to analyze how the algorithm will perform under different traffic conditions. [21]

In 2009 Pu et al. [22] presented key limitations associated with AVL technologies to estimate arterial performance measures in real-time. To address some of these limitations, the authors developed a framework that employs historic bus and car speeds, and streaming AVL bus speeds to estimate bus and car speeds, and travel times in real-time. Central to this framework is the joint relationship between bus and car speeds which has been formulated through the use of historic car and bus speeds. Despite the method's promising results, accurate estimates are dependent on streaming AVL bus data which is not always available. Also, the authors highlighted the need for further studies, before full scale implementation, to evaluate the frameworks performance under changing traffic conditions. [22]

Lucas et al. (2004) [23] presented three noteworthy limitations when using GPS and other forms of vehicle identification technologies. In part, these limitations are associated with the off-site processing of vehicle identification data which hinders real-time implementation of such methods, the cost associated with additional equipment and infrastructure investments, and privacy concerns of drivers as they traverse to transportation network. To address these limitations, the authors presented an estimation methodology that only relies on vehicle platoon information from loop detectors. Although promising a disadvantage of this method is that it requires streaming detector data which is a limitation of today's traffic controller. [23]

All of the above efforts attempt to estimate performance measures in real-time. However, this goal has been achieved with varying levels of success and accompanied by different sets of limitations. Some of these works present an entire method to extract real-time performance measures, albeit with limited success during full scale field implementations. Others are more geared towards improving a particular component of a real-time performance estimation framework and not necessarily developing a complete methodology.

2.1.4 Statistical Models

There is a large body of work of statistical estimation models that are aimed at approximating performance measures along arterials. In this category of models traffic data such as vehicle speed, occupancy, headway, traffic flow volume, etc., are used as input variables for equations or models that output performance measures such as travel time [17]. These models may be divided into sub-categories such as classical statistical models and more complex statistical models.

Classical statistical models refer to models that use traditional estimation techniques such as linear, non-linear, and Bayesian techniques to estimate arterial performance measures. The more complex model refers to model that employ techniques such fuzzy logic, neural networks, etc. or any combination of these techniques.

In terms of examples of classical statistics models Turner et al. [24] presented a series of linear expressions to estimate speeds along arterials and subsequently travel time, Zhang [16] presented a non-linear model that combines two speed estimates to calculate arterial travel time and Park and Lee [25] used a simple Bayesian estimator as the basis of a model to estimate arterial link travel speed. As for more complicated models Park and Lee [25] paired a simple Bayesian estimator with an expanded neural network to estimate link travel speeds along arterials, Cheu et al. [26] uses a multi-layer feed-forward neural network with back propagation training to fuse various data streams to estimate arterial speed, Palacharla and Nelson [27] employed the use of fuzzy logic and neural networks to dynamically estimate arterial travel time and Robinson and Polak [28] considered a k – Nearest Neighbor methodology to determine arterial travel time using loop detector data.

Some of the limiting factors of these models include that they can be site specific and must be recalibrated for different locations and a number of these have only been evaluated under simulated conditions. In addition many of the statistical models require large field data sets not only for the purposes of statistical significance but also for some of the learning algorithms to have more training before estimating arterial performance measures. [17], [18]

2.1.5 Real-Time/Online Estimation Models

Skabardonis and Geroliminis (2005 and modified 2008) proposed an analytical model to estimate travel times along arterial streets in real-time. This model utilizes data that can be had from loop detectors such as, flow and occupancy, and pairs it with signal timing data such as, cycle length, green time, and offset. Kinematic wave theory was then used as the base of this model as it was able to represent the spatial and temporal features on queues formed at signalized intersections. Similar to previous models the travel time on an arterial link is calculate as the sum of the link free flow travel time and the delay experienced at the intersection. In this model the delay incurred at an intersection is equal to the summation of the three forms of delay, the approach delay, queue delay, and delay due to oversaturation. In light of this model's ability to estimate travel time with relatively high accuracy it was validated in a simulated environment and also with limited field data. However, field data trials where offline, not utilizing a real-time data stream. [29], [30]

Tsekeris and Skabardonis (2004) examined five analytical models that have been primarily develop for use in real-time estimation of performance measures along arterials. These five models are the Spot Speed (SSM), BPR-Based, Uniform Delay-Based (UDM), Overflow Delay-Based (ODM), and the Generalized Delay-Based (GDM) models. The evaluation of these models' ability to estimate performance measures in real-time was conducted in a simulated environment. In their simulated environment they found that to fully evaluate the robustness and accuracy of these methods, aggregated travel times, at the network level, and available signal timing information should be taken into consideration. In general, the GDM and ODM were the

most promising approaches to estimate total average travel times at the network level. While the other models provided better estimates of individual link travel times. The GDM and ODM were also capable of improved network-wide travel time estimates and greater output robustness when there are discrepancies between field and simulated signal timings. However, it is not known how these simulated findings would translate to a field implementation. [31]

In 2009 Kwong et al. [32] presented a scheme for estimating the distribution of travel time on an arterial link. This scheme employed the use of wireless sensors to acquire the magnetic signature of each vehicle. An upstream signature is matched anonymously with the signature from a downstream sensor to estimate the travel time of a particular vehicle. The authors also state that other performance measures such as link volume, delay, and queue length can be determined from this methodology as distributions. The means of extracting performance measures from a vehicle's upstream and downstream magnetic signature is a statistical model of signature distance that requires no additional detector data, such occupancy, or infrastructure data such as signal timing plans. In light of the preliminary success of this model, there is a need for further field evaluations as the current evaluation procedure was done on a simple network. In addition, ground truth verification of determined performance metrics is needed. [32]

Lucas, Mirchandani and Verma in 2004, [23], presented a methodology to extract travel arterial time information without the need to indentify individual vehicles. Their methodology identified vehicle platoons as they traversed the transportation network. The platoons are identified with the use of loop detectors placed along the arterial corridor being studied. The results presented by the authors are encouraging however based on testing in a simulation environment

only. As previously mentioned, Zhang and Kwon [10] highlights that such techniques often encounter difficulties when trying to estimate performance measures in real-time as the sampling rate needed for platoon matching is often not available in the field.

A preliminary study was untaken in Melbourne, Australia to investigate the feasibility of extracting arterial travel time measures in real-time. The study was conducted along a small signalized arterial corridor controlled by SCATS (Sydney Coordinated Adaptive Traffic System). In this approach, SCATS datasets, aggregated in 60 second bins, were used in conjunction with historical travel time data from VicRoads to provide estimates of real-time travel time. A drawback of this approach is that to obtain estimated travel time data the given signal system (SCATS) must also be used. In addition additional detectors for successful field implementation may be required. [33]

A large scale attempt to extract arterial performance measures in real-time was presented by Whale [34]. In this paper, the authors presented a methodology that employed the use of a cellular automaton microscopic traffic simulation software and approximately 750 inductive loop detectors located throughout the study area, Duisburg, Germany, to estimate roadway performance. In essence, this methodology acquires traffic information, namely vehicle counts, from each of the approximately 750 detectors at a resolution of 60 seconds. The data used as input to the cellular automaton traffic simulation model. Upon receiving the data and performing the necessary data processes, the load on each link is then presented to the consumers of this information. Limitations of the approach include the use of a cellular automaton traffic model which has a few deficiencies in representing traffic and driver behavior on a microscopic scale, a lack of

flexibility in the resolution at which traffic data is sent and process, and that the vehicle load along a particular link is the only performance measure being delivered to the consumers of the results this effort. [34]

In another effort a team of researchers from the University of Minnesota developed the SMART-SIGNAL system (Systematic Monitoring of Arterial Road Traffic and Signals). This system is a data collection and performance estimation tool for arterial streets. Integral to the functionality of this system is the collection of high-resolution event based traffic data from an arterial. The primary data sources for the system are signal controller cabinets that are located throughout the arterial being studied. From these cabinets event based data such as vehicle actuations and signal phase changes are collected, archived, and processed. This rich dataset is then archived and processed to determine a variety of performance measures. Estimates of performance measures include travel time, queue length, and number of stops, under a variety of conditions. The field implantation of this system indicates that it is capable of producing accurate performance estimates in real-time. One challenge of this approach is the requirement to gain access to a signal cabinet to extract the event-based signal data. In addition, this system is more feasible for a corridor which is controlled by a network of controllers with one being a master. Where a master cabinet is not present real-time data acquisition becomes a more significant challenge particularly given the resolution required by this methodology. [35]

From the above sections one realizes that a number of advancements have been made in the field of performance measure estimation along arterials although significant limitations still exist. It is also noted that while many of these above efforts discussed their finding and underly-

ing algorithms they did not present significant information regarding data transmission methods or requirements, the impact of lost data or erroneous detections, required detector data filters, or other implementation issues. Despite the successes of the state-of-the-art methodologies and systems, there are few limitations that this research effort is looking to address while building on the capabilities of these earlier works.

2.1.6 Available Real-Time Traffic Information Services

Currently, there are number of providers that offer traffic information in real-time. A few of the major participants in this arena include Google [4], Traffic.Com (NAVTEQ) [5], INRIX [36], Total Traffic Network (TTN) of Clear Channel Radio [37], and SpeedInfo [38]. Although this short list highlights individual organizations that are currently providing information regarding traffic performance, it is noted that a number of these and similar organization offer these services in collaboration with similar organizations.

The primary means by which these service providers obtain data to estimate real-time traffic performance measures is through infield sensors and GPS enabled devices. For instance, Google relies on individuals that have their GPS based, mobile Google Maps smart phone application enabled. Google aggregates these individuals' data to estimate the current state of traffic, primarily on arterial streets [4]. As for freeway data, Google as well as other traffic service providers also rely on point sensor data often provided by regional and local transportation agencies, such as departments of transportation. Traffic.com, an affiliate of NAVTEQ, acquires its data from its own network of digital traffic sensors, commercial and government partners, and their

own traffic operations centers [5]. SpeedInfo uses its solar powered, DVSS-100 Doppler radar Speed Sensor system which measures the speed of vehicles on both sides of the highway [38]. In addition to some of the previously mentioned data sources INRIX gathers information from GPS enabled commercial vehicle fleets to estimate traffic performance [36]. TTN employs information from Airborne/Mobile Spotter Vehicles, Digital Scanners that cover many local emergency services, Police Callouts, and Traffic "Tip Lines" [37].

Accuracy of the traffic information being offered by these service providers is highly dependent of the facility type and acceptable confidence band for the particular consumer's application. The freeway performance accuracy is commonly higher than that for surface streets. This is primarily due to limited access nature of freeways and more uninterrupted flow characteristics. These attributes of a freeway facility lends itself to accurate performance measures being extracted, particularly on the macroscopic scale, with a fairly narrow confidence band. As for surface streets, both vehicle speeds and volume are highly variable due to intersections (signalized and unsignalized) and frequent, uncontrolled access points. In addition, to date, only macroscopic level information is available for both freeway and arterial facilities, representing roadway segments instead of individual vehicle performance.

3 PROPOSED METHODOLOGY

The methodology employed by the research team utilizes point sensor traffic data to drive a microscopic traffic simulation in real-time. The data from the detectors was transmitted and used as input to a simulation model of the area being studied. Arterial performance measures are then estimated from the real time simulation. In describing the methodology this section first presents the conceptual framework for the effort followed by the current implementation status. In the current research effort the microscopic simulation package VISSIM is utilized.

3.1 Conceptual Framework

Figure 2 illustrates the conceptual framework for developing a real-time, online, data-driven simulation tool. The first step in the process is to obtain real-time traffic related data from the network's roadway detectors. These data are then processed by the data processing server. Next, the current traffic state is estimated by streaming the processed detector data into a calibrated simulation model of the area being studied. Once the traffic's current state is captured in the simulated environment, the model may be used to predict near-term future traffic conditions. For example, instances of the traffic's current state may be generated and run faster than real-time to provide a series of possible future traffic states. From these future states, a probable future state may then estimated. The current research effort focuses on the use of real-time data to estimate the current traffic state however future research efforts will seek to extend the current estimation platform for use in near-term traffic prediction.

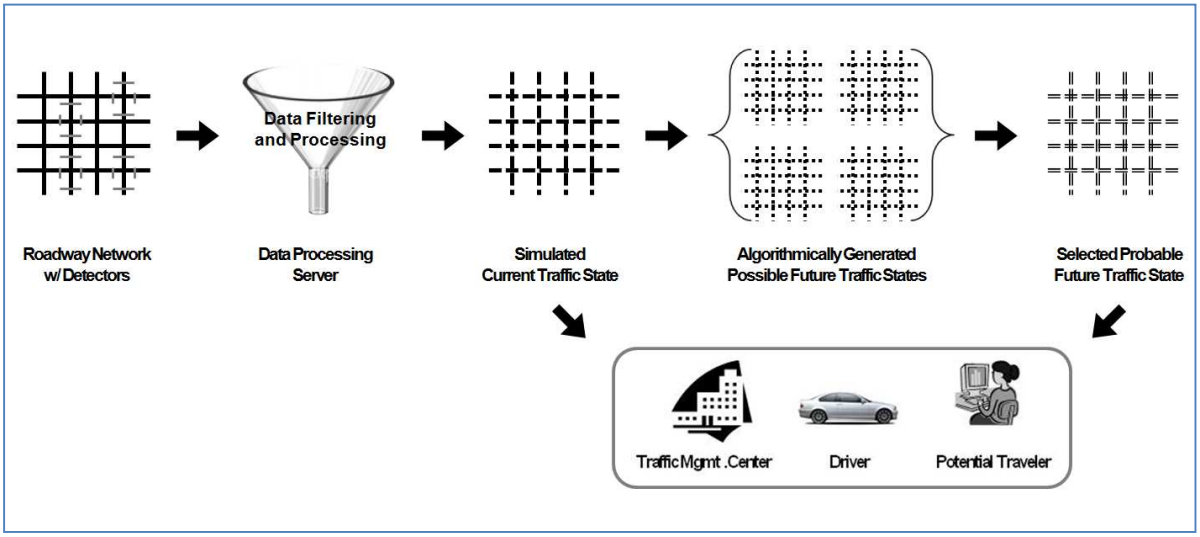

Figure 2 Conceptual Framework for Proposed Methodology

3.1.1 The Network and Detectors

As stated, the goal of this project is to deliver arterial performance measures in real-time using an online data driven microscopic traffic simulation. This research assumes an arterial network where point sensor (i.e. loop detectors, video detection, etc.) detection equipment is available, or may be deployed, capable of transmitting detection data in real-time. It is noted that while real time transmission capabilities are not commonly utilized such technology exists and is being increasingly adapted. It is further assumed that the detector location is known and may be mapped to the simulation environment. Minimum required data streamed from the detector include individual vehicle actuations and speed. Other traffic related data such as occupancy, headway, and volume may also be available however is not required for the current research effort.

3.1.2 Data Processing and Communication

The communication infrastructure to implement the real time simulation has three primary tasks: 1) manage the transmission of traffic data between the point sensors and the data processing unit, 2) facilitate the communication between the data processing unit and the simulation, and 3) broadcast the current and most probable future traffic states.

For the current implementation in the first task the data that is sent from the point sensors is processed by a central data processing unit to facilitate implementation of the data into the simulated environment. The data processing unit reads the data from the detector technology and converts this data into the appropriate message format for transmission to the simulation model.

The second task facilitates the passing of information between the processing unit and the traffic simulation. Given the specific requirements for data transmission, processing, and sharing with simulation instance(s), a customized communication tool is employed. This tool is referred to as the Transportation Runtime Infrastructure (TRTI). TRTI is a High Level Architecture (HLA) inspired communication framework that manages the passing of information between clients (i.e. simulations, data processing unit, etc.). Section 4 and Appendix A provide detailed TRTI development, functionality, implementation information.

The third task broadcasts the current and estimate future states for use in traveler information systems or in traffic control optimization. A web-based application for presenting the information has been developed. For transportation facility managers, it is also envisioned that in addition to the web-based application they will have access to the raw data. This will allow for

the use of model outputs in systems capable of adjusting traffic system parameters in real time, such as signal timings, allowing for increased traffic control system responsive.

3.1.3 The Simulated Environment

VISSIM, distributed by PTV, is a high resolution simulation program that is capable of modeling multi-modal traffic flow. VISSIM also has the capability to visually represent traffic. VISSIM also provides a COM (Component Object Model) interface which allows VISSIM to be automated by other applications. The COM interface also provides users access to VISSIM objects, so that they may be created, manipulated, or deleted. For additional information regarding VISSIM and it VISSIM COM interface see [39] and [40].

It is noted that one of the most critical aspects of this research project is the need to have a well calibrated simulation model of the area being studied. Section 6 documents the calibration effort undertaken as part of this research. Current calibration efforts are focused on *a priori* calibration of the model parameters (i.e. vehicle acceleration, look ahead, safety distance, etc.). Future research will explore real-time calibration of VISSIM model parameters. However, a well calibrated base model will remain critical as it is anticipated that the real-time calibration provisions will work best where only small adjustments to VISSIM parameters are required.

3.1.4 Test Bed

Video cameras were selected as the point sensors to be used for this test bed developed as part of this research project. Ten video cameras have been installed in a test bed located next to the

Georgia Institute of Technology campus. A Video Detection System (VDS) was selected as the accompanying hardware and software, facilitated the real-time transmission of event-based traffic data to a remote location. In addition the video detection system is capable of extracting a significant portion of available roadway data. Currently, the ten cameras that have been installed transmit their video via fiber optic cable to the data processing unit. This unit then processes the videos and sends all the relevant traffic data via wired or wireless connection to a client personal computer. This client then parses the data stream and inputs it accordingly into a VISSIM model of Georgia Tech's campus. Figure 3 presents the test bed's location, camera positions and their respective views.

Figure 3 Test Bed Location and Camera Layout and Coverage [4]

3.2 Summary

In the following chapters the above conceptual framework will be expand. First the TRTI will be presented in detail. This will be followed by a series of method implementations, ranging from lab implementations to full field tests. These implementation presentations will then be followed by discussion on related research items explored as part of this effort including calibrations and the treatment of pedestrians in a real time vehicle based simulation model.

4 TRANSPORTATION RUN-TIME INFRASTRUCTURE

As discussed the real time simulation requires a communication infrastructure to facilitate the passing of information between the central processing unit and the traffic simulation. Given the specific requirements for data transmission, processing, and sharing with simulation instance(s), the use a customized communication tool is employed. This tool is referred to as the Transportation Runtime Infrastructure (TRTI).

The development of the TRTI has been conducted jointly between this project and an NSF's Division of Emerging Frontiers in Research and Innovation (EFRI) project. TRTI is a High Level Architecture (HLA) inspired communication framework that manages the passing of information between simulation instances, referred to as federates. TRTI is an application programming interface (API) or middleware that operates using a publish/subscribe model. This mode of operation allows clients and groups (federates) to publish data to other federate(s) and receive data from federate(s) that they have subscribed to. Note, one of these federates can act as a server (i.e. the central data processing unit) that orchestrates the sharing of information among the other federates. The TRTI allows users to manage, create, add or delete simulations whenever there is a need to do so. Thus, for example, a single data processing unit could serve multiple simulations, each modeling a different arterial. The reminder of this chapter provided details into the background, development, and use of the TRTI.

4.1 Related Run-Time Infrastructure Work

Simulation experts and researchers around the world have developed several Run-Time Infrastructure (RTI) frameworks for varying purposes. Many of these frameworks have incorporated features and functions defined by the US Department of Defense's High Level Architecture (HLA) specification, resulting in interoperability between them. Georgia Tech researchers have developed toolkits to address a wide range of requirements common to distributed simulations. For example, the Federated Simulations Development Kit (FDK) is a framework designed to facilitate the development of an RTI, especially in the context of distributed simulations. The FDK contains two fully functional RTI implementations: the Basic RTI (B-RTI) and the Detailed RTI (D-RTI). The B-RTI provides only the minimum services necessary for time-managed and message-passing simulations. In contrast, the D-RTI provides the entire spectrum of services detailed in the HLA specification [41].

With advances in sensor technology and the increasing ubiquity of wireless communications, simulations that incorporate real-time data (often referred to as "symbiotic" simulation systems) have been receiving increased attention. Frederica Darema categorized these simulations as Dynamic Data Driven Application Systems (DDDAS) and has described issues related to their development [42]. Considerable research and development has been devoted to the creation of such systems, yielding several application examples. The LEAD project is applying these principles to weather prediction [43]. Other work is being conducted to accurately model and predict wildfire behaviors [44]. The AMBROSia project provides a generic toolkit for collecting, analyzing, and validating data from sensors in scientific experiments [45]. Researchers at the Uni-

versity of Birmingham (UK) have been exploring the potential role of artificial intelligence (AI) agents within a DDDAS [46]. The COERCE effort is researching ways to design increasingly flexible DDDASs that dynamically adapt to conditions outside the scope of a simulation's original design [47]. Additionally, the Agency for Science, Technology and Research in Singapore (A*STAR) has been exploring the use of DDDASs to build Integrated Manufacturing and Service Systems (IMSS) that integrate and streamline several of the business processes of the manufacturing sector [48].

Research is also being performed in the context of traffic modeling and simulation. For example, Sisiopiku et. al provide a review of the use of sensor-driven simulations to optimize signal timings and individual vehicle routings [8]. Yet another specific project involves accurately predicting travel times on arterial roads by using loop detectors in a symbiotic simulation [10].

Leveraging the work done by others and recognizing that the proposed methodology requires a robust communications framework; the research team developed the Transportation Run-Time Infrastructure (TRTI).

4.2 TRTI: Overview

Inspired by the HLA specification, the TRTI is a middleware communication framework based upon the designs of the B-RTI mentioned in Section 4.1, but modified for traffic applications. It provides mechanisms for group-oriented message passing using the publication-subscription paradigm. Because of the dynamic nature of a transportation system, the TRTI was designed to

allow individual nodes (which are referred to as “federates” in HLA literature) to communicate over any available network with other federates in the system. (The total collection of nodes within a system is referred to as a “federation”.) To ensure its versatility, the TRTI remains agnostic toward the underlying network medium so long as it is IP-based. As a result, the TRTI may operate across a variety of network media, including Ethernet, Wi-Fi, 3G, 4G, and several others. In addition, the TRTI supports both the UDP and TCP protocols, thereby allowing federates to tailor individual connections to their current network conditions.

In relation to the methodology being developed, the TRTI provides a communication interface for a wide variety of federates. For example, traffic cameras, vehicle counters, vehicle-based simulators, and traffic management center simulations are classified as federates that contribute to the simulation. The TRTI allows the data from all of these federate types to communicate seamlessly in spite of their differing roles and network media.

Rather than sending messages to multiple federates, the TRTI offers the ability to arrange federates into groups. Groups are purely logical constructs that provide mechanisms for segregating messages. When a group is created, it is given a unique name that distinguishes it from other groups within a federation. When a federate wishes to subscribe to a group, the TRTI uses the target group’s name to identify the correct group and establish a subscription. Messages published to a group are automatically propagated to all members of that group. The TRTI frees federates from having to maintain an ever-changing list of message recipients, from having to transmit several copies of each message, and from managing connections to each of the other intended recipients.

Because the TRTI is designed to operate in the absence of any infrastructure, federates are entirely responsible for group management. To facilitate this, the TRTI provides federates with mechanisms to create, subscribe to, and withdraw from groups. Any federate can create a group irrespective of its role within a federation. Federates can also join and leave groups arbitrarily, as well as send messages to and receive messages from a group. When a federate publishes a message to a group, the TRTI ensures that the message is propagated to all other federates that have subscribed to the group, and prevents it from being sent to nonsubscribers. Such segregation ensures that each federate receives only messages in which it is interested. As a result, the need to broadcast each message to the entire federation is eliminated, thereby reducing its overall bandwidth consumption.

4.3 TRTI Architecture: A Closer Look

4.3.1 Initialization

Within a federation, each federate utilizes a local instance of the TRTI as its communications gateway. The TRTI serves as a middleware between federates and handles all aspects of message reception and delivery. At initialization, the TRTI provisions the necessary resources to enable message passing via both the UDP and TCP protocols. The TRTI also records the name of a message handler function that will be called when the TRTI receives a message intended for the federate. Each instance of the TRTI is identical, regardless of the role of the federate within the simulation. As a result, all federates have access to all features of the TRTI. Figure 4 provides an overview of the TRTI's architecture.

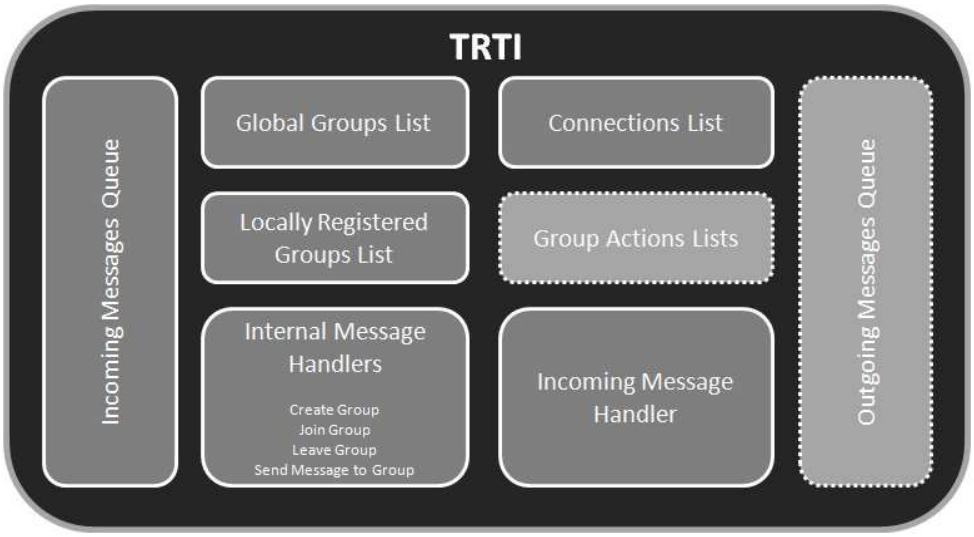

Figure 4 TRTI Architecture Overview

Each federate will initialize its local instance of the TRTI at the beginning of its participation in the simulation. In the online traffic simulation system described in Section 3, the cameras, road-side sensors, and traffic management center simulations initialize their instances of the TRTI immediately after being brought online.

4.3.2 Messages

Messages passed by the TRTI conform to a standardized format. When a federate publishes a message, the TRTI attaches a header to the beginning of the message containing its size and type, the name of the group to which the message is to be published, and the IP address of the message's source. The message is then delivered to the federate that serves as the host of the intended group which subsequently propagates the message to group subscribers. The TRTI oper-

ates under the assumption that no messages are lost in transit and therefore does not employ any delivery confirmation mechanisms. The process of message propagation is detailed in Section 4.3.6.

As an example, the cameras of the test bed system broadcast messages that typically contain the following information:

4, 2, 18, 13:00:45, 1278608487.375490

These fields represent the following (from left to right):

- Detector number - ID of the source camera for this message
- Lane Number - lane which the camera is monitoring
- Vehicle speed - measured in miles per hour
- Timestamp - formatted as hh:mm:ss
- Epoch timestamp - number of seconds from 12:00:00AM 1/1/1970

Given the fact that current efforts are limited to a small geographical area, only one group is specified. As a result, all of the simulators in the system all receive the same messages.

However, not all of the messages sent by the TRTI are utilized by federates. Because disparate TRTI instances require a collaborative means of managing groups, the TRTI employs group management messages separate from federate-generated group messages. When a federate creates a group, its local TRTI instance builds a group management message that details the new group and delivers it to the intended group host. The group host's local TRTI instance then processes the message internally and performs the actions described in Section 4.3.6. Requests for group subscriptions and subscription terminations also result in group management messages that are handled in a similar fashion. However, when a federate requests that a message be published to a group, the TRTI creates a group message and delivers it to the appropriate recipients.

When a group message is received, the local TRTI instance delivers the message's data to the federate by calling the message handler function (described in Section 4.3.3).

4.3.3 Handlers

The TRTI employs two types of handler functions. First, message handler functions serve as a federate's inbox for messages from the TRTI. As group messages are received, the TRTI passes the contents of the incoming message to the federate's message handler. Similarly, the TRTI employs internal message handlers for processing incoming group management messages. These handlers operate independently and asynchronously from the federate's software, thereby freeing the federate from any group management and message propagation tasks. While these internal handlers are defined within the TRTI framework, the federate's incoming message handler function is defined entirely by the federate. Only one incoming message handler function can be defined for each instance of the TRTI. The incoming message handler must be defined when the TRTI is initialized.

Second, the TRTI allows for group handlers to be defined by federates. Group handlers are used to perform processing tasks on messages prior to their delivery to each of the intended recipients. Group handlers also allow for common processing tasks to be consolidated, thereby eliminating duplicative effort by the individual federates. They also allow for group-level information to be reported to group members. For example, a transportation simulation may implement a group handler that determines the number of vehicles subscribed to the current group and

appends it to each message, thereby providing a rough estimate of how many vehicles are in the area.

Unlike message handlers, there is no limit to the number of group handlers that can be associated with a group. Group handlers are executed by group hosts and can be associated with or disassociated from a group at any time. When a federate publishes a message, its local TRTI instance transmits the message to the group's host. The host TRTI instance then executes the group handlers associated with the group and propagates the processed message to the group subscribers. Group handlers are executed independently and asynchronously from the federate's software.

4.3.4 Connections

As mentioned in Section 4.2, the TRTI supports message passing via both TCP and UDP protocols. Federates can use unreliable datagram services in areas where weak signal strengths disallow reliable connections, and use persistent connections where strong signals prevail. This flexibility maximizes a federate’s ability to remain connected with a federation in spite of changing network conditions.

When a federate subscribes to a group, it designates which protocol is to be used when transferring messages both to and from the group. If a federate specifies a persistent TCP connection, the TRTI takes responsibility for maintaining the connection. In transportation simulations, connections often become disrupted when vehicles drive through “dead zones” in wireless network coverage. When this occurs, the TRTI reestablishes any persistent connections as soon

as the vehicle returns to an area with adequate signal coverage. However, if a federate specifies that the UDP protocol is to be used, no such connection maintenance procedures are required due to the connectionless nature of UDP.

4.3.5 Message Queues

The TRTI handles the delivery and receipt of messages asynchronously from the federate's software. To facilitate this, the TRTI employs a series of queues to store messages until the federate is prepared to accept them. For example, when messages are received, the federate's local TRTI instance stores them in the incoming message queue until the federate calls for them to be processed. The messages are then passed to the federate in the order they were received. In the context of transportation simulation, this queue enables the federate to control when new data is incorporated into the simulation.

When handling outgoing messages, the TRTI can be configured in one of two ways. By default, it is configured to deliver messages immediately. In this case, when the federate passes the message to its local TRTI instance, it immediately begins publishing it. An alternate configuration allows outgoing messages to be stored in a queue. The messages remain queued until the federate explicitly requests that they be delivered. At this point, the TRTI publishes all queued messages in the same order that the federate provided them. In both configuration scenarios, the TRTI publishes messages asynchronously from the federate's software.

4.3.6 Groups

Any federate within a federation can create and join a group. When a federate creates a group, it specifies a group name and the address of the federate that will host the group. Each group host's TRTI instance will maintain a list of all federates that are currently subscribed to the group and ensure that each published message is propagated to all group subscribers. When federates subscribe to a group, they must specify both the target group name and the address of the group host. Once subscribed, the federates will receive all messages from the group and may broadcast messages to all other members of the group.

Naming conventions for groups can be based on a variety of criteria. Examples include generating names based on a federate's geographic location, its role within the federation, the type of messages being sent, or numerous other factors. Group naming is completely arbitrary from the TRTI's perspective and is left entirely to the federates to determine. In a transportation simulation system, possible naming conventions include using street address ranges, sensor-specific names, and/or latitude-longitude coordinates.

Group creation involves three steps illustrated in Figure 5. First, a federate sends a group creation message that includes the new group's name to the intended group host. (Any federate can send and/or receive these messages to any other federate. They can even send these requests to themselves if they intend to host the new groups.) Upon receipt, the message is placed in the group host's incoming message queue (described in Section 4.3.5). Second, the group creation request is relayed to the group host's group creation message handler (described in Section

4.3.3). Third, the group host creates an entry in its global groups list for the new group. (The global groups list contains a list of all groups for which this federate serves as the group host.)

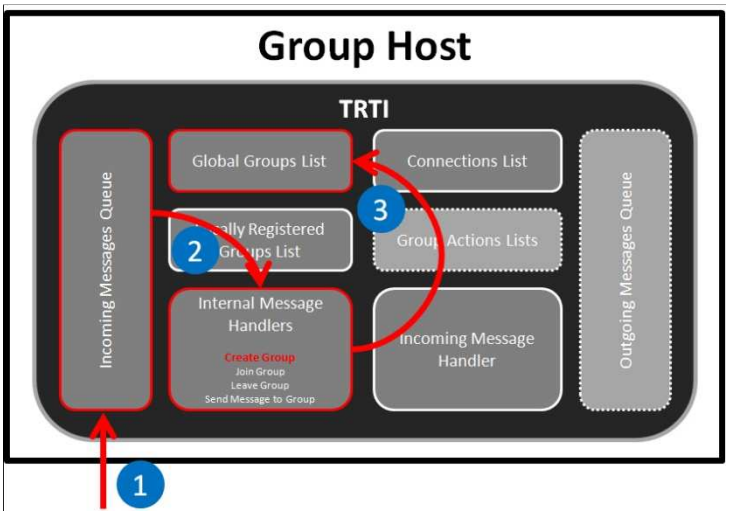

Figure 5 Steps taken by TRTI when groups are created

When a federate subscribes to a group, the TRTI instances of both the group subscriber and group host take several steps as illustrated in Figure 5. First, the subscriber's TRTI instance adds an entry to its locally-registered groups list to indicate that it has joined the target group. Second, the subscriber opens a connection to the group host and stores it in its connections list (described in Section 4.3.4) for later use. If the subscriber is not using a persistent connection or had already stored an open connection to the group host previously, this step is skipped. The third step only occurs if the subscriber's TRTI instance is configured to use an outgoing message queue (described in section 4.3.5). In this case, the subscriber creates a group subscription message and adds it to the outgoing message queue. Next, the message is transmitted to the group

host and placed in its incoming message queue. (If the target group does not yet exist on the intended host, the group host creates the group by performing the steps shown in Figure 5.) Fifth, the group subscription request is relayed to the group host's group subscription handler (also described in section 4.3.3). Finally, the handler modifies the target group's entry in its global groups list to reflect the new subscription.

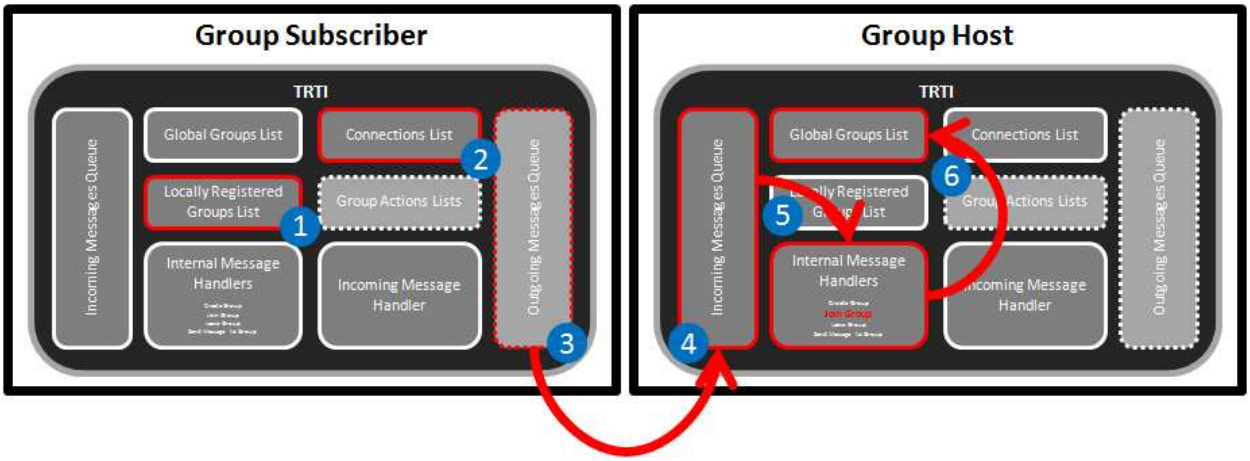

Figure 6 Steps taken by TRTI when federates subscribe to groups

After a group has been formed and federates have joined, the subscribers can begin publishing messages to the group as shown in Figure 7. First, a federate generates a message and passes it to its local TRTI instance for publication to a target group. The TRTI finds the target group in its locally-registered group list and transmits the message to the group's host. Upon receipt, the group host's TRTI places the message in its incoming message queue. Second, if any group message handlers (described in Section 4.3.3) have been associated with the target group, the

group host's TRTI relays the message to them for processing. Third, the group host generates a copy of the processed message for each of the group's subscribers as indicated by the host's global groups list. Fourth, if the host's TRTI is configured to use an outgoing message queue, copies of the processed message are then placed in the queue. Fifth, the copies are transmitted to all group subscribers and subsequently placed on their incoming messages queues. (If the message's source is a subscriber, it will also receive a copy of the message.) Finally, each subscriber's TRTI instance relays the message to the federate's incoming message handler that was designated during the TRTI's initialization (as mentioned in Section 4.3.1).

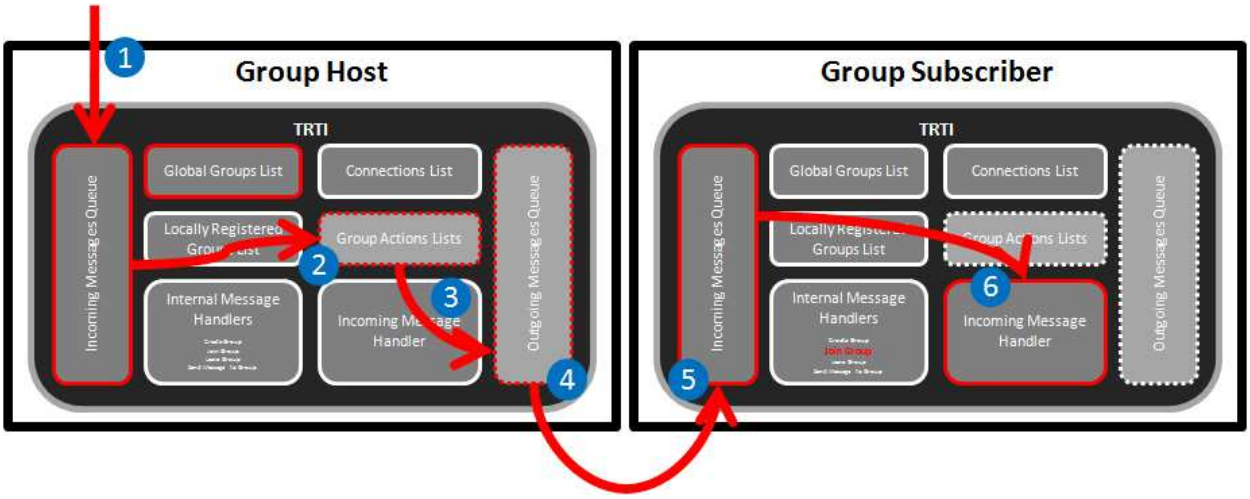

Figure 7 Steps taken by TRTI when group messages are published

The steps required for leaving a group are similar to the subscription process shown in Figure 6. First, the departing federate removes the group's entry from its locally-registered groups list. Second, the federate generates a group removal message and, if configured to do so, places the message in its outgoing message queue. Third, the message is transmitted to the group host and subsequently added to its incoming message queue. Next, the group host relays the request to its

subscription termination message handler. Fifth, the handler modifies the group's entry in its global groups list to reflect that the departing federate has terminated its subscription. Finally, if the departing federate was using a persistent connection and has terminated its subscriptions to all of this host's groups, the group host closes the federates connection. The departing federate subsequently disposes of the corresponding entry in its connections list.

4.3.7 Miscellaneous

The TRTI is written in the C programming language and has been optimized to minimize the overhead of message propagation. While many elements of the TRTI are conceptually inspired by the HLA, its design deviates significantly from the original specification in order to compensate for the highly dynamic nature of transportation systems.

Some of the commercially-available traffic simulation platforms on the market today, such as VISSIM, provide developers with a Visual Basic (VB) interface for expanding the platform's functionality. To accommodate this, the TRTI has been compiled as a dynamically linked library (DLL) to maximize compatibility with VB and other languages with DLL support. For additional details on how to initialize and use TRTI functions, Appendix B provides the Application Programming Interface (API) for TRTI.

4.3.8 Limitations of the TRTI

Because it was not designed as a peer-to-peer framework, the TRTI's architecture is its most significant limitation. Specifically, no mechanism exists for federates to "explore" a network, the-

reby preventing them from finding one another without using some form of directory lookup service. Section 4.3.6 illustrates this limitation by explaining that federates must provide the IP address of group hosts, implying that the address is already known. Such is the case for the method being proposed. To compensate, a single statically-addressed federate (whose address was hard-coded into each federate's software) was designated as the host of all groups. However, in cases where the address of group hosts is not previously known, a directory service must be used to provide federates with the IP address of each group's host.

Another related limitation stems from the requirement that groups be hosted by a specific federate. When a group host goes offline, the group is dissolved. Any messages published to that group in the future will no longer be propagated. For the group to be restored, it must be recreated on a new host, and each federate must subscribe to the new group.

Several minor TRTI limitations are dictated by the computing hardware. For example, the maximum number of queued messages, groups, and group members is determined by the amount of memory available on the host machine. (The TRTI can be configured to enforce arbitrary maximums on the size of these structures.) Also, message propagation speed is limited by both processor speed and network bandwidth. Groups with large numbers of subscribers may experience significant latency in message delivery times due to these factors.

Another issue arises from the wide variety of hardware used in distributed simulations. Not all hardware manufacturers construct their products to use the same endian format. Because of the TRTI's agnostic approach toward message payloads, it does not modify any numerical data in the message and thereby does not ensure compatibility between federates of different endian-

ness. As a result, federates may receive messages that appear corrupt. To avoid this, federates should implement standards for bit ordering within their federations. A simple solution involves utilizing the functions provided by the standard sockets library to encode numerical values both to and from network bit order. If messages are properly encoded before being sent to and after being received from the TRTI, bit ordering problems will be averted.

5 EXPERIMENTATION AND EVALUATION

Three experiments were conducted to determine the feasibility of the proposed methodology. The first of was a proof of concept test which was conducted in a simulated environment. The second and third were field tests, with the primary difference being the use of temporary versus permanent detectors. The following presents the details and results for each experiment.

5.1 Experiment #1: Simulated Environment - Proof of Concept

The proof of concept seeks to provide insight into the feasibility of the proposed real time simulation framework. This experiment uses two VISSIM simulation instances. One instance represents the “real-world” or field and the other attempts to replicate the “real-world” simulation in real-time (referred to as the “modeled-world”). The inputs to the real-world model include traffic volumes over a 4-hour period (reflective of a peak period), signal timing data, and vehicle turning movements. The modeled-world simulation has the same roadway configuration, signal timing data, and historical turning movement percentages. The modeled-world simulation is not given any vehicular volumes as part of the input files. Instead, as will be discussed, vehicles are generated according to the data obtained from the detectors in the real-world simulation instance. This initial experiment explores the feasibility of approximating traffic conditions of the real-world simulation in the modeled-world simulation. To determine how well the modeled-world replicates the real-world travel time and delay over representative paths, and queue lengths at the approaches of the various intersections, are collected and compared.

5.1.1 Experimental Design

A three intersection arterial was created using VISSIM, with each intersection under two-phase semi-actuated signal control. Each roadway is a two-way arterial, with one lane in each direction. In the real-world simulation a loop detector is placed 100 feet from the upstream end of each entrance link, for a total of eight boundary loop detectors. These detectors are responsible for capturing the presence and speed of a vehicle as it enters the network. In both the real-world and modeled-world there are 6 additional detectors, one on each intersection cross street approach. These detectors are used to implement semi-actuated traffic signal control. No data is currently passed from these detectors in the real-world simulation to the modeled-world simulation. Both models simulate a 4 hour time period during which the maximum network volume reached is approximately 1200 vehicles/hour and a minimum of approximately 550 vehicles/hour.

A framework in C++ was developed to implement the system shown in Figure 8. In this framework VISSIM COM is utilized to provide a direct means of interacting with a simulation during runtime. To establish communication between the two simulation models a unidirectional named pipe is created. A pipe is a specific section of memory that is used for the purposes of communicating between a server and one or more clients. When using pipes the pipe-server is the process that creates the pipe and the pipe-client is the process that connects to the created pipe [49]. In the named pipe that was created the real-world simulation model served as pipe-server and was able to write to the pipe. The pipe-client was the modeled-world simulation and was able to read from the pipe. While pipes are capable of two-way communication for

the purposes of this experiment a unidirectional pipe was sufficient. Subsequent experiments replace pipes with the TRTI.

Each of the eight detectors that are placed at the edge of the real-world simulation network are polled for vehicle speed, location, and lane data once every simulation second. In this example, given the fixed detector locations, a detector ID would be sufficient in place of the location and lane data, however, passing location and lane data was undertaken to allow for more robust data streams in future experimental iterations. At the end of each second the pipe server writes an [8] x [3] array to the pipe containing the detector information over the last second. The array is then read by the pipe-client and the information is implemented in the modeled-world simulation. For a graphical representation of the experimental design, see Figure 8 Experimental Design for Proof of Concept.

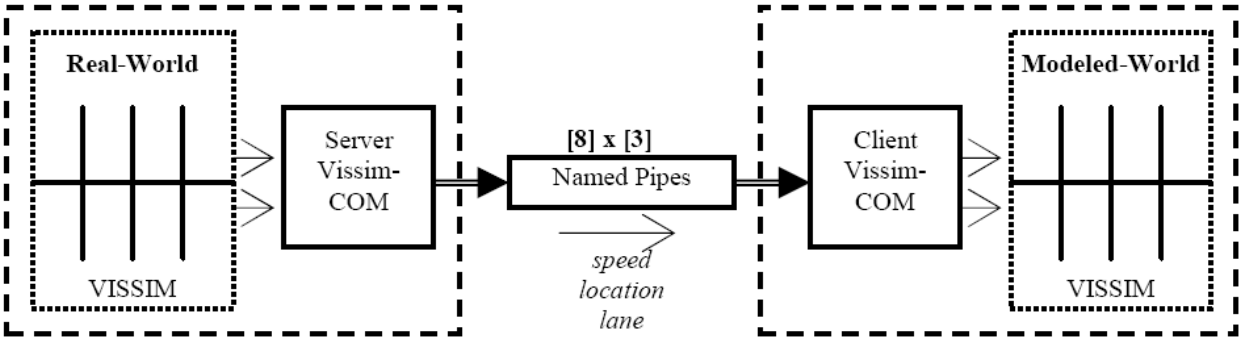

Figure 8 Experimental Design for Proof of Concept

The execution of the model world is driven by the real-world model, with the modeled-world executing a simulation second only when a second of data is received from the real-world data server. In this experiment, reliable, ordered communications are assumed with the named pipe operating on a first-in-first-out (FIFO) basis ensuring that the modeled-world and real-world simulations remain synchronized. Subsequent versions of the framework using the TRTI integrate timestamps directly into the data stream and incorporate data consistence checks. The following pseudo-code further illustrates the structure of the server – client relationship.

```
Pipe-server (Real-World)
for (i = 0, i <= simulation period, i++)
{ advance simulation 1 sec
read  vehicle speeds from the 8 detectors
write [8]x[3] to pipe }

Pipe-client (Modeled-World)
for (i = 0, i <= simulation period, i++)
{ read [8]x[3] from  pipe
input vehicle speeds into simulation
advance simulation 1 sec }
```

5.1.1.1 Simulated Time Frame

A four hour simulation time period is used, capturing the transition into and out of the peak period. The flow rate is 500 vehicles per hour on the main arterial for the first hour, increasing steadily to 900 vehicles per hour over the second and third hours and then returning to 550 vehicles per hour in the fourth hour. At the end of the simulation period the average travel times and delays from seven representative paths, along with the queue lengths at each intersection ap-

proach are collected from both the real-world and modeled-world simulations (Figure 9 and Table 4). These performance measures are presented in 10-minute interval aggregations.

5.1.1.2 Scenarios

The results from two scenarios are presented. Scenario 1 assumes ideal detector performance, with every real-world vehicle and its associated speed accurately detected and passed to the modeled-world. Under such an assumption the primary difference between the real-world and modeled-world results will be due to randomness in driver and vehicle characteristics and potentially different path selection decisions of a vehicle in the real-world and its simulated counterpart in the modeled-world. Scenario 2 introduces some of the variability expected in a field implementation from detector failures and speed measurement inaccuracies. The detectors randomly failed to detect vehicles with a frequency of approximately 2%. Additionally, the detected speeds were allowed to randomly vary higher or lower by up to 10% of the actual vehicle speed.

In both scenarios the vehicle speed measured over the detector in the real-world is used as the desired vehicle speed for the vehicle placed in the modeled-world. However, if the vehicle speed was lower than the expected range of desired speeds (48 to 58 kph) it is assumed the vehicle is within congested conditions and the desired speed is randomly set within the preceding desired speed range. In this instance the vehicle is placed in the modeled-world at the highest speed possible given traffic conditions without exceeding the desired speed. If the vehicle is traveling more slowly than its desired speed it will attempt to accelerate to its desired speed as quickly as possible.

5.1.2 Results and Analysis

Five replicate runs (R-1 through R-5) were performed. Each replicate run consisted of a modeled-world being driven by the streamed detector data of the real-world simulation, allowing for paired comparisons of the real-world and modeled world simulations. Each replicate run utilized different random seeds for real-world and modeled-world simulation instances.

Travel time and delay results for seven paths and queue lengths for three approaches were compared between the real and modeled-world simulation instances for the two scenarios.

Figure 9 presents the network link naming conventions and Table 4 the performance measure links considered. All links in the network are single lane.

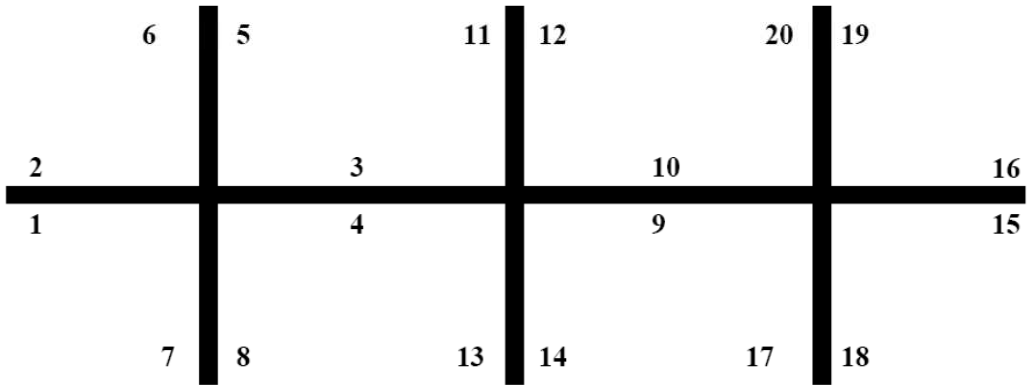

Figure 9 Roadway Network and Link Names

Table 4 Description of Performance Measures

Measures		Path Links	Distance (m)
Travel Time	Delay		
TT-1	DL-1	1-4-9-15	1308
T-2	DL-2	16-10-3-2	1309
TT-5	DL-5	11-13	290
TT-8	DL-8	4-12	366
TT-9	DL-9	10-13	382
TT-10	DL-10	4-9	381
TT-11	DL-11	10-3	383
Queue Length			
QL-1		1	
QL-6		14	
QL-7		10	

5.1.2.1 Individual Performance Measures

For most of the monitored performance measures the Scenario 1 and Scenario 2 modeled-world simulations captured the performance of the real-world simulations accurately. For example, consider Figure 10 and Figure 11 which present the values of the travel time for path 2 (TT-2), from replication 2 (R-2), and of the queue length for path 6 (QL-6), from replication 3 (R-3), respectively, over the four-hour simulated time period. As seen, the modeled-world in both scenarios is able to reasonably track performance measures of the real-world through the four hour period.

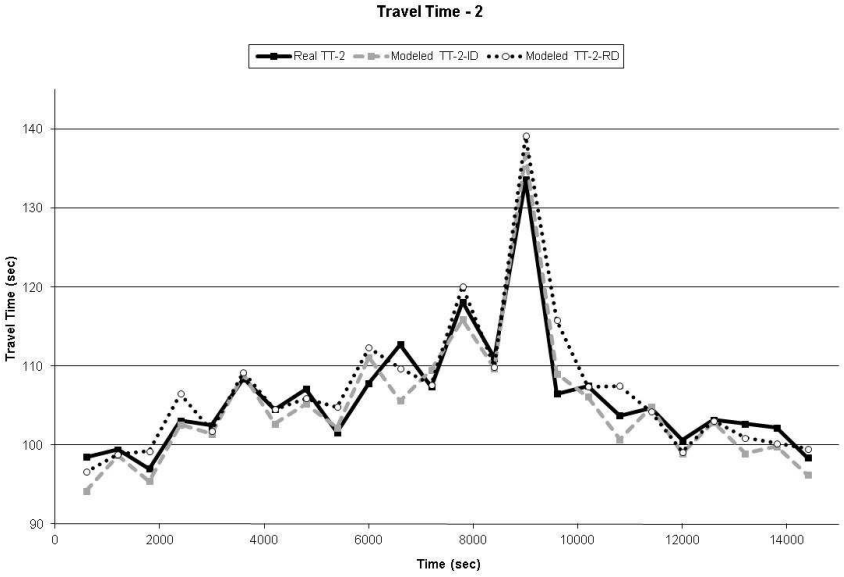

Figure 10 Average Travel Time for Travel Time Path 2 (TT-2), Replication 2 (R-2), for the Real-World and the Modeled World Scenarios 1 and 2.

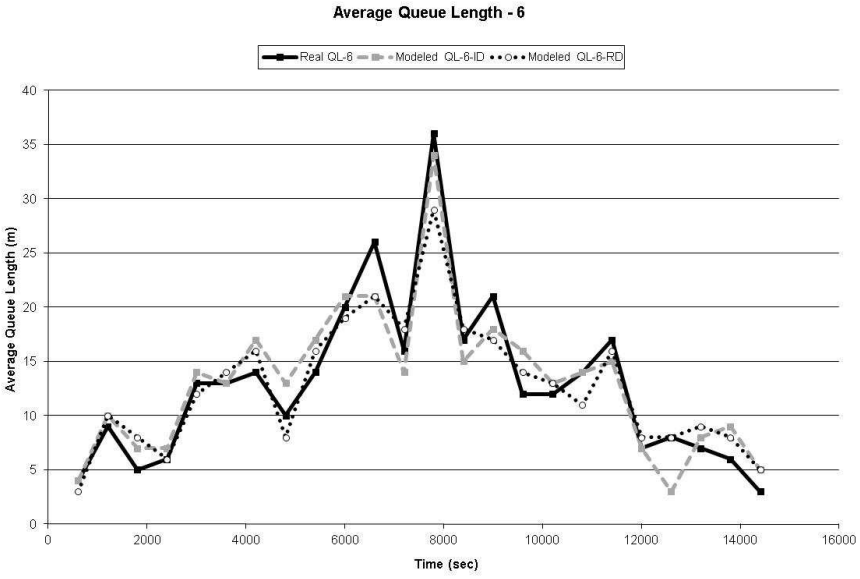

Figure 11 Average Queue Length for Queue 6 (QL-6), Replication 3 (R-3), for the Real-World, and the Modeled-World Scenarios 1 and 2

For instance, in Figure 10 and Figure 11 the absolute differences among the measures from the various scenarios analyzed are minimal. The average and standard deviation of the difference between the values of TT-2 from Scenario 1 are 2.06, and 1.55 seconds; and 2.10, and 2.12 seconds, respectively for Scenario 2. Similarly, the average and standard deviation of the difference between the values of QL-6 from Scenario 1 are 1.96, and 1.46 car-lengths; and 1.96, and 1.57, car lengths, respectively for Scenario 2.

However, when considering all replicated experiment instances it was found that the model-world did not always consistently track the real-world. For instance, consider Figure 12 and Figure 13, which represent the travel time for path 1 (TT-1) from replication 4 (R-4) and the delay for path 1 (DL-1) from replication 3 (R-3), respectively. There is a large discrepancy in the estimates of these particular performance measures between 8000 and 11000 seconds, the highest demand period of the simulated time frame. The modeled world travel time estimate approximately 73% of the real world travel time for both Scenario 1 and Scenario 2. The delay estimate from the modeled world is approximately 44% of the estimate from the real-world.

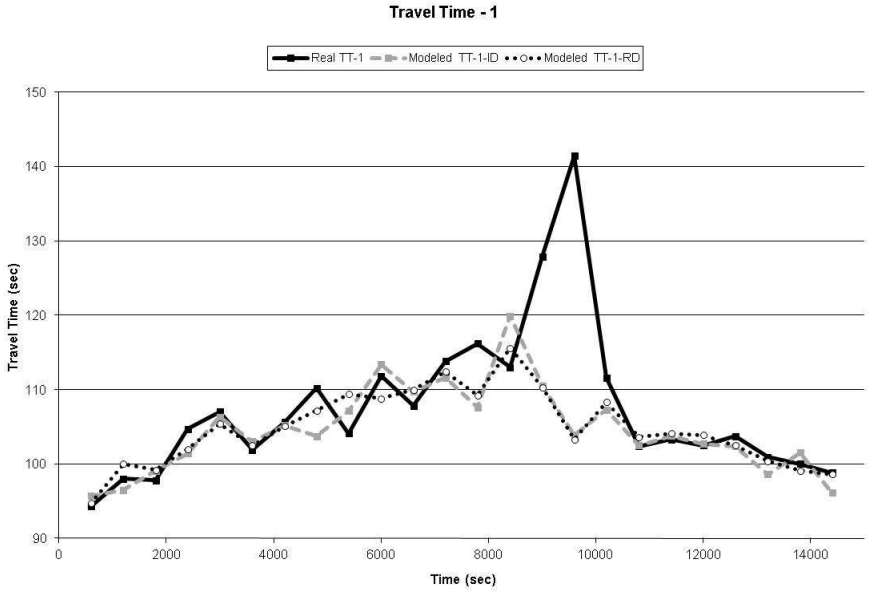

Figure 12 Average Travel Time for Travel Time Path 1 (TT-1), Replication 4 (R-4), for Real-World and Modeled-World Scenarios 1 and 2

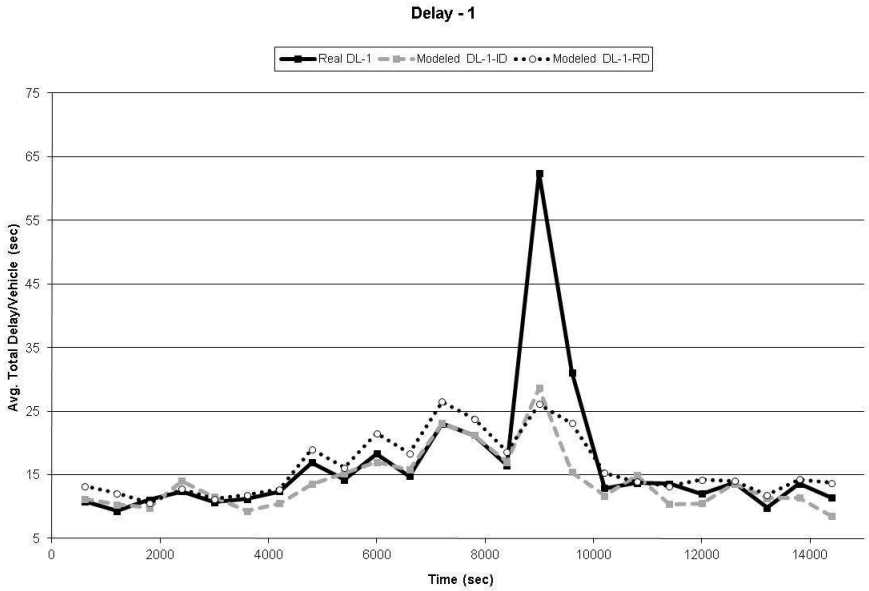

Figure 13 Average Delay for Approach 1 (DL-1), Replication 3 (R-3), for the Real-World, the Modeled-World Scenarios 1 and 2

Two potential sources of these errors are: 1) randomness in vehicle routing and 2) a smoothing of flows in the model-world. In these experiments the randomness in vehicle routing is limited to a vehicle's turning movement selection at an intersection. Of primary concern is the selection between through and left turn movements. For example, the intersection midway through the arterial has the highest left turn movement percentage at 16% in each direction. The impact of the randomness in left turn movement selection is seen through which vehicles in a particular platoon turn left. The left-turn vehicle placement in the queue can dramatically impact operations as flows approach capacity, particularly in this study network as a left-turning vehicle waiting for a gap will block all following (left, through, or right turning) vehicles. For example, if the 1st vehicle in a platoon is attempting to negotiate a left turn at the arterial's middle intersection and is unable to do so the waiting delay is incurred not only for the turning vehicle but also for those vehicles queued behind the turning vehicle. Should the last vehicle in the platoon attempt to make a left turn, any delay while waiting for a gap will be experienced only by that left-turning vehicle.

This particular source of error cannot be addressed by boundary point sensors without knowledge of every real-world vehicle's desired path through the network. The currently data-driven simulation is based on the hypothesis that such data is likely to be unavailable, at least in the near future. However, detector data from internal network detectors may provide a means to address this issue. For example, a mainline detector at the stop-bar could be used to identify when vehicles are not moving during a green phase and this information could be passed to the

modeled-world simulation. The use of internal network detector information will be one direction of future research efforts.

The second issue, a smoothing of flows in the modeled-world, has the potential to "smooth" out traffic fluctuations. Currently, irrespective of the headway with which cars enter the real-world, the modeled-world implementation algorithm has the effect of rounding the headway to the nearest second. This is particularly noteworthy for actuated traffic control, where a few tenths of a second can be the difference between a signal gaping out and a car receiving an extension of the green phase. For example, in the replicate runs where the divergence in travel time was seen at the middle intersection it was also noted that the side streets tended to receive slightly more green time. Overall this would decrease the time given to the mainline and decrease the modeled-world delays. Headway smoothing of the entering flows is a likely explanation of the extended side street green time. Future efforts will consider methods to eliminate this unintended bias.

5.1.2.2 Consistency of Results

The consistency of the performance measures across replicate runs was explored by calculating the difference between the real-world and modeled world performance measures for each replicate trial and then averaging over the 5 replicates. Table 14 and Figure 15 illustrate the concept of stability using average differences in queue lengths from Scenario 1 and travel times from Scenario 2, respectively.

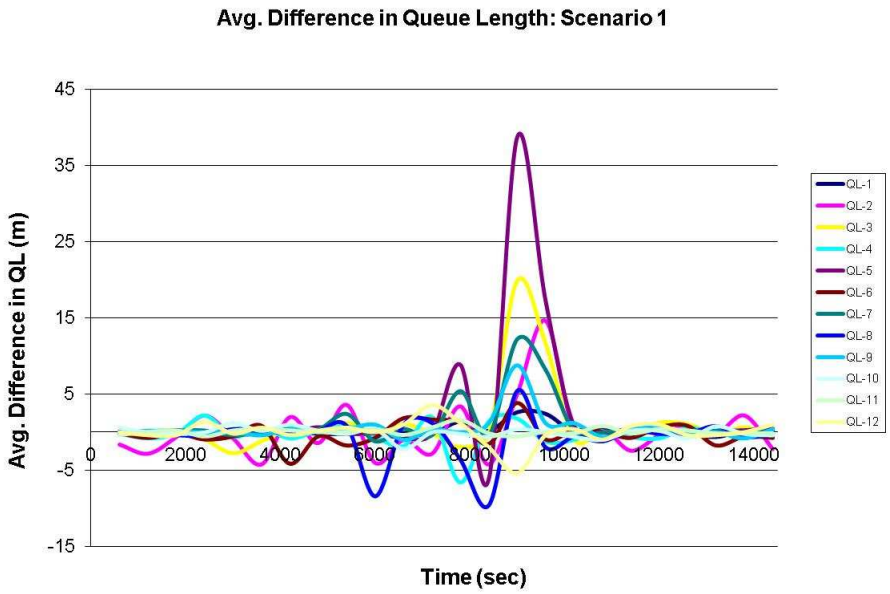

Figure 14 Average Difference in Queue Length, Scenario 1

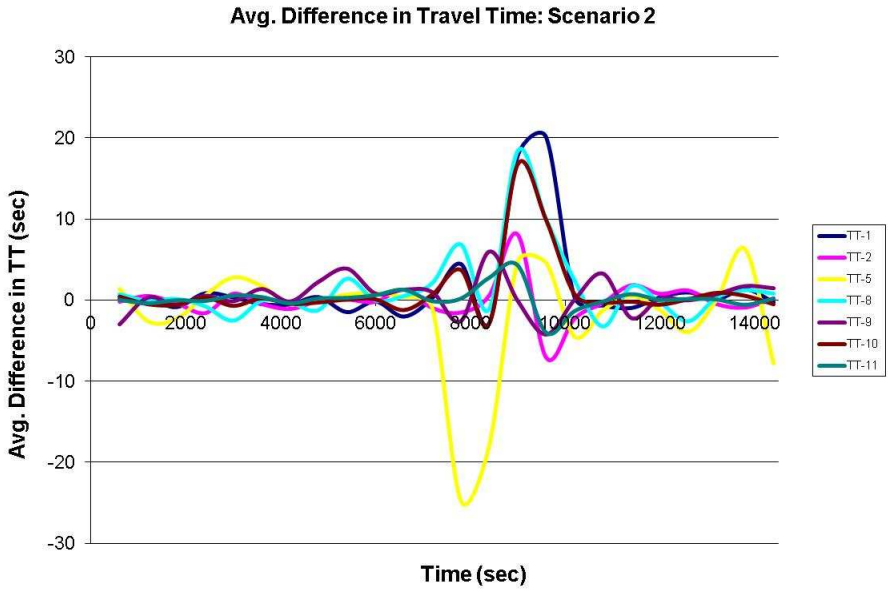

Figure 15 Average Difference in Travel Time, Scenario 2

The above figures indicate that the methodology being considered is rather stable except for a few instances were performance measures differed during the period being considered in a particular replicate trial. The reason for these differences is discussed in the previous section and will be the focus of future efforts. Overall, the modeled-world is generally successful at replicating performance measures of the real-world. In addition the method is seen to be resilient to reasonable detection errors, that is, drastically faulty data or complete detector failure is not considered in this analysis.

5.1.3 Limitation and Future Direction

In designing the proof of concept experiment, the research team limited the data passed from the real-world simulation to the modeled-world simulation to data that could be obtained in a field implementation. That is, the modeled-world was not provided with more information than may be detected on today's roadways. However, in VISSIM there are approximately 12 potentially influential parameters that are used for the purposes of calibrating traffic simulation models. Table 5 lists these parameters [39]. In the discussed experiment these 12 parameters are the same in the real-world and modeled-world simulations. This results in the modeled-world simulation having "perfectly" calibrated parameters relative to the real-world.

Table 5 Description of VISSIM Calibration Parameters

Parameters	
Emergency stopping distance	Minimum headway
Lane changing distance	Desired safety distance parameters
No. observed preceding vehicles	Maximum deceleration
Maximum look ahead distance	-1 m/s^2 per distance
Average stand still distance	Accepted deceleration
Waiting time before diffusion	Distance of standing and 50km/h

One of the key next steps is the exploration of the impact of these calibration parameters and other sources of randomness in the simulation. Section 6 presents an in depth discussion on model calibration. In additional next research steps also include identifying, quantifying, and addressing the factors that resulted in the significant variation noted during the peak demand period. Of primary interest will be two issues discussed in section 5.1 however other possible sources for the variation will also be sought.

Finally, the current model is limited to detection at boundary points of the model. Future work will seek the incorporation of detection data from internal detectors into the model calibration. This will consider standard detections (i.e. typical actuated control layouts) and the possible of new detector placement specifically designed to aid a real-time simulation.

5.1.4 Experiment #1 Summary

This experiment explored a methodology to develop a data-driven online simulation tool to deliver real-time performance measures with the aid of microscopic traffic simulation. The major objective of this experiment was to demonstrate the feasibility of such as real-time simulation. A

proof of concept experiment was designed to have one microscopic traffic simulation instance reflect the performance measures of second model, using only data that could be polled from a detector. This experiment was accomplished through the use of two VISSIM simulation instances, where one represented the real-world and the other, the modeled-world.

The results from this experiment demonstrated that the modeled-world is capable of reflecting the performances measures of the real-world with a relatively high level of accuracy. However, some notable discrepancies were seen. Despite the current discrepancies and limitations of the experimental design, the results presented support the likely feasibility of this approach.

5.2 Experiment #2: Field Test with Temporary Detectors

In experiment #1, the results of preliminary studies to determine the feasibility of the proposed framework are presented. Given the feasibility of the proposed methodology in a simulated environment, a field test was developed to explore the methodology's robustness. The goal of the initial field test was, in part, to determine whether a VISSIM simulation instance could be driven by real-time, real-world, detector data and produce performance measures that reflect those of the area being simulated. To conduct this experiment, the 5th Street / Ferst Drive corridor in the midtown Atlanta area on the Georgia Tech campus was selected as the arterial to be studied (see Figure 16). The experiment was conducted for 90-minutes, during the peak noontime period on July 16, 2009.

A VISSIM model for the test bed area was developed. Real time detector data was streamed into the VISSIM simulation model from boundary detectors (Figure 17). While not used in this experiment midblock detector data was also streamed and logged for potential use in future concept development efforts. For this experiment temporary detectors where utilized. Detector data was transmitted over Georgia Tech's wireless network to a central data processing server. A time stamped message was sent for each vehicle that crossed a detector. The time stamped data included the link number and lane number of the reporting detector and the measured vehicle speed. In addition, the corridor was outfitted with temporary cameras located at each of the six intersections that record arterial operations during the experiment. The cameras facilitate the post-hoc extraction of travel time data to be used in the evaluation of the real-time simulation performance. In addition, two GPS equipped vehicles logged their location and speed data as they traversed the study corridor during the experiment. Figure 17 shows the VISSIM representation of the test site and the locations of detectors and cameras along the 5th Street NW and Ferst Drive NW corridor. At the end of the 90-minute test period the logged data was processed and various performance measures extracted for comparison with the simulation output.

Figure 16: 5th Street NW/Ferst Drive NW Study Corridor (red line), Atlanta GA [4]

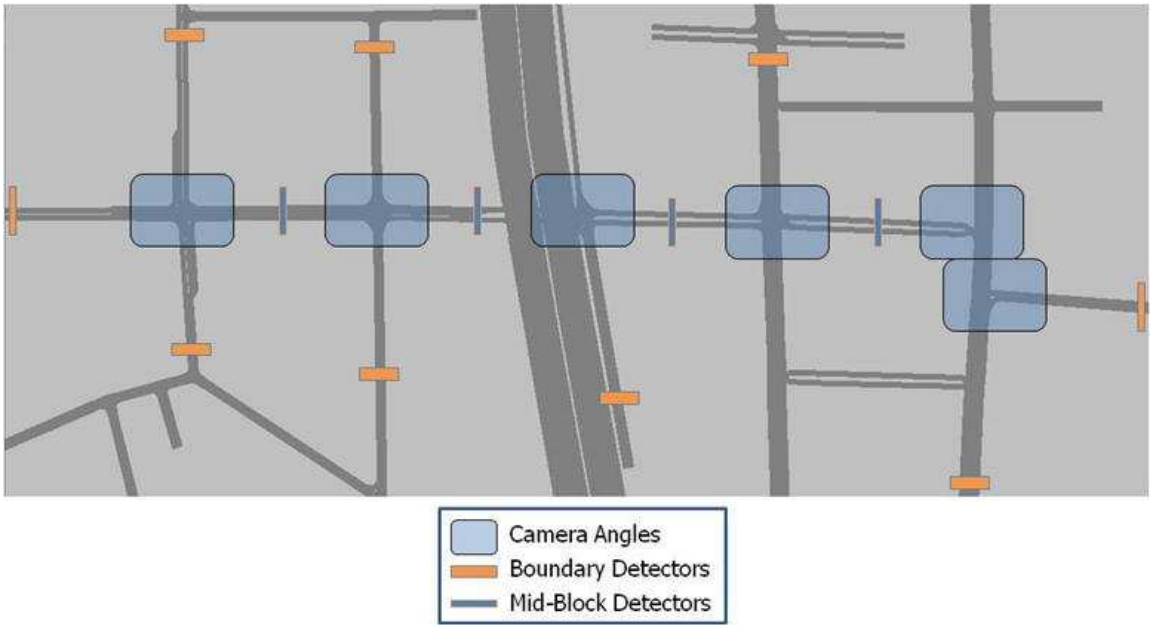

Figure 17 VISSIM Representation of the Study Corridor

5.2.1 Results and Analysis

The camera and video based field travel time data were compared with the VISSIM model to determine how well the data-driven simulation was able to reflect field travel times. Two primary sets of travel times were obtained: eastbound (EB) and westbound (WB). Scatter plots of the data are shown in Figure 18 and

Figure 19. For the eastbound data,

Figure 19, one can readily infer that the VISSIM travel times are similar to the field travel times, with exceptions at the boundaries of the graphic where the VISSIM travel times appear to be higher than the field travel times. For the westbound data sets, Figure 18, there is less similarity between the VISSIM and field travel times. From the westbound graphic the field travel times appear systematically in the lower range of travel times output by VISSIM.

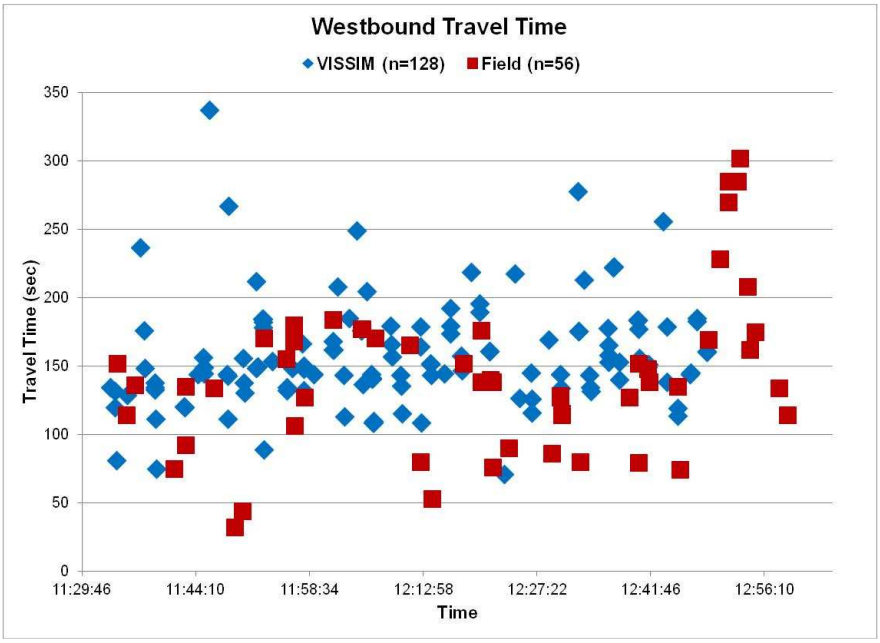

Figure 18 Westbound Travel Times - VISSIM vs. Field

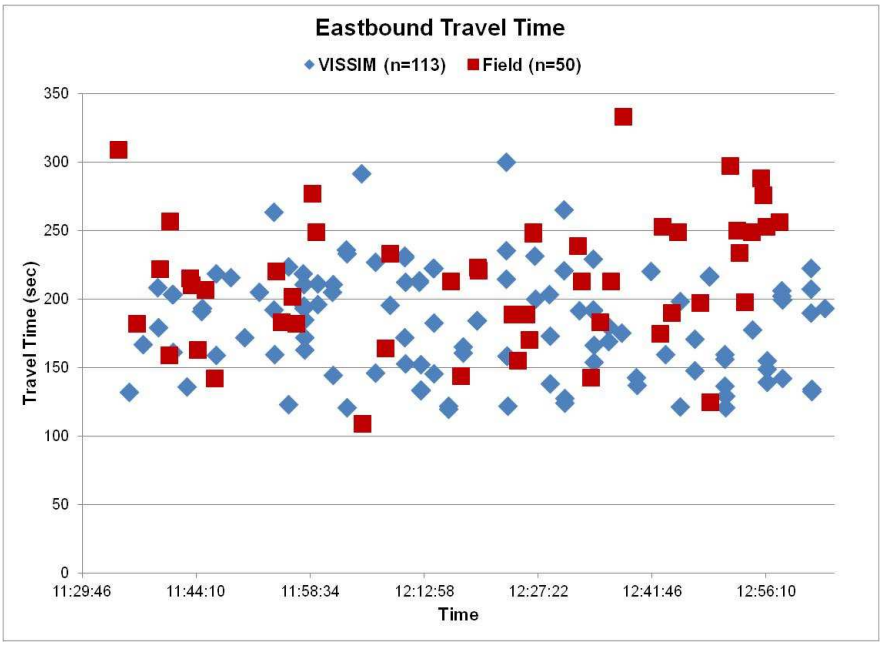

Figure 19 Eastbound Travel Times VISSIM vs. Field

The descriptive statistics were next examined (Table 6). In the eastbound dataset, the VISSIM travel times have a mean of 183.1 seconds and a standard deviation of 39.3 seconds. The field measured travel times have a mean of 218.4 seconds and a standard deviation 50.1 seconds. The higher eastbound field measured travel time does not appear to be systematic but heavily influenced by a cluster of high values near the end of the run. An analysis of the data removing the last fifteen minutes reduces the difference in average travel time between the Eastbound simulated and field results by approximately 45% percent, from a travel time of 218.4 to 202.3 seconds. Potential reasons for this cluster will be discussed later in the section. For the westbound direction, the mean and standard deviation of the VISSIM travel times are 157.5 seconds and 38.9 seconds respectively, while the field measured travel times the mean and standard deviation are 113.4 seconds and 63.0 seconds, respectively.

Table 6 Descriptive Statistics for Eastbound and Westbound Travel Times

Statistic	Eastbound Travel Time		Westbound Travel Time	
	VISSIM	Field	VISSIM	Field
Mean	183.1	218.4	157.5	113.4
Standard Deviation	39.3	50.1	38.9	63.0

Next, statistical tests were conducted to determine whether the VISSIM and the field measured travel times are statistically different. First the distributions were tested for normality as this will influence the statistical test chosen. Lilliefors normality tests were conducted on all the travel time data sets. The results of the normality tests are presented in Table 7. From these results one is unable the reject the null hypothesis that the eastbound VISSIM and Field travel times are normally distributed. However for westbound VISSIM and Field travel times the nor-

mality test results provides sufficient evidence for one to reject the assumption that these datasets are normally distributed. These conclusions were further corroborated after examining a series of density plots, Figure 20 and Figure 21, and Q-Q plots, Figure 22 and Figure 23.

Table 7 Statistical Test Results

Statistical Test	p-Value	Interpretations
Normality Test		
EB VISSIM	0.3255	Unable to reject normality assumption
WB VISSIM	0.0001	Reject normality assumption
EB Field	0.6760	Unable to reject normality assumption
WB Field	0.0088	Reject normality assumption
2 Sample t-Test		
EB VISSIM vs. EB Field	0.0001	Reject equal mean assumption
WB VISSIM vs. WB Field	0.1125	Unable to equal mean assumption
Wilcoxon Sum Rank Test		
EB VISSIM vs. EB Field	0.0001	Reject equal median assumption
WB VISSIM vs. WB Field	0.0408	Reject equal median assumption
Chi-Square Test		
EB VISSIM & EB Field	0.3654	Unable to reject same distribution assumption
WB VISSIM & WB Field	0.1560	Unable to reject same distribution assumption
Kolmogorov-Smirnov Test		
EB VISSIM & EB Field	0.0016	Reject same distribution assumption
WB VISSIM & WB Field	0.0235	Reject same distribution assumption

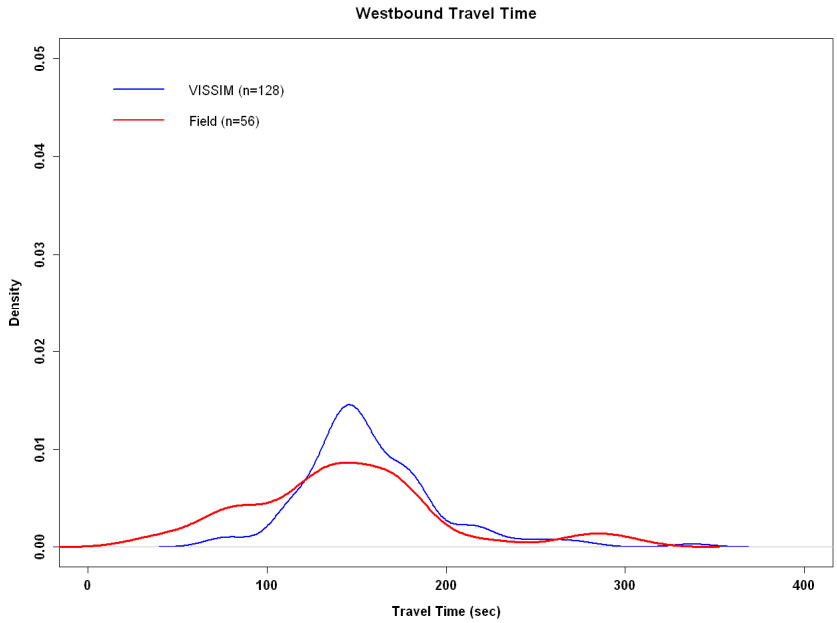

Figure 20 Density Plot of VISSIM vs. Field Westbound Travel Times

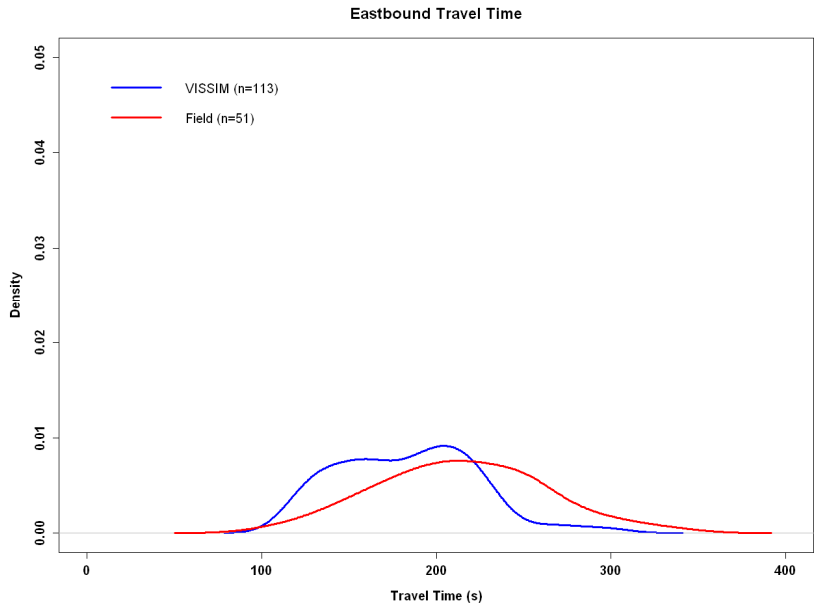

Figure 21 Density Plot of VISSIM vs. Field Eastbound Travel Times

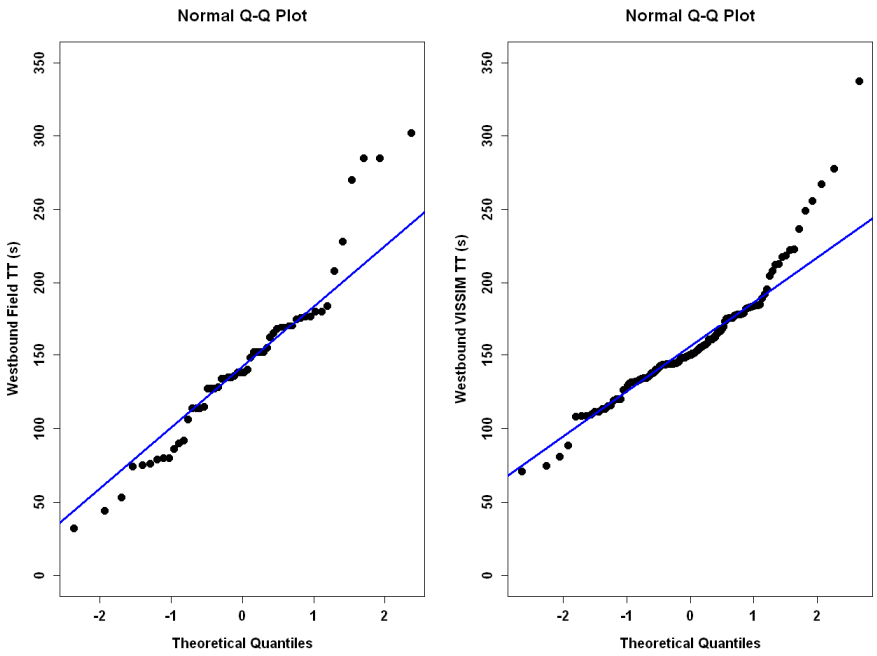

Figure 22 Q-Q Plots of Field and VISSIM Westbound Travel Times

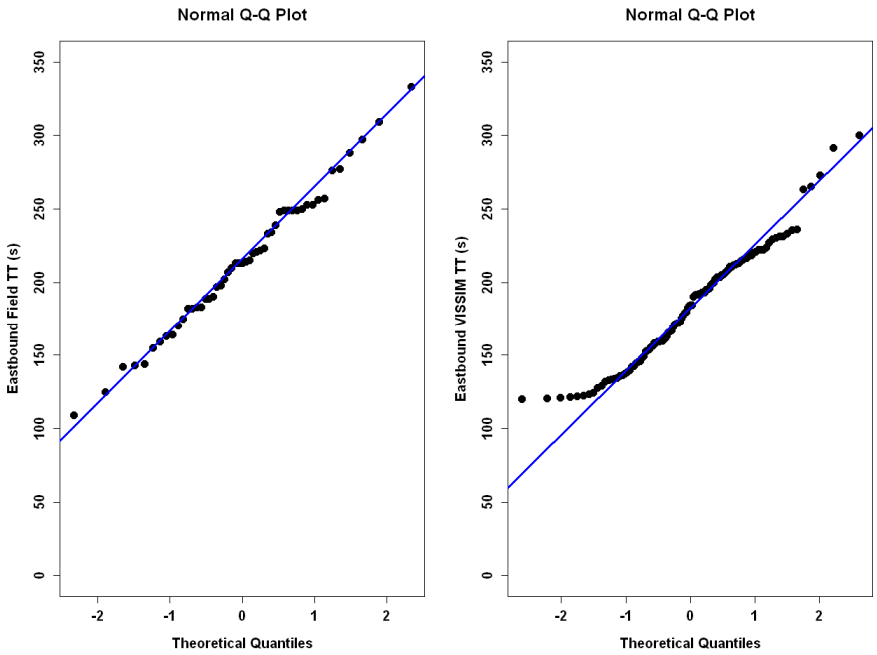

Figure 23 Q-Q Plots of Field and VISSIM Eastbound Travel Times

A series of other statistical tests were conducted to further explore the differences between Field and VISSIM travel time estimates. These tests were also used to quantify some of the similarities and dissimilarities that were observed, especially from the density plots. The test results are also included in Table 7.

From the above results one can conclude that there is a statistical difference between the VISSIM and the actual (mean / median) travel times, in both the eastbound and the westbound directions. However, it is again noted that if the last fifteen minutes of data were not included in the eastbound analysis the result is reversed, with the test failing to reject equal means. This further indicates an event specific issue rather that a systemic problem eastbound.

Several areas are perceived as potential sources for the discrepancies between the estimated and actual performance measures. These areas are generally related to model calibration and facility representation. For model calibration the parameters that reflect driver behavior were left unchanged in VISSIM, potentially indicating that the default driver behavior in the VISSIM model may not be representative of the behavior along the study corridor. Accurately capturing driver behavior may improve VISSIM estimates of travel times. In addition, considerable differences in simulated vs. field volumes were observed on some links. In part this is a result of simulated turning movement distributions at the various intersections throughout the corridor differing significantly from the field movements. Historical turning movement percentages where utilized as real-time turning counts were not available. It is also noted that volume discrepancies could result from detector errors. The Tech Trolley (an on-campus shuttle) was also not represented. By not capturing the Trolley behavior, VISSIM is not able to simulate the increase in travel time for other vehicles that the Trolley may inhibit as it traverses the corridor.

There are two aspects of the study corridor that were not represented in the VISSIM model of the area. The first was the roadway gradient, which is positive from west to east, and the second, the pedestrian and pedestrian facilities along the corridor. Thus, any influence from these factors is not reflected in the VISSIM model. Pedestrians in particular were noted as a potential significant factor. The probe vehicle drivers noted instances where pedestrian movements significantly interfered with traffic flow. For example, at the intersection of 5th Street and Spring Street left turning vehicles yielding to crossing pedestrians would prevent through vehicles behind the left turning vehicle from traversing the intersection. As no pedestrians were modeled in

VISSIM this behavior was not reflected. For the test bed the pedestrian interference was particularly notable as given the nature of a college campus there tends to be periods in which significant, short duration, increases in pedestrian activity occur. The influence of pedestrian activity on simulation models is investigated and discussed in detail in Section 8.

5.2.2 Experiment #2 Summary

In experiment #2 the researchers were able to demonstrate the fundamentals of the proposed methodology in a field test using readily available technology. The microscopic traffic simulation model was able to be driven in real-time by real-world data streams. The comparative analysis demonstrated some success particularly when considering the eastbound travel times. It is anticipated that once sources of identified discrepancies are addressed the VISSIM model will be able to produce better estimates of travel times.

5.3 Experiment #3: Field Test with Temporary and Permanent Detectors

Test #3 is a full scale test of the methodology. The field test was conducted on July 8, 2010, between 1:00PM and 3:00PM. The study area is the same as the previous test (Figure 16:). Both permanent (Video Detection System (VDS)) and temporary detectors, capable of streaming individual vehicle records, were employed during this test. In addition to the temporary and permanent detectors six camcorders were used to collect additional traffic information for post processing. Four camcorders were used to detect boundary conditions (i.e. when vehicles enter and exit the network) while two were used to collect signal phase information at the intersections of 5th Street and Spring Street, and 5th Street and W. Peachtree Street. The location of each detector, and their respective detection zones, including the camcorders and their view angles are shown in Figure 24. In addition, probe vehicle travel routes were added to allow for a more robust evaluation of the system. In this field test four routes are monitored, each of which are traversed by two probe vehicles, see Figure 25.

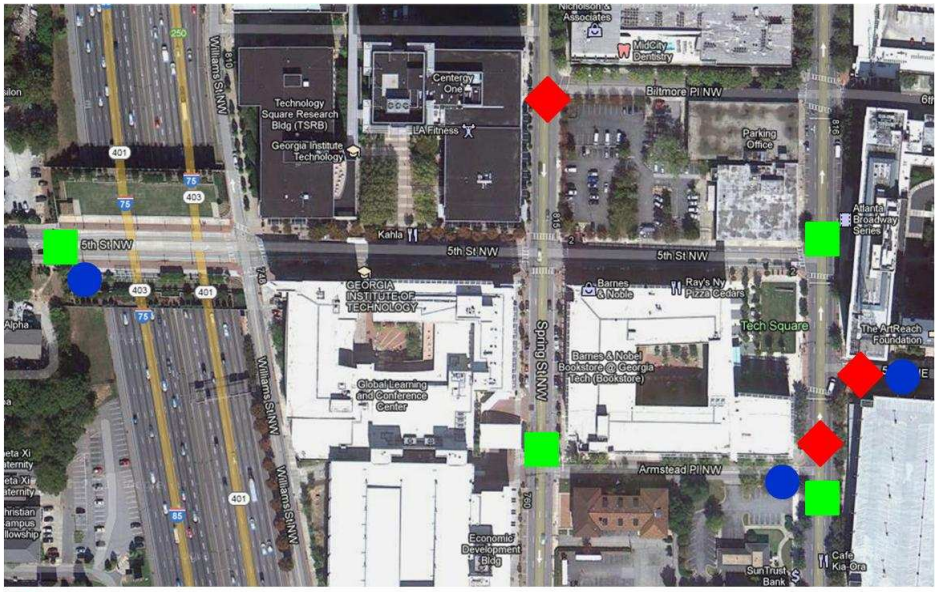

Figure 24 Detector Locations Throughout the Study Area

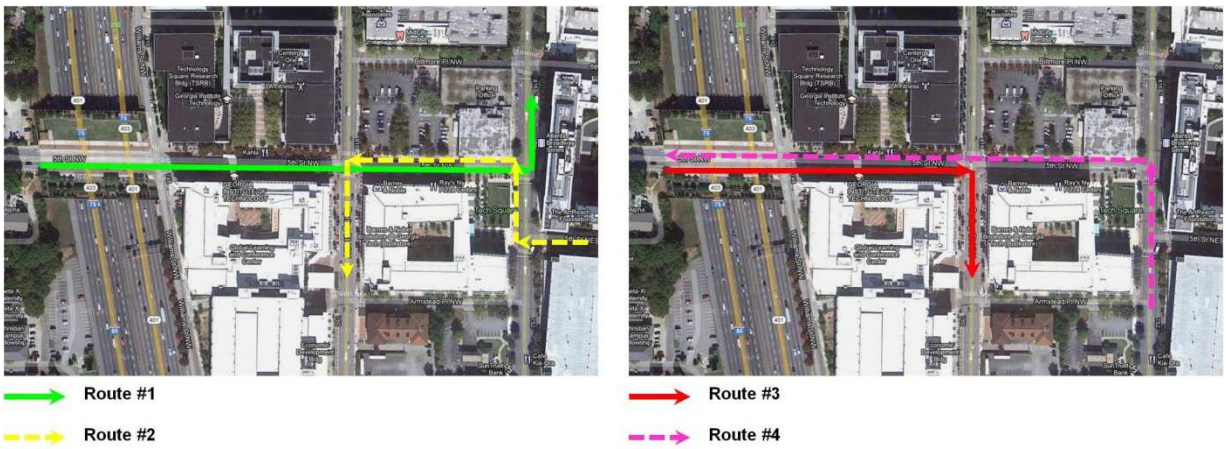

Figure 25 Probe Vehicle Routes Through Study Area

Each permanent VDS camera is connected to the Georgia Tech fiber network and is capable of detecting and transmitting individual vehicle records in real-time. The temporary detectors consisted of research assistants with laptop computers using a script to record and transmit individual vehicle data back to the server in the laboratory. These detectors were primarily tasked with detecting the four probe vehicles. By identifying the probe vehicles in the field in real time they could be identified as they entered the simulation, allowing for a more robust paired travel time comparison in the later analysis. The temporary detector on the 5th Street bridge was also tasked with detecting non-probe vehicles as a permanent VDS camera was not available for this site.

Each packet of transmitted detector data includes six fields. They are detector number (each detector location having a unique number), lane number, speed (in miles per hour), detector time, and epoch time. Table 8 provides a sample of streamed data. Clock time is also presented in the sample below but it is determined from the epoch and not transmitted by the detectors.

Table 8 Sample of Streamed Detector Data

Detector #	Lane #	Speed (mph)	Timestamp	Epoch Time	Clock Time
4	2	18	13:00:45	1278608487.375490	13:01:27
11	1	22	11:04:17	1278608487.578350	13:01:28
11	3	8	11:04:17	1278608487.677290	13:01:28
11	2	6	11:04:17	1278608487.779180	13:01:28
10	1	17	13:01:25	1278608487.935580	13:01:29
5	1	26	13:00:20	1278608487.200850	13:01:29
1	1	6	12:57:53	1278608487.419210	13:01:29
11	3	9	11:04:19	1278608487.778030	13:01:30

During a preliminary test, videos feeds were compared to VISSIM animation to verify that as a vehicle entered a detection zone the detector data was successfully transmitted and VISSIM generated a vehicle in the appropriate position. Figure 26 is an example image from the verification process.

Figure 26 Permanent Detector Generating Vehicle in VISSIM in Real-Time

Data was collected for approximately 120 minutes. At the end of this data collection, six different data streams were available:

- GPS data from the 4 probe vehicles
- Signal phase information from the two signalized intersections
- Vehicle presence from permanent video detectors
- Probe vehicle presence from temporary detectors
- Individual vehicle travel times over the pre-defined routes
- VISSIM trajectory data for all vehicles generated from the arriving data stream

5.3.1 Results and Analysis

Where the previous tests focused on aggregate travel times this experiment sought to evaluate the real time simulations ability to estimate an individual vehicle's travel time through paired travel time comparisons. Probe vehicle travel times were extracted from the video footage and from the simulation's equivalent vehicle. These two sets of travel times were then compared.

The following discussion focuses on travel times for probe vehicles traveling along routes #2 and #4 as similar inferences can be made from the analysis of the data from routes #1 and #3. Route #2 is approximately 1300 feet in length and traverses three signalized intersections (Figure 25). Route #4 is approximately 1600 feet in length and includes three signalized intersections.

Twenty four pairings of travel times were collected from Route #2 and 36 from Route #4. Each pairing consists of a field probe vehicle travel time and the respective simulation estimate. The average field travel time for Route #2 is approximately 94 seconds and the simulation estimate is approximately 85 seconds. The Route #4 field travel time estimate is approximately 136 seconds and the simulation estimate is approximately 121 seconds. These and other descriptive statistics can be seen in Table 9. Figure 27 and Figure 28 present scatter plots of individual travel time estimates. Figure 29 and Figure 30 are also included to present travel time data from Route #1 and Route #3. Figure 31 presents four pairs of density plots to further compare each pair of travel time estimates for each route.

Table 9 Descriptive Statistics of Travel Times for Route #2 and #4

	Mean Travel Time		Standard Deviation Travel Time	
Route #	VISSIM	Field	VISSIM	Field
1	138.6	141.5	20.9	20.6
2	84.8	93.5	27.7	27.1
3	42.8	45.65	23.0	31.8
4	121.3	135.6	30.6	27.2

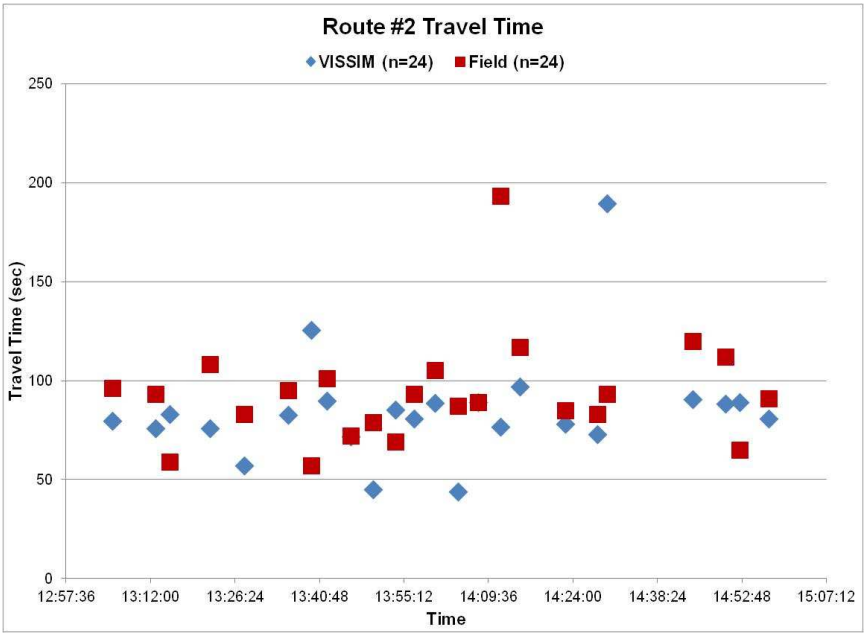

Figure 27 Route #2 Travel Times - VISSIM vs. Field

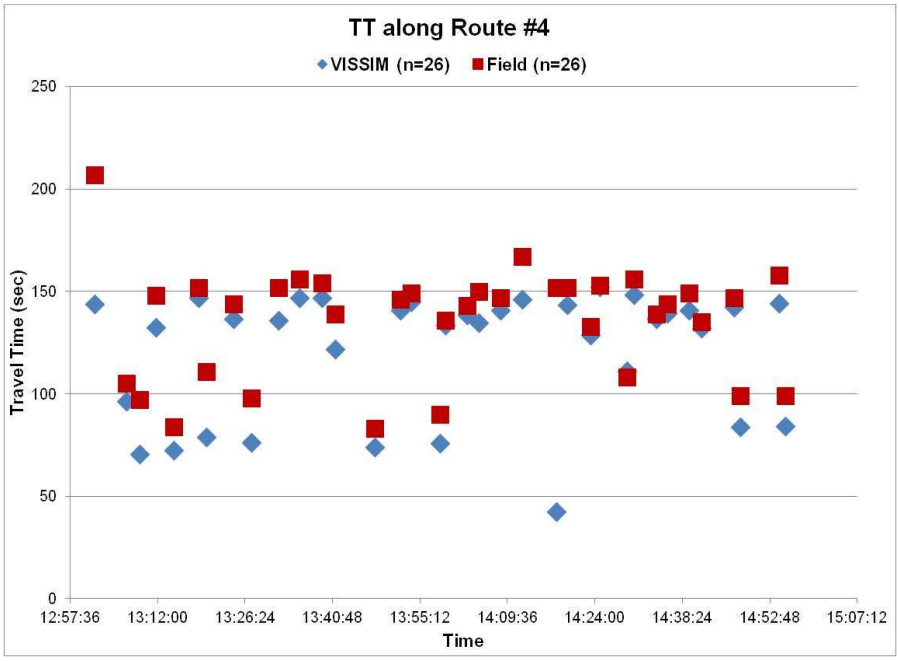

Figure 28 Route #4 Travel Time - VISSIM vs. Field

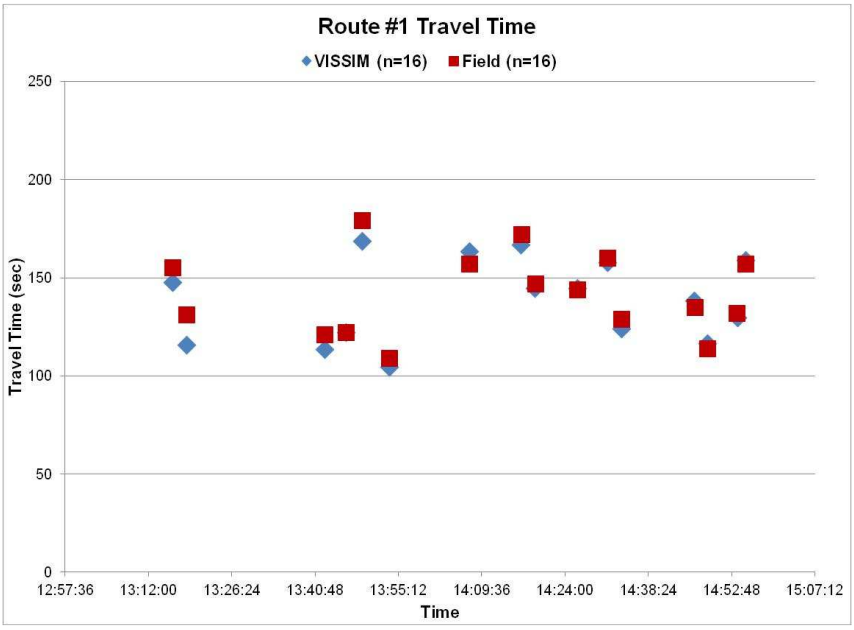

Figure 29 Route #1 Travel Time – VISSIM vs. Field

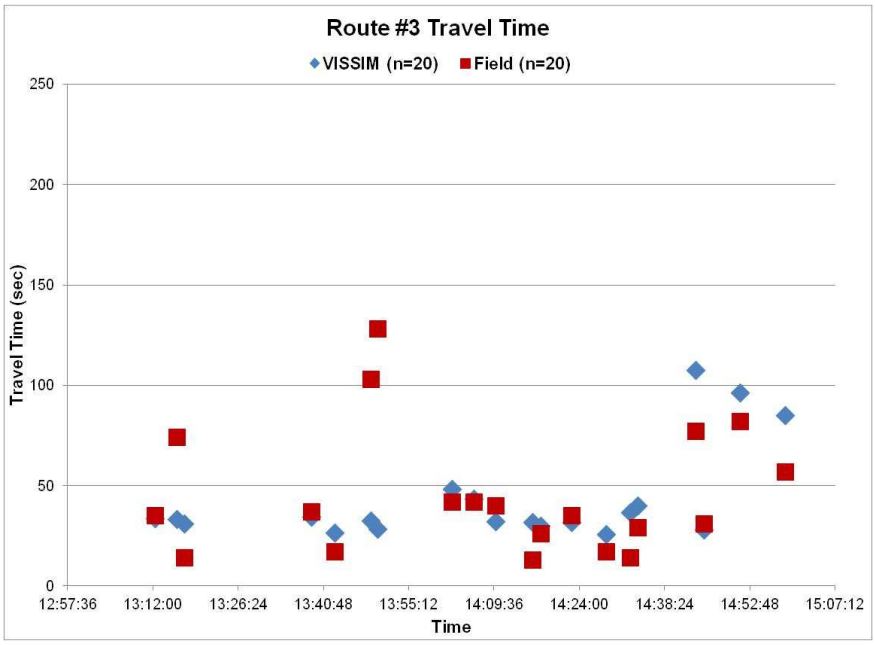

Figure 30 Route #3 Travel Time – VISSIM vs. Field

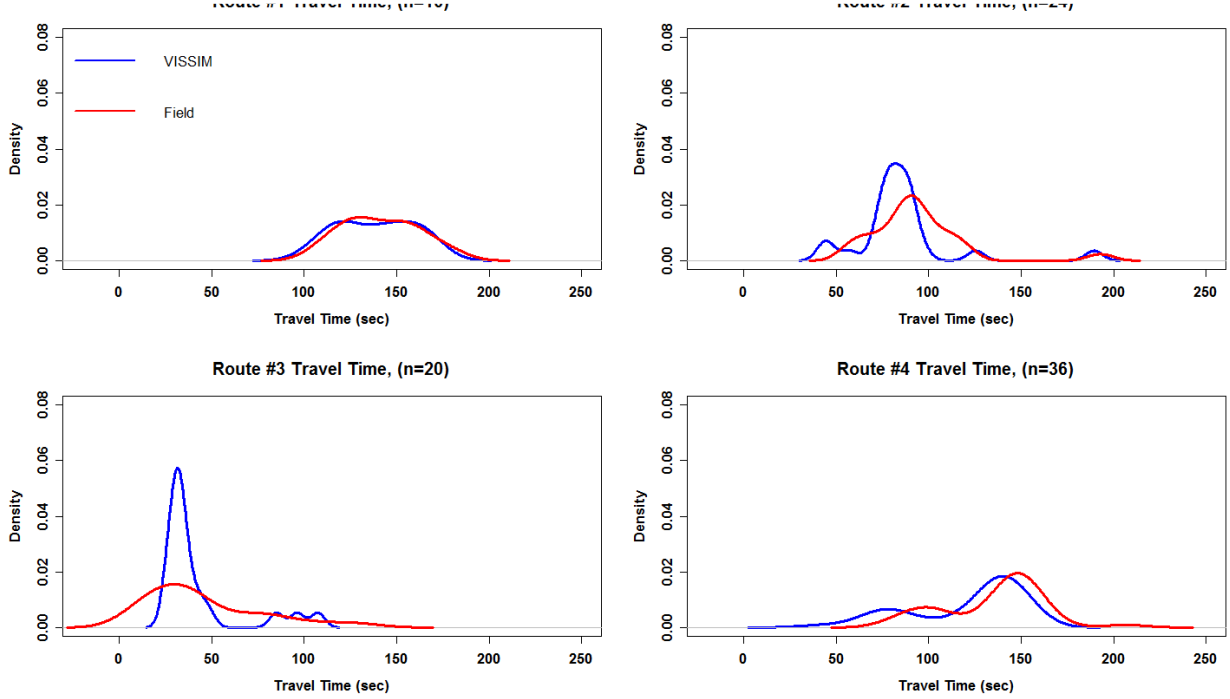

Figure 31 Density Plots of VISSIM and Field Travel Times for Routes #1 - #4

Similar to the previous analysis a series of statistical tests was conducted. The conducted tests include a paired t-test and a sum rank test, to compare means/medians, and chi-square test and a Kolmogorov-Smirnov test, to compare distributions. The results of these tests are presented in Table 10.

Table 10 Test Statistics

Statistical Test	p-Value	Interpretations
Normality Test		
Rt. #2 VISSIM	0.00001	Reject normality assumption
Rt. #4 VISSIM	0.00000	Reject normality assumption
Rt. #2 Real-World (RW)	0.06387	Unable to reject normality assumption
Rt. #4 Real-World (RW)	0.00198	Reject normality assumption
2 Sample t-Test (Paired)		
Rt. #2 VISSIM vs. Rt. #2 RW	0.28670	Unable to reject equal mean assumption
Rt. #4 VISSIM vs. Rt. #4 RW	0.00013	Reject equal mean assumption
Wilcoxon Sum Rank Test		
Rt. #2 VISSIM vs. Rt. #2 RW	0.05382	Unable to reject equal median assumption
Rt. #4 VISSIM vs. Rt. #4 RW	0.00549	Reject equal median assumption
Chi-Square Test		
Rt. #2 VISSIM & Rt. #2 RW	0.28930	Unable to reject same distribution assumption
Rt. #4 VISSIM & Rt. #4 RW	0.15740	Unable to reject same distribution assumption
Kolmogorov-Smirnov Test		
Rt. #2 VISSIM & Rt. #2 RW	0.03101	Reject same distribution assumption
Rt. #4 VISSIM & Rt. #4 RW	0.00864	Reject same distribution assumption

Based on the scatter plot data and the statistical tests it may be concluded that the simulation reasonably reflects the real world however differences do exist. It is noted immediately that a significant improvement from the previous test was the synchronization the signal in the simulation with the field, likely accounting for much of the improved performance.

However, several issues may be readily noted when reviewing the analysis. Firstly, the simulated estimates of the probe vehicles' travel time tend to be lower than the field measured travel time. One potential reason for this result is vehicle acceleration rate in the field versus the simulation. During the test run the research team noted that the vehicles in the simulation appeared to accelerate to their desired speeds more aggressively than vehicles in the field. Acceleration rates can be a significant factor, particularly in a network dominated by signalized inter-

sections. These rates can determine whether a vehicle arrives on red or green at a downstream intersection, which directly affects travel time estimates as well as other performance measures. For instance, on several occasions it was observed that a simulated vehicle successfully traversed a downstream signal with the corresponding vehicle in the field arriving a few seconds later stopped at a red light. While differences in acceleration rates do not often lead to such dramatic differences, they also can lead to more subtle changes. This again highlights the need for underlying calibration of the simulation model.

There are a several other subtleties that may be contributing to the discrepancies in travel time estimates. As mentioned previously, three of the more significant contributing factors are signal synchronization, vehicular volume traversing the network, and turning movement distributions. In the preceding experiment the research team was able to develop a methodology to synchronize the signals in the simulated environment and the field. However, real time methodologies are not yet available to address the other two issues. The next reported test attempts to remove these issues and explore the capabilities of a real time simulation given (near) perfect data.

5.4 Experiment #4: NGSIM's Peachtree Corridor Study

5.4.1 Motivation and Background

Experiment #4 may be described as a pseudo field test. The experiment utilizes a near ideal data set (tenth of a second resolution of vehicle positions on the corridor, route data for every vehicle, individual vehicle turning movement data, and signal status at a tenth of a second resolution) to

determine the performance of the real time simulation under ideal conditions. That is, under ideal data collection conditions is a real time simulation capable of providing a reasonable reflection of the real world. This experiment uses previously collected field data as input to the real time simulation, streamed in wall clock time. This data was collected as part of the FHWA Next Generation Simulation (NGSIM) program [50]. The NGSIM program created high fidelity data sets intended for use in the study of traffic behavior and the development of the next generation of traffic simulation tools and algorithms.

The NGSIM data set utilized is for Peachtree Street, Atlanta GA. The studied segment extended just south of the intersection of Peachtree and 10th Street and north of the intersection of Peachtree and 14th Street, Figure 32. [50]

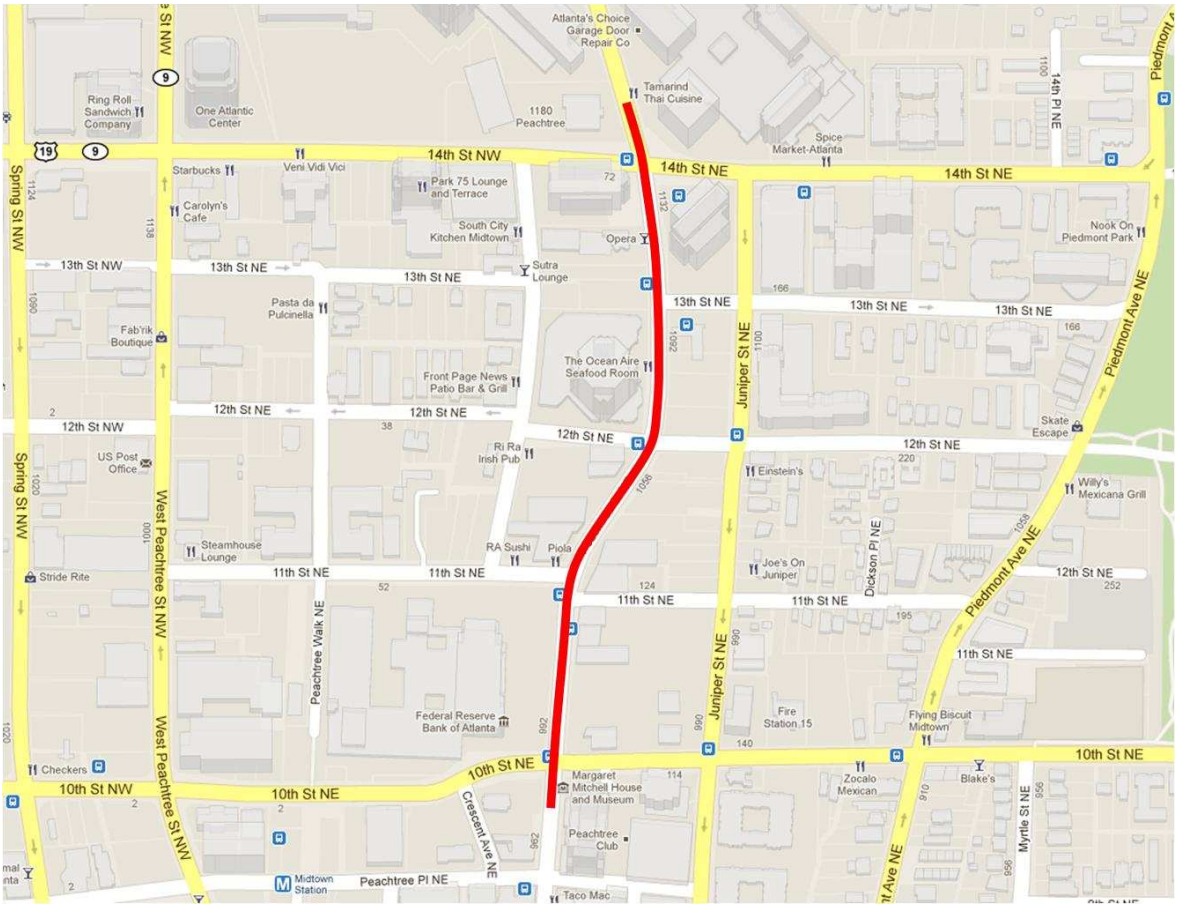

Figure 32 Peachtree Study Corridor [4]

The NGSIM Peachtree dataset comprises of trajectory data (with a resolution of a tenth of a second) for all vehicles traversing the corridor during the study period. Trajectory data was gathered on November 8, 2006, between 12:45PM and 1:00PM and 4:00PM and 4:15PM. In addition signal phase information at each intersection, origin-destination data (OD) for each vehicle, turning movement distribution at each intersection, and a series of other traffic related informa-

tion were also collected. Video of the entire corridor is also available during data collection periods.

5.4.2 The Study

For the experiment, a detailed VISSIM model of the study area (Figure 33) was created. Roadway geometry was based on existing conditions at the time of the experiment and additional information such as vehicle volume, turning movement distribution, routing decisions and signal timing plans were added based on the NGSIM data set. Several verification iterations were completed to ensure that the model correctly represented the area being studied, as well as the traffic conditions during the study period. During this verification process issues related to the number of vehicles traversing the corridor and to signal timing plans were identified.

Figure 33 VISSIM model of Peachtree Study Corridor [4]

For instance, the number of vehicles, and subsequent turning movement distributions, were initially based on the summary reports produced by the NGSIM program. However, the team noticed that there were discrepancies between these summaries and counts extracted by hand from the videos. To address this issue, a software tool was developed to help record vehi-

cular volume and turning movement counts from the videos. Errors identified in the NGSIM data were corrected, as best as possible, in the utilized VISSIM data set.

The NGSIM data also provided a direct observation of the signal indications. The observed signal indication did not appear to coincide with the provided signal timing controller data, likely indicating that the provided controller data was out of date. Thus, the signal indication data and engineering judgment was utilized to develop likely signal timing plans that would match the indication observations. The final simulation model is based on these plans, which includes offset observations. It is noted that during the observation periods (approximately 15 minutes) the offsets did appear to drift by a few seconds in the NGSIM data. To address this issue an average estimated offset is utilized.

5.4.2.1 Simulating Data Stream

To simulate streaming detector data the team used trajectory and OD data to create a VISSIM trip-chain file which approximates the process of streaming detector data into the real-time simulation. A trip chain file is able to approximate a detector stream as each file's record consists of a time-stamp, indicating when a vehicle entered the network (i.e. crossed a boundary link detector), and a zone number indicating a vehicle's origin (i.e. the boundary detector crossed) and destination. This string of information is similar to that from a detector, except for a vehicle's destination. However, destination zones are often times approximated through historical turning movement.

With this method of approximating streaming detector data, a number of issues were encounter during the creation of the trip-chain file. The most important piece of information that is needed to create a trip-chain file is correct OD pairs. However after examination of the OD information given by the NGSIM program it was noticed that a number of OD pairs were potentially incorrect. For example, there were OD pairs that suggested an unusually large number of vehicles performed a u-turn maneuver. To verify these maneuvers the OD distribution tables from NGSIM's Summary Reports and the corresponding videos were examined [51], [52].

Simultaneous examination of the distribution tables and videos revealed errors associated with assigned OD pairs. For instances, the u-turns were often left turns from the mainline to approaches leaving the network. In addition, there were assigned OD pairs that were not traversed by any vehicles during the study period. These errors largely occurred when the tracking software lost its handle on a vehicle that it had identified and began a new track for the same vehicle. To correct these issues engineering judgment was use to identify potentially erroneous OD pairs and necessary corrections were made by observing the vehicle on the video.

5.4.3 Preliminary Results and Analysis

Using the corrected NGSIM data final trip-chain files where created and used for the VISSIM data input. Ten replicate runs were conducted for the comparison between field and simulated performance measures. Similar to previous tests, travel time is the performance measure monitored and compared. Table 11 presents a summary of the simulated travel times from each of the

10 replicates and a summary of the field travel times. Note, data corresponding to the 12:45PM – 1:00PM period is referred to as the Noon period and 4:00PM – 4:15PM is referred to as Evening.

Table 11 NGSIM versus VISSIM (VSM) Travel Time Results

		Noon - North		Noon - South		Evening - North		Evening - South	
		Avg (s)	Std Dev	Avg (s)	Std Dev	Avg (s)	Std Dev	Avg (s)	Std Dev
VSM Run #	1	120.0	31.7	102.0	20.5	108.1	28.8	100.3	29.0
	2	120.7	33.9	100.9	21.7	113.3	32.4	99.3	29.8
	3	117.4	34.5	98.4	22.9	111.5	30.4	94.6	27.6
	4	118.1	32.2	98.6	25.1	118.8	29.8	100.2	28.2
	5	116.0	31.5	96.6	22.6	116.7	34.0	103.1	29.5
	6	112.5	31.1	98.8	23.4	112.5	32.1	104.8	30.1
	7	113.7	32.2	96.4	24.6	114.2	32.2	102.4	29.8
	8	119.0	33.1	99.3	22.9	113.6	36.0	99.8	28.9
	9	116.5	31.8	100.0	20.4	108.7	33.6	104.2	31.5
	10	113.8	31.2	95.1	25.8	113.1	32.7	103.1	28.8
VSM Avg.		**116.8**	**32.3**	**98.6**	**23.0**	**113.1**	**32.2**	**101.2**	**29.3**
NGSIM		**131.5**	**36.7**	**106.6**	**17.1**	**140.4**	**35.4**	**133.9**	**29.6**
% Error		**11.2**	**11.8**	**7.5**	**34.1**	**19.5**	**9.0**	**24.4**	**0.9**

In the following discussion the referenced VISSIM results are the average of the 10 replicate runs. It is noted that there are some discrepancies between the simulated and field travel time estimates. A key difference is that VISSIM tends to under estimate field travel times. The smallest difference between VISSIM and field travel time is approximately eight seconds, occurring for the Noon-South time period. While the largest difference, 32.7 seconds, occurred for the Evening-South period. The simulation does a slightly better job estimating travel times for the noon period versus the evening. When comparing the standard deviations in Table 11, the values

produced by VISSIM are similar to those from the field. This is observation is encouraging as it indicates that VISSIM's approximation of the variation travel time estimates is rather similar to that of the field. With dissimilar means and "similar" standard deviations the research team anticipates that the observed discrepancies may be addressed through a more rigorous calibration effort. Density plots were examined to further corroborate this hypothesis, see Figure 34.

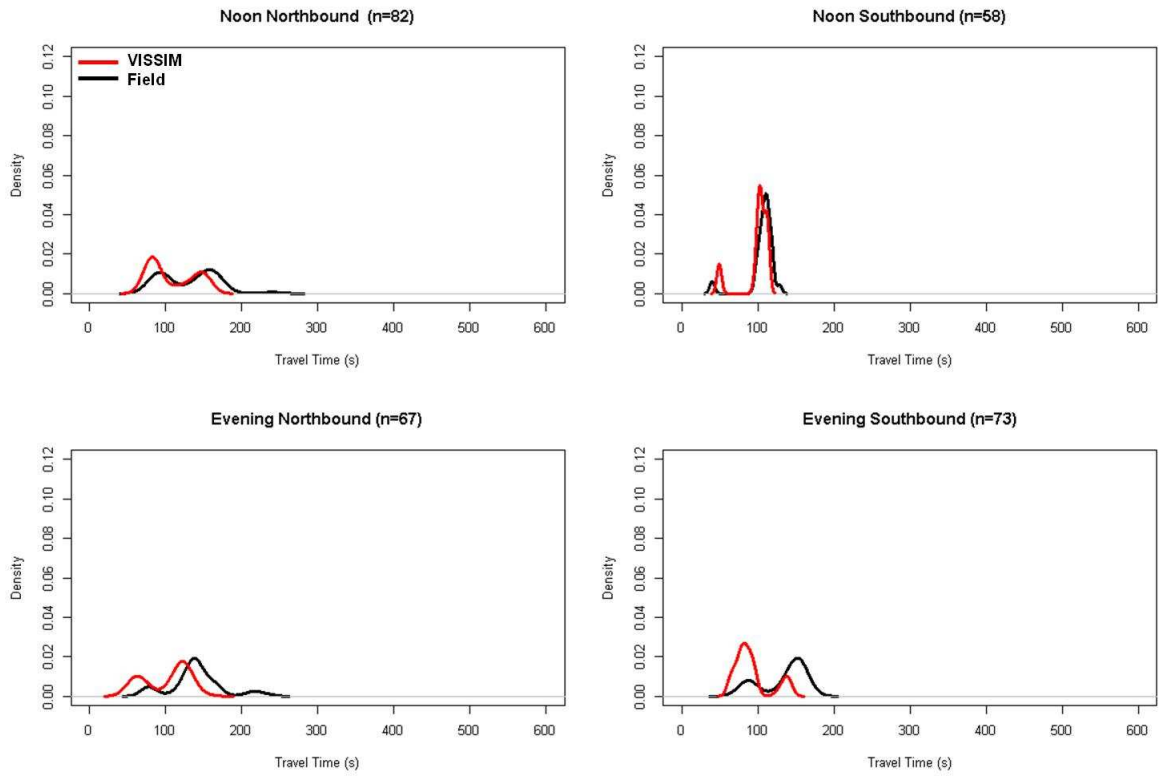

Figure 34 Density Plots of Field vs. VISSIM (single run) Travel Times

The density plots of the simulated travel times generally capture the bi-modal or tri-modal form of the field travel times. The differences between the plots tend to be a shifting of the centroid of the modes or proportionality between the different modes. However, in all cases

the general form of the distribution is reflected, a very encouraging finding, likely indicating many of the differences can be addressed in calibration.

Finally, in addition to the travel time distribution plots the Time-Space-Diagrams for the field and simulated data were generated. Distinct discrepancies in driver behavior were observed as illustrated in Figure 35 and Figure 36.

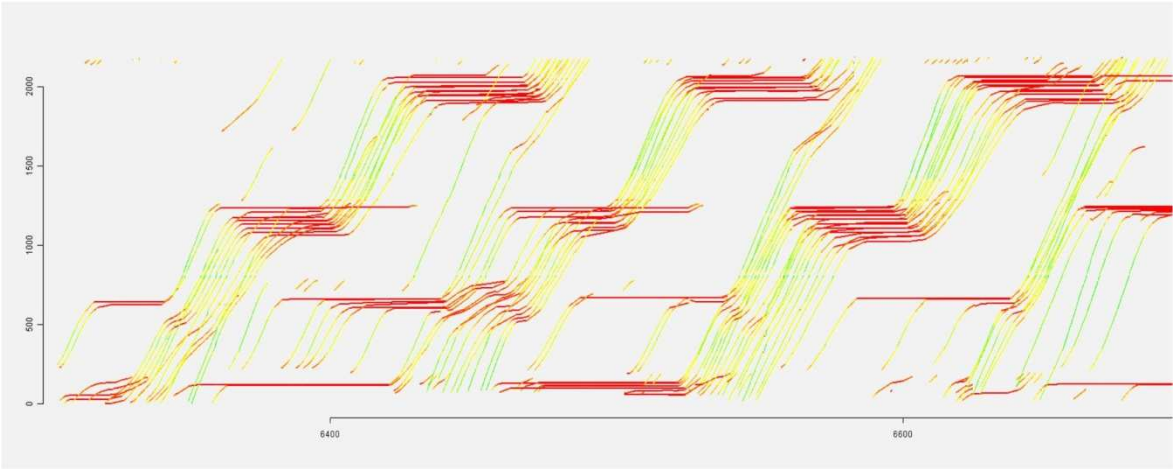

Figure 35 Northbound Real-World Time-Space Diagram

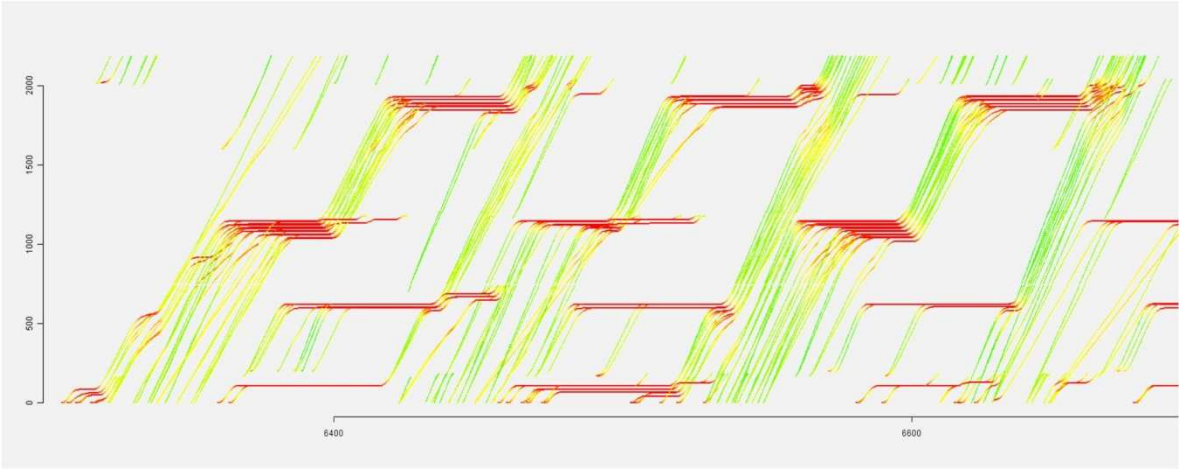

Figure 36 Northbound VISSIM Time-Space Diagram

In the above figures each line represents the trajectory of a vehicle as it traverses the length of the study corridor with respect to time. The colors along each trajectory represent current vehicle speed relative to the maximum speed along the corridor. Red represents speeds of approximately zero mph, green represents speeds of approximately 35 miles-per-hour, and shades of each color represent speeds between 0 and 35 miles-per-hour. In comparing field and simulated trajectories it is apparent the simulated traffic is less variable (i.e. the traffic flow is "smoother"), with less interaction between vehicles. One of the more recognizable differences is that simulated vehicles tend to achieve their desired speed more quickly and maintain that speed for longer periods. A likely reason for this difference is that simulated drivers are being modeled with more aggressive tendencies than their field counterparts and less variability in aggressiveness across drivers. As a result of this more aggressive driving by simulated vehicles they will tend to traverse the corridor in less time versus vehicles in the field, and may clear an intersection during the green or amber phase while their field counterpart may not make through that intersection at that point in time. Such scenarios are supported by the travel time measurements that are presented in Table 11 as VISSIM tends to underestimate real-world travel times.

Given the above results for the NGSIM pseudo field experiment and the insights afforded by the time space diagrams the research team anticipates that more accurate estimates of field travel times may be achieved through an advanced calibration procedure. This procedure will involve a Monte Carlo parameter selection method which determines the most effective parameters to calibrate a VISSIM simulation model. Chapter 6 will present this proposed calibration procedure in detail.

6 ADVANCED MODEL CALIBRATION PROCEDURE

As seen calibration is a key step in developing an accurate simulation model. The calibration process involves the selection of values for adjustable modeling parameters that allow a particular model to most accurately reflect the specific network conditions under consideration. A number of procedures have been proposed for calibrating traffic simulation models. While most of these procedures focus on determining values for a small set of parameters for relatively simple models, many modern simulation tools include an increasingly complex array of parameters available for calibration. Many of these additional parameters may have little influence on simulation results, while others may have a significant impact.

The following will summarize a sensitivity procedure for determining which model parameters are most important for calibrating a simulation model. As a case study, this sensitivity procedure is applied to an arterial simulation model based on the VISSIM microscopic simulation tool to identify critical parameters that would need to be evaluated during subsequent model calibrations. For greater details regarding this method, readers are encouraged to consult [53].

6.1 The Method

The developed sensitivity-based process for the selection of parameters to be included in model calibration is comprised of four sequential steps: 1) initial parameter selection, 2) performance

measure selection, 3) Monte Carlo simulations, and 4) parameter elimination. Steps 3 and 4 are repeated until the stopping criterion is satisfied.

6.1.1 Initial Parameter Selection

In the first step of the process, model parameters that are known a priori to have little, if any, impact on simulation results due to the structure of the model are eliminated prior to the sensitivity analysis. For example, in the VISSIM modeling system the Wiedemann (1974) and Wiedemann (1999) car following equations are used to define arterial operations and freeway operations respectively [54], [55]. If the model being calibrated does not include one these facility types, parameters related to the respective car following equations may be removed from the calibration.

A priori elimination of parameters that do not influence a model will reduce the computational effort in subsequent analysis, lessening the time and resources required to select the final set of parameters for calibration. However, if it is uncertain whether a parameter should be eliminated it is recommended that the parameter remain in the experiment. Also, if resources permit, this step may be eliminated in its entirety and all parameters included in the subsequent selection process.

6.1.2 Performance Measure Selection

As part of the calibration process it is necessary to select the performance measure(s) that will be used to gauge the acceptability of the simulation model. Common performance measures include travel times, flows, capacities, delay, queue lengths, etc. Measures of effectiveness should

be selected such that critical network components, such as key intersections or interchanges, and the overall network, i.e. end-to-end corridor travel time, may be evaluated. The measure(s) must also be field measurable, allowing for the collection of field data to be used in the calibration process. Analyst judgment is normally required in the selection of performance measures for the particular model under study. However, in the initial stages, it is recommended to include a wide cross section of potential measures, paring down the measures in later analysis to those that are most informative.

6.1.3 Monte Carlo Simulation Experiment

A Monte Carlo experiment is next used to determine the likely influence of the remaining parameters on the simulation model performance. In the Monte Carlo simulation experiment simulation runs are generated based on randomly selected parameter values with the results aggregated in an effort to find underlying relationships between parameter values and model performance measures.

6.1.3.1 Parameter Range Selection

Before generating random parameter values for the Monte Carlo experiment it is necessary to determine parameter ranges over which the random values will be assigned. There is generally no exact method for this determination. These ranges must be determined through a combination of past experience, simulation documentation, results of other studies, and engineering judgment.

For instance, the VISSIM documentation provides insight into model behavior and reasonable ranges for a number of parameters. The objective of range selection is to cover all feasible parameter values while excluding values which may introduce impractical or flawed behavior in the model. When the analyst is uncertain of a reasonable parameter range it is recommended in the initial step to use a more inclusive range and, if necessary, narrow the range in later process iterations.

6.1.3.2 Random Parameter Generation

Random parameter values within the given parameter ranges must be generated. A random set of parameters is required for each simulation run. Random numbers should be generated using a reasonable random number generator [56]. The number of parameter sets needed is determined using standard sample size statistics [39] influenced by level of effect in the selected performance measure deemed to be significant (e.g. 1%, 5%. etc. changes), the reasonable range of parameter values, and the sensitivity of performance measure to changes in the parameters. While the sensitivity to parameters must be based on analyst expertise, initial assumptions may be validated using the observed variability from the initial iteration of the methodology. For instance, it was seen in this effort that the modeling variability based on parameter variation (parameters varied within a reasonable range) was typically well within ten percent.

6.1.3.3 Simulation Runs and Sensitivity Analysis

Each set of randomly generated parameter values is used to generate simulation trials in the Monte Carlo study. The results of the simulation runs are evaluated to determine which parameters appear insignificant. It is important to note that this step is not attempting to quantify the mathematical relation-ship between the performance measure and parameter; it is only intended to identify the potential existence of a relationship. A convenient method to quickly identify these potential patterns is to visually inspect a scatter plot of the parameter value versus the performance measure (a unique plot for each parameter). The analyst may also wish to include a best fit line to aid in the visual assessment. Scatter plots allow for a quick visual assessment of the influence of the given parameter over its considered range, allowing for a ready recognition of any potential relationship between the parameter and performance measures since human analysts are more likely to identify patterns when none exist than to miss patterns that are actually present.

In addition to the scatter plot it is also recommended to evaluate the effect each parameter has on the mean value of the performance measure. The effect on the mean is equal to the slope of the best fit line of the scatter plot multiplied by the absolute value of the range of values for the given parameter, Equation 1. These values may then be used to rank each parameter based on its effect on the mean of each selected measure of effectiveness.

$$\textit{Effect of the mean} = \textit{slope}((\textit{MOE values})_{1 \to n} * (\textit{Parameter Values})_{1 \to n}) * \textit{abs}(\textit{Parameter Upper Bound} - \textit{Parameter Lower Bound}) \quad (1)$$

This ranking requires a simplifying assumption of a linear relationship between parameter values and the performance measure. Based on the scatter plots for the study described in this effort this was deemed to be a reasonable assumption when considering parameter values within a reasonably narrow range. However, in inspection of the scatter plots it should be considered if the relationship between the parameter value and performance measure differ significantly from linear. Should this exist, then a more robust ranking metric should be considered.

Finally, the variance of the performance measure, due to changes in parameter values, should be considered. If the variance increases or decreases then the corresponding parameter should remain in the analysis, even if the impact on the mean value is minimal.

6.1.4 Parameter Elimination

Parameters found to display minimal impact on simulation model output through either visual inspection of the scatter plots or the effect on the mean should be eliminated from further consideration. To avoid analyst bias in the parameter selection it is useful to develop guidance for determining whether a parameter should be considered significant. Such guidance would be specific to each model and performance measure. The analyst must decide what level of impact is deemed significant for the particular study. For instance in an initial alternative analysis a 10% error may be tolerable and therefore the effort and resources should not be expended to calibrate parameters whose effect is under 10%. Whereas in a detailed final design application it may be desirable to consider any parameter whose possible impact on the performance measures may be within just a few percent.

To avoid eliminating parameters that may be significant it is advised that conservative elimination guidance be employed, particularly in the initial iteration of the parameter selection. Additionally, it may be desirable to carry forward a parameter that intuitively seems significant but does not appear to be significant in the current iteration, allowing for confirmation of significance (or insignificance) in the next iteration. The number of variables to be eliminated per iteration is ultimately an analyst judgment. While the parameter reduction should be a function of the findings, a general guideline for good practice is that number of parameters eliminated should not exceed approximately one-half of the total parameter set in the initial iteration and one-third in subsequent iterations.

6.1.5 Iteration

After parameter elimination the Monte Carlo simulation experiment (random parameter generation, simulation trails, and sensitivity analysis) should be repeated using the reduced parameter set. Based on the updated Monte Carlo simulation results the remaining parameters should again be considered for potential elimination. This process should be repeated until no parameters are eliminated after a Monte Carlo simulation experiment.

After each iteration the parameter ranges of should be reexamined using the scatter plots. If there are obvious abnormalities in the data, such as extremely high travel times, or large numbers of recorded errors during the simulation then the range for that parameter should be reconsidered. Similarly if there is reason to believe that the range of values for that parameter should be larger, then that range should be modified as well.

6.2 Procedure Application Case Study: Cobb Parkway Model

The model area is a 1.4 mile, eleven intersection segment of Cobb Parkway (U.S. Highway 41) in Cobb County, GA Figure 37. Cobb Parkway is a primary arterial in Cobb County, with four lanes in each direction. The model was constructed using 2004 intersection AM peak count data. Controller signal timing data was obtained and modeled using the VISSIM NEMA signal controller. The posted speed limit is 45 mph. Prior to model parameter calibration significant effort was spent on model development to ensure the correctness of the underlying model construction. Details on the base model development, corridor geometry, signal timing, etc, may be found in [40] and [57].

Figure 37 Cobb Parkway Model and VISSIM Overview

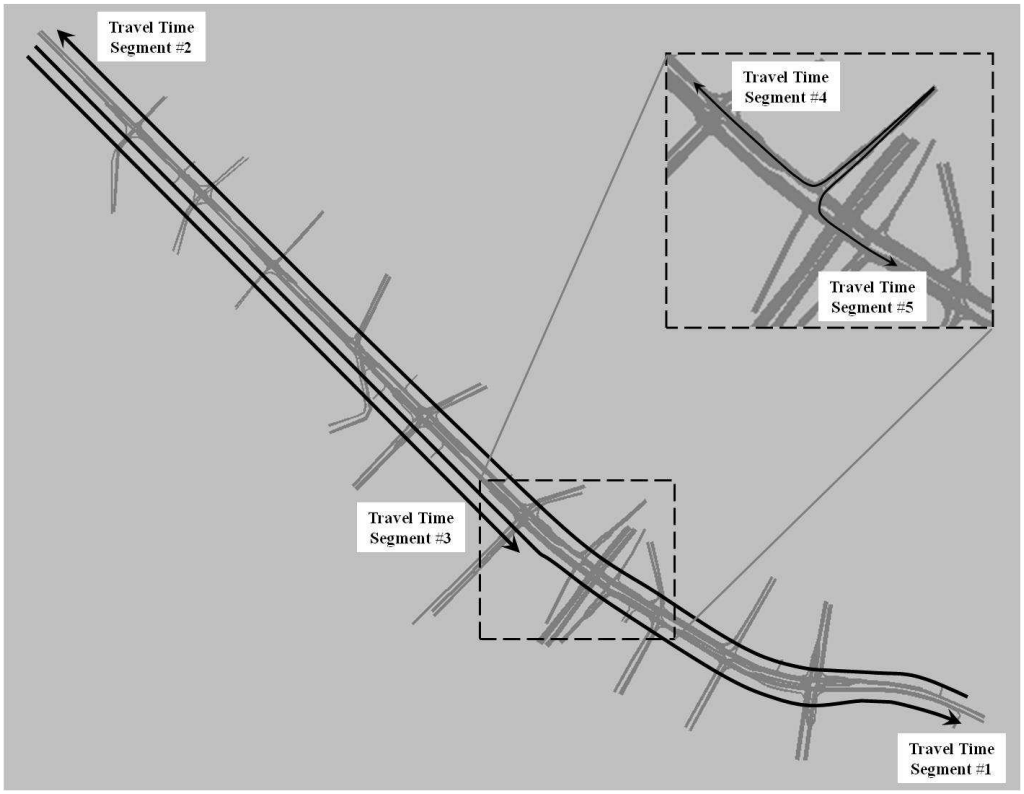

Figure 38 Travel Time Segments along Cobb Parkway

6.2.1 Initial Parameter Selection

In the initial step, parameters that can be eliminated from consideration due to specific model characteristics are identified. For the Cobb Parkway model twenty-eight of the available parameters were eliminated, leaving twenty-two parameters for further consideration. Twelve of the eighteen car following parameters were eliminated as this model only includes parameters related to Wiedemann (1974). Parameters associated with vehicle the acceleration and deceleration functions were also eliminated because the model focused only on signalized arterials (i.e. the Wiedeman (1999) equations for freeway operations were not considered). Additional parameters

that are based on the mechanical capabilities of the average vehicle on the network were also not considered as there is little justification for changing their default values. Parameters relating to the acceleration functions were also not considered as the driver's acceleration decisions are likely dominated by car following considerations due to the close spacing of signals and level of congestion.

In addition, the general lane change behavior was set to free lane selection as Cobb Parkway does not have a designated "fast lane" and vehicles often pass each other on both the left and right sides. This also eliminates a parameter used only in conjunction with right-side rule instead of free lane selection behavior. All of the lateral behavior parameters were also eliminated as there is no lateral behavior present in this model.

These reductions left twenty-two parameters for consideration. One additional parameter for the simulation run, random seed value, was added to allow for an exploration of the impact of randomness due to inherent model stochasticity to bring the total parameter set to twenty-three.

6.2.2 Performance Measure Selection

For the performance measures five travel time segments were chosen. Travel time data provides the advantages of being straightforward, easily interpreted, and reflective of model changes. The five travel time segments include two end-to-end segments, a segment over the most traveled route in the network, and two short two-intersection segments, Figure 38. Segment #1 is the southbound end-to-end segment. It is 11,294 feet long and includes 10 intersections. Segment #2 is the northbound end-to-end segment. It is 11,334 feet long and also includes 10 intersections.

The third segment is representative a typical commuter route. It is 6955 feet long and covers the most heavily traveled route on the network, from the northern arterial entrance to the intersection of Cobb Parkway and I-285. Segments #4 and #5 are shorter segments at 1670 feet and 1426 feet respectively that include two heavily traveled routes from the I-285 exit ramp to Cobb Parkway northbound and southbound. Each of these routes includes two traffic signals.

6.2.3 Parameter Range Selection

The parameter value ranges were chosen to be larger than typically used in similar studies but within any limits described in the VISSIM documentation. An initial set of simulations were undertaken to evaluate the reasonableness of these broader limits using randomly varied parameter sets to ensure model stability and performance. Where parameter values resulted in unrealistic performance measures or a significant number of reported modeling errors the range is adjusted to exclude those values.

The initial and final parameter ranges for the first iteration of the methodology are shown in the Table 12. An empty value in the final range column indicates that the parameter was not changed.

Table 12 Selected Parameter Ranges

	Parameter	Initial Range	Final Range
1	Desired Speed Distribution Range	±0.0-10.0 mph	±0.5-10.0 mph
2	Look-ahead distance min	0-900 ft	0-300 ft
3	Look-ahead distance max	500-1000 ft	500-1200 ft
4	Number of observed vehicles	2-8	
5	Average standstill distance, ax	0.0-20.0 ft	2.0-8.0 ft
6	Additive part of safety distance, bx_{add}	0.0-8.0	0.0-3.0
7	Multiplicative part of safety distance, bx_{mult}	0.0-8.0	0.0-3.0
8	Maximum Deceleration (own)	-20.0 - -3.0 ft/s²	
9	Maximum Deceleration (trailing)	-20.0 - -3.0 ft/s²	
10	Accepted Deceleration (own)	-6.0 - -0.33 ft/s²	
11	Accepted Deceleration (trailing)	-6.0 - -0.33 ft/s²	
12	Reduction rate (own)	50-300	50-200
13	Reduction rate (trailing)	50-300	50-200
14	Waiting time before diffusion	20–80 sec	40–80 sec
15	Min. headway (front/rear)	1.64-25.00 ft	
16	Safety distance reduction factor	0.0-1.0	
17	Max. deceleration for cooperative braking	-35.0 - -3.0 ft/s²	
18	Reduction factor for changing lanes before a signal	0.3-0.9	
19	Start upstream of stop line	200–600 ft	
20	End downstream of stop line	200–600 ft	
21	Emergency stop distance	6.56–30.0 ft	
22	Lane change distance	300–1000 ft	500–1000 ft
23	Random seed value	1-999	

6.2.4 Calibration Parameter Set Determination

To determine the final calibration parameters, a series of Monte Carlo simulation experiments are undertaken and parameters with minimal influence on the simulation outputs are eliminated. This process is repeated until no remaining parameters can be eliminated based on the results of the Monte Carlo simulations.

In the case study, three iterations were required before no parameters could be eliminated. Each iteration began with the creation of 1000 sets of random parameter values (23 parameters in the initial round) within their stated ranges using Microsoft Excel in conjunction with a Visual Basic script. These parameter sets were used to create 1,000 corresponding VISSIM input files, for each of two volume cases (i.e. 100% AM volumes and 75% AM volumes) for a total of 2000 runs using a PERL script. While this value is approximately one order of magnitude higher than the minimum number required by the simulation variability at our selected level of significance (approximately 85 tests for each volume case, assuming a 10% run variability and 4% desired accuracy) the greater number of tests allowed for easier visual examination of the resulting scatter plots. A modified version of the "multi-run" script, provided with VISSIM, was used to automate the model runs and to collect the output data *(9)*.

For this study a parameter had to demonstrate least a 4% effect on the mean travel time of at least two segments or an observable relationship in the scatter plots to be retained for subsequent iterations. Other thresholds could, of course, be considered and future studies will explore the impact of the threshold selection on method convergence.

6.2.4.1 Iteration I

The results from the 100% volume runs led to the elimination of 11 parameters that had a negligible effect on the travel time measurements. The retained and eliminated parameters and their impacts on travel times (Equation 1) are shown in Table 13 and Table 14 below.

Table 13 1st Round - Retained Parameters' Effect on Mean Travel Times

		Travel Time Segment				
#	**Parameter**	**#1**	**#2**	**#3**	**#4**	**#5**
1	Desired Speed Distribution Range	-0.32%	1.58%	-0.18%	-0.59%	3.15%
5	Average standstill distance, ax	**5.97%**	**7.62%**	**6.19%**	**8.44%**	**14.99%**
6	Additive part of safety distance, bx_{add}	**6.20%**	**19.28%**	**7.14%**	2.59%	**-5.61%**
7	Multiplicative part of safety distance, bx_{mult}	**4.45%**	**11.17%**	**4.86%**	2.20%	-0.72%
8	Maximum Deceleration (own)	**11.41%**	1.15%	**7.30%**	-1.11%	**-20.93%**
9	Maximum Deceleration (trailing)	**4.48%**	-0.87%	2.60%	-0.87%	**-7.94%**
15	Min. headway (front/rear)	**17.71%**	**4.27%**	**12.54%**	-1.87%	**-28.78%**
16	Safety distance reduction factor	**11.14%**	-0.70%	**7.28%**	-1.85%	**-20.61%**
17	Max. deceleration for cooperative braking	**7.85%**	-1.82%	**4.45%**	-1.42%	**-9.90%**
18	Reduction factor for changing lanes before a signal	1.61%	**14.61%**	2.96%	0.32%	-0.08%
22	Lane change distance	**-17.91%**	-0.85%	**-11.85%**	1.45%	**22.94%**

Table 14 1st Round - Eliminated Parameters' Effect on Mean Travel Times

		Travel Time Segment				
#	**Parameter**	**#1**	**#2**	**#3**	**#4**	**#5**
2	Look-ahead distance min	1.52%	-1.94%	0.86%	-1.26%	-6.73%
3	Look-ahead distance max	-2.31%	-0.39%	-1.42%	-0.05%	2.92%
4	Number of observed vehicles	-2.10%	0.52%	-0.68%	-0.15%	-0.72%
10	Accepted Deceleration (own)	1.91%	-0.37%	1.71%	0.45%	-2.31%
11	Accepted Deceleration (trailing)	1.38%	-2.50%	0.87%	0.40%	-1.90%
12	Reduction rate (own)	-2.84%	3.28%	-2.03%	-0.25%	5.56%
13	Reduction rate (trailing)	1.42%	2.10%	1.76%	0.34%	-0.24%
14	Waiting time before diffusion	2.06%	0.67%	1.65%	-0.24%	-3.68%
19	Start upstream of stop line	-0.41%	-3.24%	-0.47%	-2.15%	-5.38%
20	End downstream of stop line	-0.31%	-2.80%	-1.03%	0.40%	2.50%
21	Emergency stop distance	1.59%	4.25%	3.10%	0.30%	0.62%

Figure 39 shows the average travel time along segment #3 versus parameter value for the minimum headway parameter and is illustrative of how scatter plots are used in the analysis. The plot shows a potential relationship between increasing travel times and increasing minimum headway values. Both this result and two results from two segments above the 4% impact threshold result in this parameter being retained for a subsequent iterations. Figure 40 illustrates the lack of an observable impact due to an elimated parameter (look ahead distance minimum).

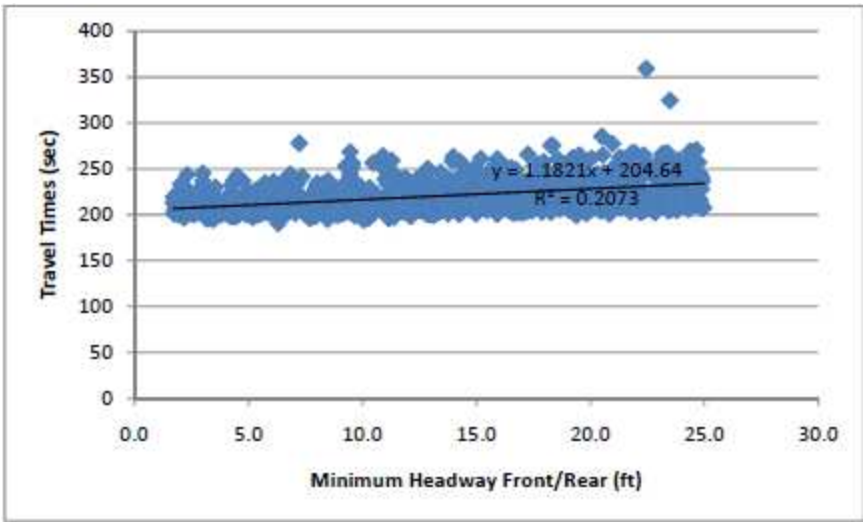

Figure 39 Mean Travel Times on Segment #3 vs. the Minimum Headway

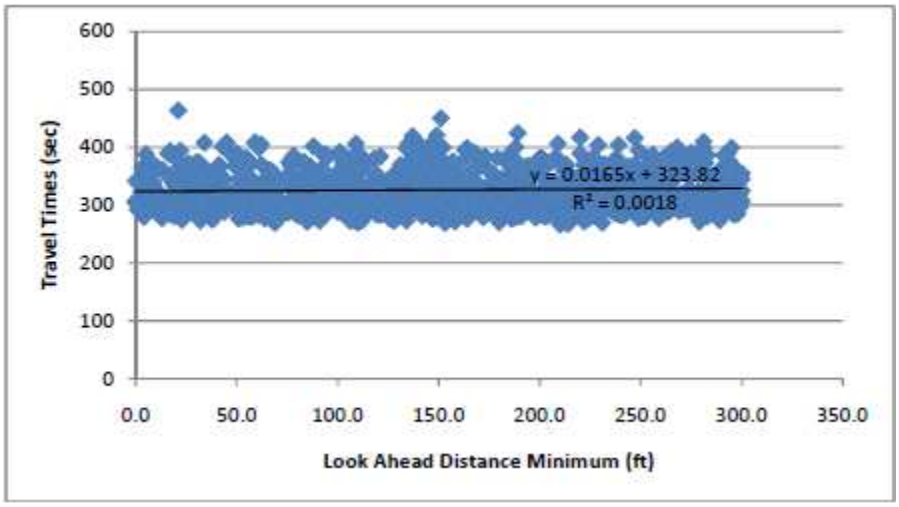

Figure 40 Mean Travel Times on Segment #1 vs. the Look Ahead Distance Minimum

It is noted that parameter #1, desired speed distribution range, was retained for the second iteration even though it failed to meet the sensitivity threshold since this parameter had shown significant impacts in other studies. Also, parameter 18, reduction factor for changing lanes before a signal, was retained. While only one travel time segment exceeded 4% the difference was large, exceeding 14%. In addition the scatter plots indicated the parameter to be potentially significant.

Similar results were obtained for 75% volume case. The only difference between the two scenarios is that the 75% volume case did not include parameter #9, the maximum decelerating (trailing) parameter.

6.2.4.2 Iteration II

For the second iteration the 11 remaining parameters from the 100% volume case and the 10 remaining parameters for the 75% volume case were carried forward. For those parameters eliminated in the first iteration, the default values from the initial model are used. As mentioned previously, the random seed value is also included as an additional parameter to capture inherent stochasticity. The results from the second iteration are analyzed in a manner similar to that of the previous runs. In addition, comparisons were made between the results of the simulations from the first and second iterations to identify any changes in travel times that might result from undetected interactions of the eliminated parameters. In Figure 41 the average travel times for all 1,000 runs from each travel time segment are compared for both parameter sets. The similarity between these results helps support the first iteration parameter eliminations.

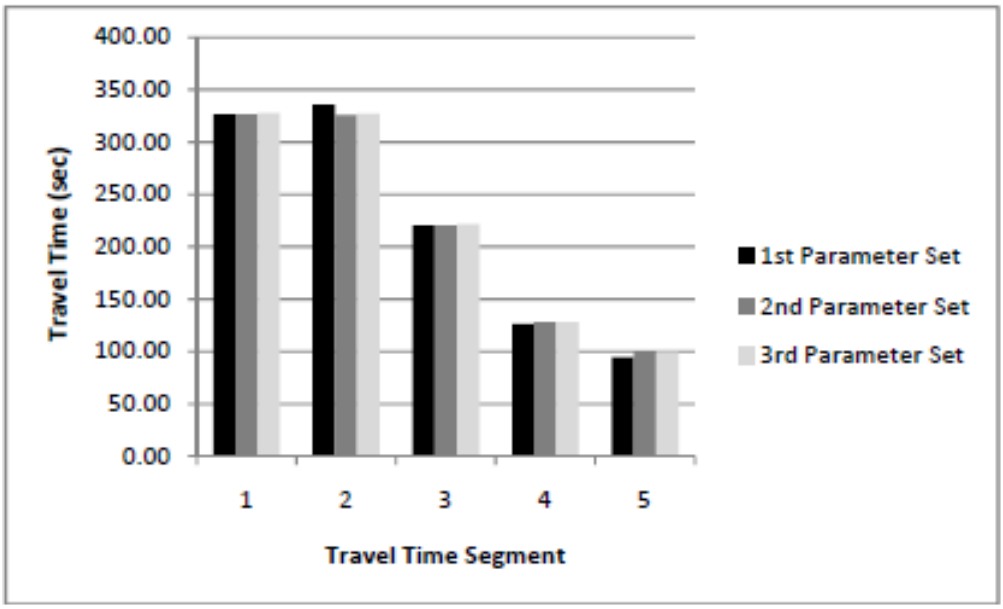

Figure 41 Comparison of Mean Travel Times from 1st, 2nd and 3rd Parameter Set Runs

After completing the second iteration a list of retained parameters was generated for each scenario. Note, the list of retained parameters was determined in a manner similar to that described in the first iteration. After second iteration of runs and analyses, parameters #1, desired speed distribution range, and #18, reduction factor for changing lanes before a signal, were eliminated – for both the 100% and 75% volume cases.

6.2.4.3 Iteration III

Similar to the second iteration, the nine remaining selected parameters from the 100% volume case and the eight remaining selected parameters for the 75% volume case were carried forward. For those parameters eliminated in the second iteration the default values from the initial model were used. Similar to iteration two Figure 41, above, shows the average travel times on each

segment from the third parameter set runs compared to the average travel times on each segment from the first and second parameter set runs. Overall, the results from the third iteration are very similar to iteration one and two, supporting the selection of the parameters thus far eliminated. From the results of the third iteration no parameters were identified as insignificant. Thus, the third iteration is the last and these parameters represent the parameters that should be included in the model calibration process. See Table 15 and Table 16 below for the final list of effective calibration parameters.

Table 15 Final 100% Vol. Scenario - Retained Parameters' Effect on Mean Travel Times

		Travel Time Segment				
#	**Parameter**	**#1**	**#2**	**#3**	**#4**	**#5**
5	Average standstill distance, ax	**6.25%**	**5.74%**	**6.54%**	**9.19%**	**11.11%**
6	Additive part of safety distance, bx_{add}	**4.95%**	**10.46%**	**5.62%**	1.65%	**-11.67%**
7	Multiplicative part of safety distance, bx_{mult}	3.80%	**6.47%**	**4.32%**	1.15%	**-4.96%**
8	Maximum Deceleration (own)	**9.86%**	1.29%	**7.00%**	-2.08%	**-24.32%**
9	Maximum Deceleration (trailing)	**5.54%**	1.09%	3.78%	-1.75%	**-10.37%**
15	Min. headway (front/rear)	**17.50%**	**4.85%**	**13.10%**	**-5.69%**	**-40.46%**
16	Safety distance reduction factor	**10.57%**	2.39%	**7.22%**	**-4.96%**	**-28.45%**
17	Max. deceleration for cooperative braking	**8.59%**	0.66%	**5.48%**	-2.85%	**-15.16%**
22	Lane change distance	**-16.61%**	-0.53%	**-12.14%**	**4.60%**	**32.19%**

Table 16 Final 75% Vol. Scenario - Retained Parameters' Effect on Mean Travel Times

		Travel Time Segment				
#	**Parameter**	**#1**	**#2**	**#3**	**#4**	**#5**
5	Average standstill distance, ax	2.94%	1.89%	3.47%	**4.75%**	**27.08%**
6	Additive part of safety distance, bx_{add}	3.34%	3.49%	**4.65%**	3.38%	-3.11%
7	Multiplicative part of safety distance, bx_{mult}	2.30%	2.00%	2.87%	2.41%	-0.25%
8	Maximum Deceleration (own)	**4.75%**	0.77%	2.50%	3.45%	**-10.24%**
15	Min. headway (front/rear)	**8.09%**	1.01%	3.86%	1.88%	**-18.11%**
16	Safety distance reduction factor	**4.75%**	0.26%	2.26%	1.04%	**-9.70%**
17	Max. deceleration for cooperative braking	3.90%	0.33%	0.91%	0.25%	**-8.84%**
22	Lane change distance	**-7.25%**	-0.36%	-3.03%	0.20%	**9.63%**

6.2.5 Desired Speed

Of particular note in the preceding analysis is the elimination of the desired speed range parameter. Both iteration 1 and iteration 2 found the desired speed range to be insignificant. To further explore this somewhat counterintuitive result, we examined why this result might have an insignificant effect on performance measures. The working hypothesis was that due to traffic conditions on this corridor vehicles were unable to reach their desired speed (45 mph) thus greatly reducing its significance as a model parameter.

To test this hypothesis the runs were repeated using the 100% volume scenario and the iteration #2 parameter set with the average desired speed was lowered from 45 mph to 30 mph. Thus the considered maximum potential range of desired speeds would now be from 20 mph and 40 mph respectively. The results from the Monte Carlo simulation experiments results for this new scenario now showed that for all three of the long travel time segments the desired speed

distribution range was one of the most influential parameters. Thus, while for the original model the desired speed range was found to be insignificant it is seen that for other model configurations the parameter can be highly significant. This highlights the need to consider parameters for each model as the impact of parameter calibration can vary from model to model.

To further explore the effects of the desired speed range calibration parameter, while corroborating the above hypothesis, an additional experiment was conducted using the NGSIM model introduced in Section 5.4. In the experiments discussed in Section 5.4 the desired speed range varied from 0 to 10 mile-per-hour. For the following experiments the desired speed parameter is allow to range from 0 to 20 miles-per-hour. Approximately 300 replicates of NGSIM corridor model were created, with each replicate using a different desired speed range expressed as the difference between maximum and minimum desired speed. The desired speed range parameter was the only parameter varied between replicates. For each replicate run the relevant travel time measurements extracted. Figure 42 presents a scatter plot of desired speed range versus average travel time for each segment. The red horizontal line in Figure 42 represents the average field travel time.

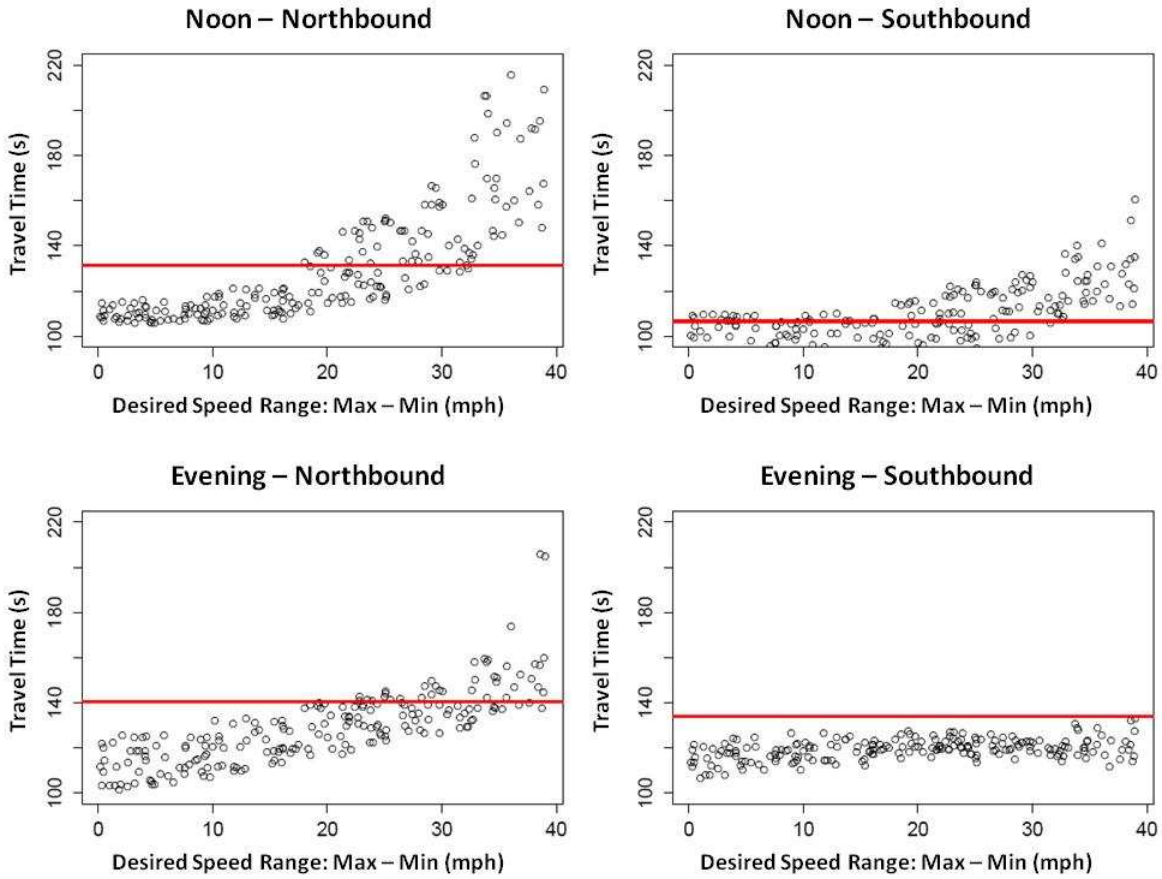

Figure 42 Average Travel-Time versus Desired Speed Range

In all four cases there is little change in the mean or variability in travel over the desired speed ranges (Max – Min) of 0 to 20 mph. This result underlies the elimination of the desired speed range parameter from the list of calibration parameters, in the final stage of the advanced calibration procedure discussed previously as the maximum allowed variation was average desired speed +/- 10mph. However, from the figure above, as the desired speed range increases beyond 20mph (i.e. average desired speed +/- 10 mph) the average travel time estimates and travel time

variability increase in three of the four segments. Thus it is again seen, that depending on the underlying base conditions (for instance, the variability in desired speed selected by drivers on a corridor) the importance of parameter change. For this particular instance it is recommended to generally retain desired speed as a calibration as it has been demonstrated to influence model operations under certain conditions.

6.3 Advance Calibration Procedure Summary

The previous sections described a general procedure for identifying parameters which should be considered for calibration of particular simulation models. For the case study (Cobb Parkway in Cobb County GA), application of this procedure resulted in the selection of nine parameters and eight parameters for two volume cases.

The sensitivity-based procedure was effective in determining which parameters had a significant effect on the model. However, ultimately the construction of the model itself is more significant than the parameter values, as evidenced by only a few parameters influencing measured travel time by more than 10%. As such, parameter calibration should be used to fine tune a model, but the results using the default parameter values must already be reasonably close to the values from the field data in order for the calibration to be successful.

The results from the application of this procedure also show important differences from previous studies. For instance, seven parameters previously used for calibration purposes were shown to be insignificant for calibration of the Cobb Parkway model. These seven parameters include: waiting time before diffusion, emergency stop distance, number of observed preceding

vehicles, accepted deceleration (own), accepted deceleration (trailing), reduction rate (own) and reduction rate (trailing). These parameters were included in the previous studies for varying reasons however it is clear that a general set of critical parameters requiring calibration in all models does not exist. Application of the sensitivity-based parameter selection method avoids the expense of unnecessary calibration, including the potential costs of field data collection of these parameters. Thus, without confirmation of a parameter's significance it is possible that insignificant parameters are essentially being calibrated to arbitrary values and significant parameters are being missed.

In the future efforts of this research the discussed calibration procedure will be applied to the NGSIM data based experiment. First a base calibrated model will be developed. As part of this development the critical parameter set will be identified. Given the calibrated base model the need and methodology to calibrated parameter in real time will be investigated. For instance, might it be expected that parameter values change throughout a day, congested traffic versus uncongested, morning versus evening, etc.

Finally, as noted in the experimental results presented in Chapter 5 significant pedestrian-vehicle interactions was observed but not accounted for in the simulation. This pedestrian-vehicle interaction had the potential to significantly affect arterial performance. The influence of pedestrians on vehicles should not be address through calibration of model but instead through direct inclusion of pedestrians in the model. To model pedestrian-vehicle interaction VISSIM's pedestrian model was examined to determine its ability to accurately reflect pedestrian behavior. A detailed

study was undertaken on the test bed intersection of 5th Street and Spring Street. The following chapter describes this study.

7 MODELING PEDESTRAIN BEHAVIOR

Many of the commonly utilized traffic simulation tools currently under-represent the complexity of pedestrian behavior and their interactions with the various components of the traffic network. While simulation packages have been developed specifically for representing pedestrians, their usage has generally been limited to modeling pedestrian behavior for special cases, such as a building evacuation, large pedestrian interactions (e.g. stadiums), transit centers, etc. [58–62]. Although these packages utilize sophisticated behavioral algorithms for pedestrian simulation, they are usually not designed to specifically model pedestrian-vehicle interactions in the urban traffic environment.

This section will explore the microscopic modeling of pedestrians crossing at an intersection with the use of VISSIM, while incorporating observed pedestrian behaviors at a crosswalk and the influence of pedestrian-vehicle interactions.

7.1 Previous Works in Modeling Pedestrians

The impetus of this study was a set of observations performed by the research team on the simulation test bed. While observing pedestrian behavior, pedestrians appeared relatively uninfluenced by the pedestrian signal. Instead, most pedestrians crossed whenever they found an acceptable gap in traffic, regardless of the pedestrian signal indication.

Several researchers have observed the similar issues with pedestrian rule violations. For instance, a study performed by Virkler [63] in Australia he classified pedestrians as: "complying" (those who cross during the walk indication), "runners" (those who cross during the clearance interval), and "jumpers" (those who cross during the red interval). This study found that 74.4% of pedestrians complied, and 15.8% were "jumpers" crossing on the red phase at opportune moments. Ishaque and Noland [64] noted that pedestrian compliance to signals should be taken into account, as the signal affects the perceived pedestrian efficiency of an intersection. They attempted to study the gap acceptance behavior of pedestrians crossing against the pedestrian signal. One of their more immediate conclusions was that gap acceptance was dependent on vehicular volumes at the intersections. However, the study was limited as insufficient violations were observed to determine the distribution of gaps accepted by rule-violators and of rule-violating versus rule-following pedestrians. Yang et al. [65] developed a model of Chinese pedestrian behavior that accounted for gap-seeking behavior. They theorized that there were two types of pedestrians, law-obeying and "opportunistic." They observed that an average of 85% of pedestrians were "opportunistic".

There are a number of other research efforts that are focused on modeling observed pedestrian behavior in a mixed-traffic simulation environment. Rouphail and Eads [66] used CORSIM to evaluate turning movement delay given a level of pedestrian flow. They compared this to other methods, including the 1994 HCM and Canadian method of predicting delay due to pedestrians. CORSIM assigns delay values based on the level of pedestrian volumes (none, light, moderate, and heavy). Neither the HCM nor the Canadian methods include adjustments for vi-

olating pedestrians, although the Canadian method specifically calls for the volume of pedestrians who cross during the walk and pedestrian clearance phases. Wan and Rouphail [67] had previously looked at a gap-seeking models for roundabouts using ARENA. Schroeder and Rouphail [68] also looked at signalized crossing behavior in VISSIM at crossings near roundabouts.

Numerous researchers have also studied simulating pedestrian activity to quantify its effects on turning movements at signalized intersections. Milazzo et al. [69] noted that the Highway Capacity Manual (HCM) has measures for empirically determining delay for right and left turning vehicles from one way streets. They investigated the impact of total pedestrian volumes on turn movement delays. They determined that the HCM should add an adjustment factor for pedestrian and cyclist saturation rates. Coyemans and Herrere [70] also investigated factors that could be applied to delay equations based on pedestrian volumes, but did not consider gap-seeking pedestrian behavior. Hubbard et al. [71] reversed the question and examined the delay that turning vehicles imposed on pedestrians at crosswalks. Based on their study, the authors recommended that the HCM be modified to include the impacts that turning vehicles have on pedestrians.

Expanding beyond the individual intersection, Virkler [72] simulated pedestrian behavior in a traffic network. In the Virkler study, the author developed a method of determining travel time along pedestrian corridors that incorporated link travel times and time spent in queues at nodes. Virkler also noted the effect of non-compliance at walk signals and found that pedestrians who did not comply with signals, on average, reduced their delay by 22%.

These studies recognize the same general pedestrian behavior that was observed in the research test bed. It is apparent that, to varying degrees, pedestrians across cultures can be grouped into complying (i.e. those who follow the pedestrian indications), and gap-seeking (i.e. those who cross the street, regardless of the pedestrian signal indication, if the gaps in traffic are sufficient). This behavior is even acknowledged in the HCM 2010, where effective pedestrian walk time may be increased to reflect "illegal pedestrian behavior" [73]. Thus, to realistically model pedestrians in today's traffic simulation tools these behaviors must be reflected. Therefore, the objective of the efforts reported in this paper is focused on an attempt to replicate observed pedestrian behavior at a crosswalk, accounting for pedestrian-vehicle interaction within a microscopic simulation environment.

7.2 Methodology

Pedestrian data were collected for the south crosswalk at the intersection of Spring Street and Fifth Street in midtown Atlanta, Figure 43. Spring Street is a four lane, one-way, southbound street with a 35 mph speed limit. Fifth Street is a two lane, two-way, east-west street, with a 25 mph speed limit. This intersection is located in an area known as Technology Square (Tech Square) and is home to a number retail shops (including the campus bookstore), instructional buildings, and commercial businesses, as well as the Georgia Tech Hotel and Conference Center. Given the relatively consistent pedestrian demands, this site offers a desirable location observing pedestrian behavior.

7.2.1 Data Collection and Processing

The primary means of collecting pedestrian and vehicular data is by video recording. Tech Square is outfitted with VDS cameras that stream video and traffic data as a part of a NSF real-time simulation project. Covered zones include the intersection proper as well as upstream on each approach (Figure 44 and Figure 45). Data were extracted from the video using both manual methods and using automated reduction software.

7.2.1.1 Pedestrian Data

Pedestrian data collected includes the number of pedestrians, walk speed, and individual pedestrian arrival and departure times. Data collection was conducted on July 8, 2010 from 12:00 PM to 1:00 PM, September 16, 2010 from 12:00 PM to 1:00 PM and from 5:00 PM to 6:00 PM. Figure 44 provides the intersection camera view and Figure 45 contains the upstream approach view for Spring Street. Approximately 400 pedestrians were detected over the one-hour period. The average walk speed was estimated at 4 feet per second. The research team manually recorded time stamps from the video for the arrival and departure of each pedestrian. A pedestrian was considered to have arrived when he/she entered the waiting zone, defined as the sidewalk area within approximately 15 feet of the crosswalk curb line and departed when the pedestrian stepped from this zone into the crosswalk, see Figure 44. The difference between the arrival and departure represents the waiting time experienced by the pedestrian while waiting to use the crosswalk (minus a waiting zone transition time of 2 seconds). The average waiting time per pedestrian was found to be approximately 21.5 seconds.

7.2.1.2 Vehicular Data

Traffic counts were collected on the Spring Street and 5th Street approaches. In addition, the timestamp, speed, and lane number were recorded as each vehicle crossed the upstream detectors on Spring Street, see Figure 45. Signal timing plans were obtained from the City of Atlanta and field-verified. The intersection operates under semi-actuated control with loop detectors on 5th Street. The cycle length for the signals during this time period was 110 seconds.

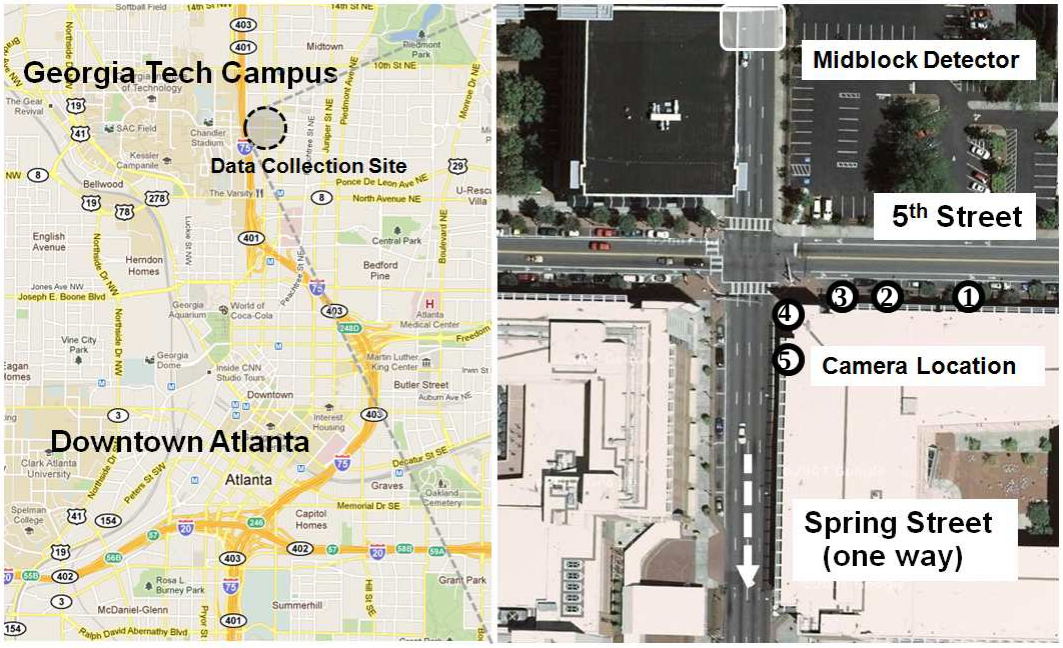

Figure 43 Data Collection Site for Pedestrian Study

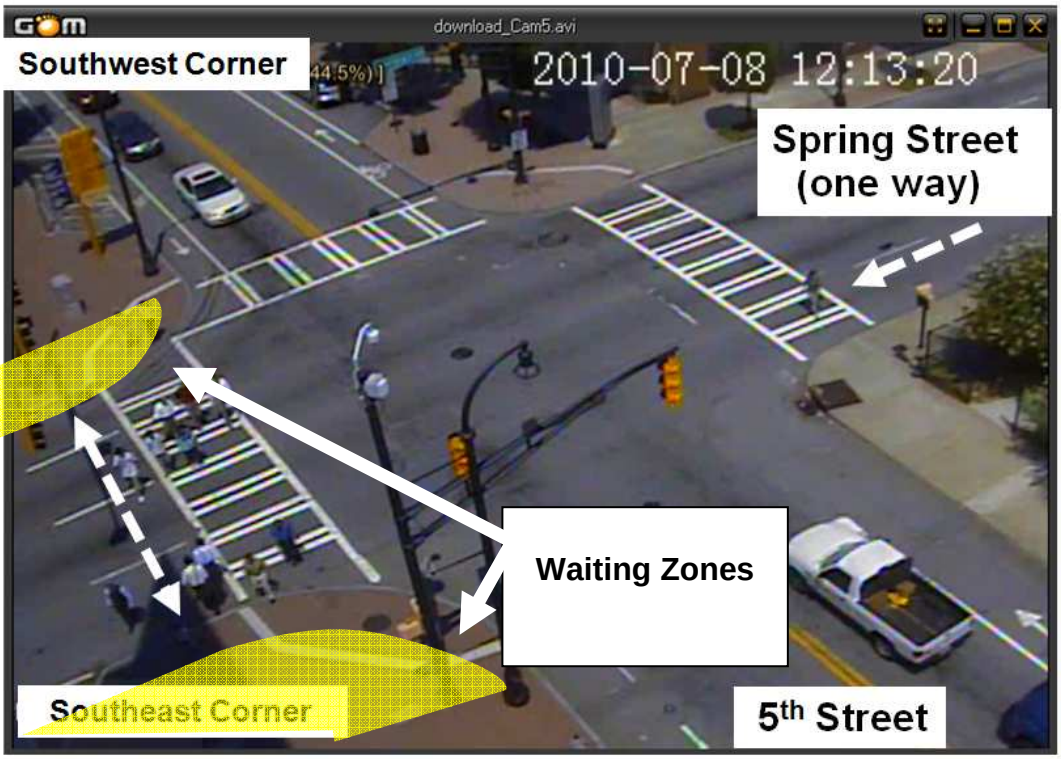

Figure 44 Camera View for Pedestrian Data Collection

Figure 45 Midblock Detector Camera Data Acquisition View

7.2.2 Simulation Model

VISSIM 5.3 was utilized for this effort. VISSIM, a widely used off-the-shelf traffic simulation program, is a discrete, stochastic, time-step-based microscopic simulation model [39]. This behavior-based multi-purpose traffic simulation program was developed to model a wide range of traffic conditions including freeway, arterial, and public transit operations. In VISSIM, all vehicles are modeled individually, based on a psycho-physical driver behavior model developed by Wiedemann [39]. Recently, to better represent pedestrian behavior, VISSIM introduced a new pedestrian model based on the Social Force Model [74]. The Social Force Model for pedestrian dynamics is based on Newtonian physics and pedestrian interaction is modeled according to social, psychological, and physical forces. A pedestrian's motion is influenced not only by their route choice but also by other pedestrians and obstacles.

7.2.2.1 Vehicle and Pedestrian Interaction Modeling in VISSIM

VISSIM can model pedestrians under one of two paradigms: vehicular traffic mode or pedestrian traffic mode. When modeling a pedestrian area (for example a room or floor of a building) the pedestrian traffic mode is utilized and the pedestrian area is defined along with the pedestrian origins and destinations. A pedestrian determines its own path through the area according to the Social Force Model. Multiple pedestrian areas may be modeled (for example multiple floors of a building) and can be connected via ramps or stairs. Interactions between vehicles and pedestrians cannot, however, be modeled in pedestrian mode. A link in vehicle traffic mode must be created then converted to a "pedestrian link" [39]. The pedestrian link then utilizes the same mechanisms

(e.g. priority rules) as vehicles to model the interaction between vehicles and pedestrians.

In contrast to vehicular traffic links, pedestrian links are multidirectional. As with vehicles, different pedestrian classes may be created and different attributes assigned to each class. Signal heads may be placed at the ends of the pedestrian link to represent pedestrian signals. Multiple signal heads may be used, each associated with a different pedestrian class. A pedestrian will consider a signal head if and only if its pedestrian type is assigned to that signal head. Two pedestrian classes were created to model complying pedestrians (i.e., those pedestrians that do not cross when the signal indication is a steady DON'T WALK), and gap-seeking pedestrians (i.e., those that do not follow the signal head indications, crossing whenever an appropriate gap is available in vehicle traffic.)

To facilitate the interaction in the crosswalk between vehicle and pedestrians, priority rules are utilized. Similar to the priority rules in vehicular traffic modeling, transportation analysts may set up priority rules between a pedestrian link and each conflicting vehicular lane. In the study area, the critical interaction is between vehicles traveling southbound on Spring Street and pedestrians crossing eastbound or westbound on 5th Street. Gap-seeking pedestrians may attempt to cross during the steady DON'T WALK when the southbound vehicle traffic is receiving a GREEN indication. During the steady DON'T WALK, individual priority rules are applied for each lane of Spring Street to realistically model pedestrian gap selection behavior. For example, westbound pedestrians are designed to yield to vehicles in Lane 1 and Lane 2 within a time headway of 4 seconds and 6 seconds of the crosswalk, respectively. Lane 3 and Lane 4 priority rules are designed such that vehicles should not be within 6 seconds of the crosswalk at the time

the pedestrian is expected to reach the lane. Figure 46 illustrates the priority rules for pedestrians crossing westbound, where gap-seeking pedestrian will not depart from the waiting area curb line if a vehicle is in the any of the zones indicated by the arrows and dotted lines.

The proceeding priority rules are not required for complying pedestrians. Crossing behavior for complying pedestrians is governed by pedestrian signal heads and pedestrians will not cross when a DON'T WALK indication is displayed. In accordance with guidance from the Highway Capacity Manual, "effective walk time" was used in estimating complying pedestrian time available to start crossing. An additional four seconds was added to the seven seconds of displayed WALK indication in the field, such that the modeled effective WALK indication is 11 seconds. Interactions may also occur between pedestrians (complying and gap-seeking) and vehicles turning southbound from 5th Street onto Spring Street. These interactions occur when pedestrians have the right-of-way, i.e. a WALK indication is displayed. For this analysis vehicles are modeled to yield to pedestrians.

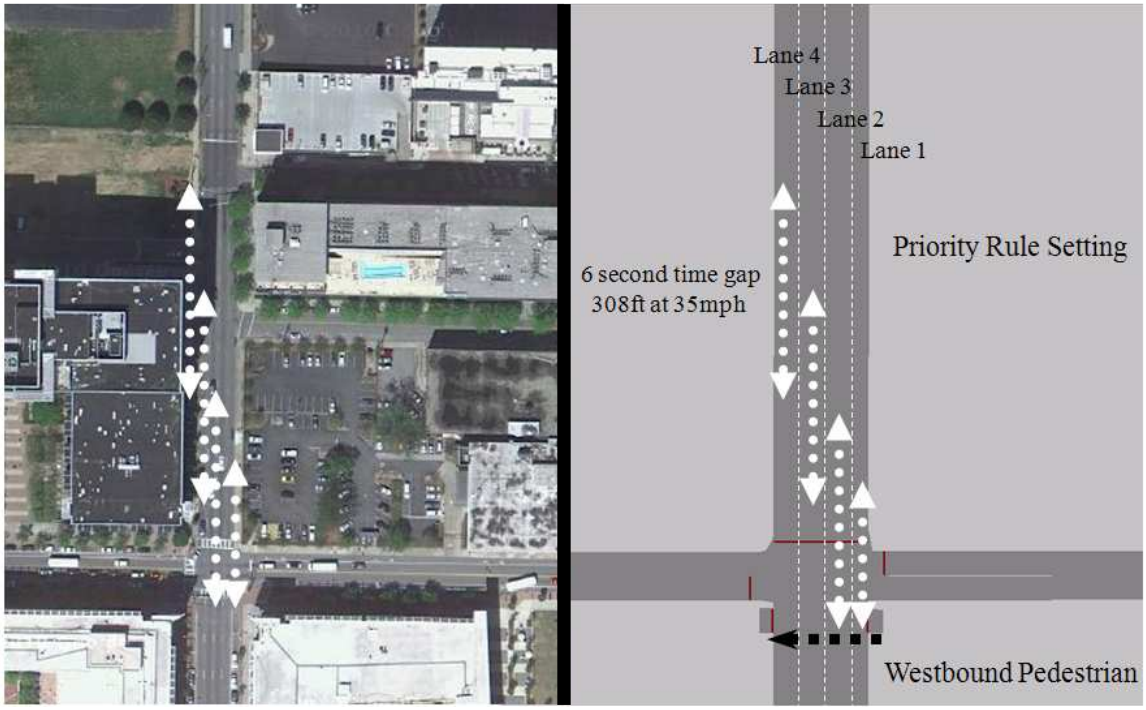

Figure 46 VISSIM Priority Rule Configuration for Gap-Seeking Pedestrians

7.2.3 Experiment

Pedestrians were assigned as complying and gap-seeking pedestrians in the simulation runs. The complying pedestrians only entered the crosswalk during modeled WALK indication (i.e. the effective walk time as discussed above). This behavior was achieved by using signal heads at the end of the pedestrian links. Gap-seeking pedestrians did not follow the pedestrian signal during the modeled steady DON'T WALK, choosing to enter the crosswalk based solely on the availability of an acceptable gap in the traffic stream. During the modeled WALK indication gap-seeking pedestrians ignored all priority rules and crossed as though they were complying pede-

strians.

Eleven ratios of gap-seeking to complying pedestrians are modeled, from 100% complying (thus 0% gap-seeking) to 0% complying (100% gap-seeking) in 10% increments. Ten replicates were completed for each selected ratio. Data collected from each replicate includes pedestrian arrival times, pedestrian departure times from the waiting area, and pedestrian waiting time.

To allow more direct comparison of the field data to the VISSIM results, the arrival pattern of the southbound traffic on Spring Street was also replicated. As previously stated, the time stamp of traffic crossing the upstream detector in the field was recorded. These data were used to generate a VISSIM fkt file. An fkt file allows a user to directly control the entry time of all vehicles on a link. Thus, the Spring Street arrival pattern over the hour was set to match the actual observed arrival stream.

7.3 Results

The following presents results from the field data and simulation experiment.

7.3.1 Field Results

While processing the data from the video, one of the more prominent pedestrian behaviors that was noticed was the number of gap-seeking pedestrians using the intersection. A majority of pedestrians that arrived during the DON'T WALK indication appeared to be gap-seeking, crossing when an acceptable gap was available. For instance, the Figure 44 snapshot was taken during a

DON'T WALK interval (indication not visible in image), however a number of pedestrians were crossing. This behavior was observed throughout the data collection period, over a majority of the cycles. Figure 47 displays the total crossings (y-axis) over the data collection period as a function of time of cycle (x-axis). Pedestrian data are included from approximately 32 cycles. For example, over the data collection period, 10 pedestrians were observed entering the crosswalk 86 seconds into the cycle. This figure clearly indicates that a significant number of pedestrians enter the crosswalk during the DON'T WALK interval.

To determine whether there is a notable relationship between pedestrian arrival and departure patterns, the pedestrian arrivals into the waiting zone are plotted in Figure 48. It appears that the departure pattern is generally independent of the arrival pattern. However, the departure pattern does appear correlated with the pedestrian signal (Figure 47). At the start of the pedestrian DON'T WALK interval (t = 21) there is a generally low likelihood of pedestrian crossing. Approximately 55 seconds into the DON'T WALK interval (t=75), the number of pedestrians crossing increases significantly. The likelihood of pedestrian crossing remains high through the remainder of the DON'T WALK interval. At the start of the WALK and Flashing DON'T WALK, the pedestrian departures are similar to the arrivals.

This crossing pattern results from gap-seeking pedestrian behavior. At the start of the DON'T WALK interval, the southbound vehicle traffic receives a GREEN indication. While the southbound vehicle queue is clearing, the gap-seeking pedestrians are unable to cross Spring Street. Once the queue dissipates the likelihood of a gap-seeking pedestrian finding a gap increases, depending on the southbound vehicle arrivals. Thus, the observed behavior of gap-

seeking pedestrians using the later portion of the DON'T WALK interval is directly related to the southbound traffic queue clearance time and subsequent traffic flow, not the pedestrian signal indication.

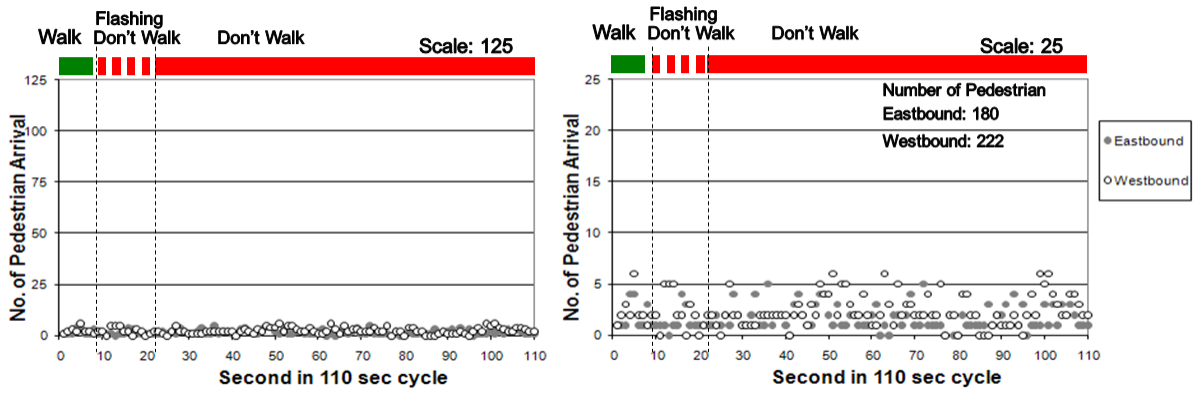

Figure 47 Number of Pedestrian Crossings versus Cycle Time

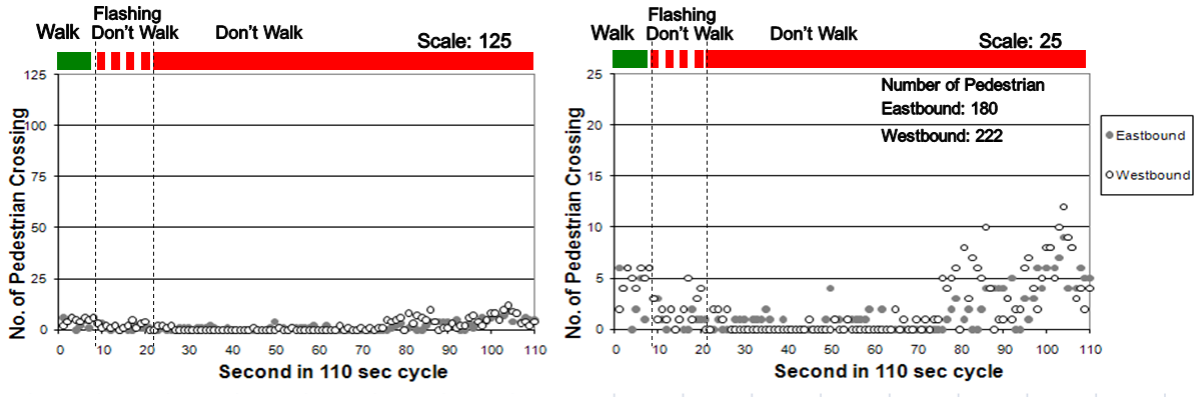

Figure 48 Pedestrian Arrival Pattern versus Cycle Time

7.3.2 Simulation Results

Figure 49, , and Figure 51 shows representative results from a typical replication for complying

to gap-seeking ratios of: 100% to 0%, 50% to 50%, and 0% to 100%, respectively. As with Figure 47 and Figure 48, the pedestrian crossings (y-axis) represent the cumulative crossings over the full data collection time period (i.e. 1 hour). Figure 49, with 100% complying, limits pedestrians crossing to the effective WALK interval. The simulated departure behavior clearly fails to match field observations. **Figure 50**, with 50% complying and 50% gap-seeking, demonstrates some of the aspects of the field data (i.e. pedestrians crossing after southbound queue clearance) however the ratio of pedestrians crossing during the WALK indication to the steady DON'T WALK appears higher than field observations. Figure 51, with 100% gap-seeking provides the closest match to the observed field data. Pedestrian arrival rate was also examined to investigate potential correlations between the arrival and departure distribution. As with the field data, it was observed that the arrivals and departures appear independent, with the simulated and field arrival patterns looking very similar, implying that the simulated departed rates are not determined by the distribution of pedestrian arrivals.

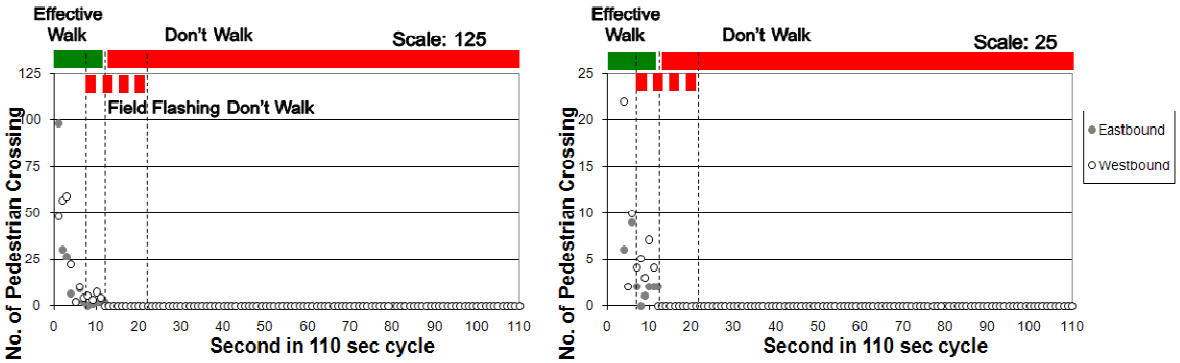

Figure 49 Simulated Pedestrian Crossing Behavior, Complying to Gap-Seeking Ration 100% to 0%

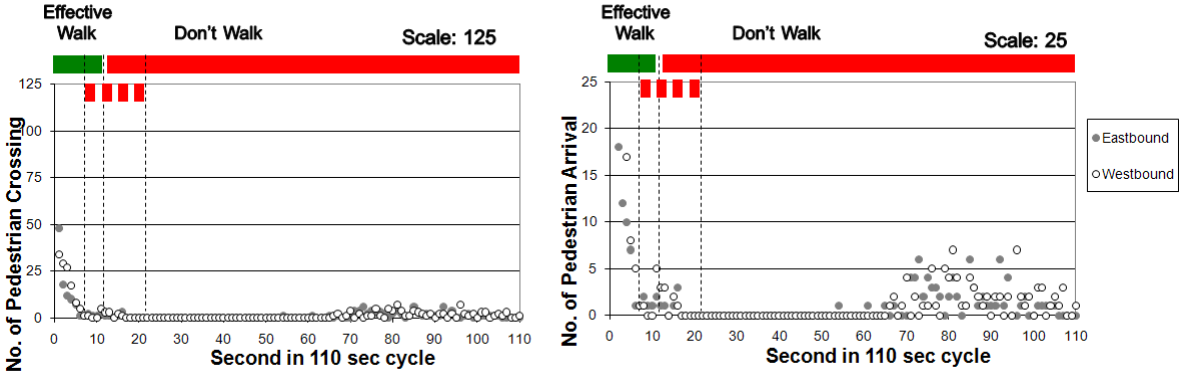

Figure 50 Simulated Pedestrian Crossing Behavior, Complying to Gap-Seeking Ration 50% to 50%

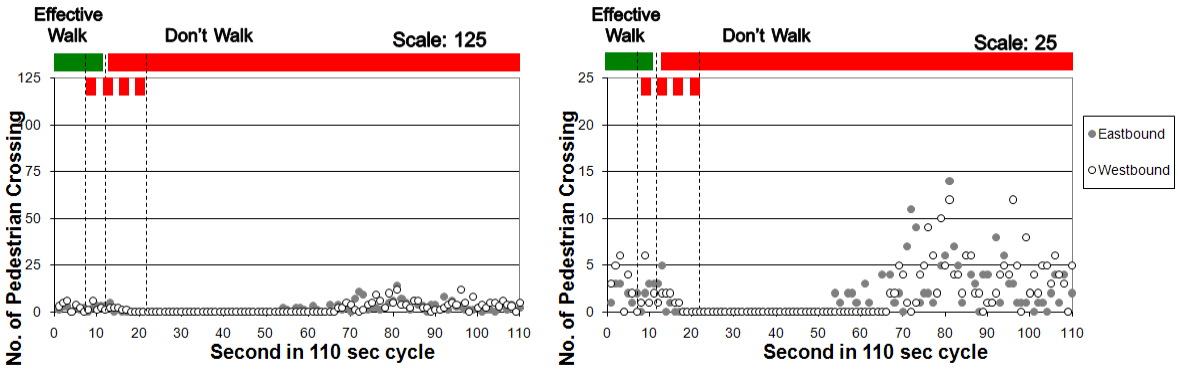

Figure 51 Simulated Pedestrian Crossing Behavior, Complying to Gap-Seeking Ration 0% to 100%

Table 17 provides a breakdown of the various complying pedestrian to gap seeking pedestrian ratios and their respective average waiting times across the ten replications. The average pedestrian waiting time decreases as the gap-seeking fraction increases, with the ratio of 90% to 95% gap-seeking to complying pedestrians most closely matching the field waiting time observations of 21.5 seconds.

Table 17 Complying-Gap-Seeking Ratios versus Average Waiting Time

Percent Complying	Percent Gap-Seeking	Average Waiting Time	Maximum of 10 Replicate Runs	Minimum of 10 Replicate Runs
100%	0%	46.9	50.6	44.0
90%	10%	43.0	44.9	41.1
80%	20%	40.9	43.9	37.4
70%	30%	38.5	40.9	35.5
60%	40%	36.1	39.4	32.7
50%	50%	32.8	35.7	30.5
40%	60%	29.9	31.9	29.0
30%	70%	27.2	29.1	24.9
20%	80%	24.4	27.9	22.8
10%	90%	22.2	23.7	20.4
0%	100%	20.3	22.5	18.7

7.4 Discussion

It is readily seen when comparing the curb departure behaviors over a cycle observed in Figure 47 (field data) and Figure 49 (100% complying pedestrian) that the simulation model fails to capture the real world. The field data clearly demonstrates a high willingness of pedestrians to cross during the DON'T WALK interval. Modeling 100% complying pedestrians does not allow this behavior to be reflected, yielding significantly higher pedestrian waiting values (which could

lead to errors if applied in multi-modal transportation policy analyses**). Figure 50** displays the crossing behavior for a mix of pedestrian types, 50% gap-seeking and 50% crossing. In this simulation, the pedestrian behavior begins to more closely resemble the field data. However there are still notably lower percentages of pedestrians crossing during DON'T WALK than are observed in the field (and the simulated pedestrian waiting time values are still significantly higher than observed in the field).

The patterns of curb departures shown in Figure 47 and Figure 51 (100% gap-seeking pedestrians) are very similar. However, a notable difference between these two figures is that more pedestrians in the field observation data cross earlier during the DON'T WALK interval. One potential reason for this observation is that pedestrians in the real-world have more varied gap acceptance criteria than pedestrians in VISSIM, including pedestrians that force a crossing and cause approaching vehicles with the right-of-way to slow down. This supposition is supported by a few noted field observations where pedestrians are seen running across the crosswalk or crossing the street in stages, waiting in the street as conflicting vehicles pass by in an adjacent lane.

These observations regarding the similarity between the field data and simulation model are support by the waiting time data. As the percentage of complying pedestrians deceases and percentage gap-seeking pedestrians increases (Table 17) the average pedestrian wait time decreases. This decline is expected as increasing the proportion of gap-seeking pedestrians lowers the average waiting time due to their willingness to disregard the traffic signal and depart from the curb sooner than complying pedestrians. With 100% complying pedestrians, the average waiting time per pedestrian is 46.9 seconds, compared to a field measured waiting time of 21.5

seconds, a 118% higher simulated waiting time than field measured waiting time. For 100% gap-seeking pedestrians, the simulated waiting time was 20.27 seconds, around 6% lower than the field data.While additional effort is needed (see challenges below) it is reasonable to infer from these results that the percentage of complying pedestrians is high and failure to account for this behavior will result in an inaccurate reflection of real world behavior.

In light of the strong similarity between the observed and simulated pedestrian behavior, it is important to recall that in this modeling effort that the simulated vehicle arrival stream was set to match the field arrivals. Thus, the gaps seen by the simulated pedestrians were very similar to those noted in the field observations. If the arrival stream was modeled using VISSIM vehicle generation (for the same flow rate) the modeled pedestrian behavior is likely to change. For instance, ten replications of the simulation were run using VISSIM vehicle generation for 100% gap-seeking pedestrians. The average simulated pedestrian waiting time increased to 24.2 seconds/pedestrian (from 21.5 seconds/pedestrian with the arrivals matched). While practically this is a small change in waiting time it does demonstrate that the vehicle arrival pattern influences the model performance, representing an area of future needed research.

7.4.1 Simulation Challenges

As seen in the previous section, the simulated environment is capable of providing a reasonable reflection of the observed pedestrian behavior. However, there are a number of caveats that should be highlighted which will play an integral role when duplicating this methodology.

Firstly, the VISSIM model's output appeared to be highly sensitive to the pedestrian related parameters. For instance, pedestrian gap acceptance criterion, priority rule configurations, and effective crosswalk width all had the potential to significantly influenced model results. In this effort the value(s) of each of these parameters were established by examining previous works, seeking professional input, conducting condensed field studies, and performing limited sensitivity analyzes. However, ultimately final parameter values are selected based on the modeler's judgment in an attempt to reflect realistic crossing behaviors. Future efforts should explore methods to field measure these parameters, determine the model sensitivity to these parameters, and develop guidance to model developers on the selection and calibration of parameter values. For example, to account for the potential effect of pedestrians walking outside of the painted crosswalk limits, an *effective crosswalk width* should be used. This width will typically result in the modeled crosswalk having a greater width than that painted in the street. When choosing an effective crosswalk width, it is important that the analyst be careful when estimating this value. An improper estimate may produce inaccurate results, as this width affects pedestrian *throughput rate* across the street, and subsequently pedestrian delay.

Secondly, the variability in pedestrian and vehicle arrival and discharge process, pedestrian gap selection, pedestrian to turning-vehicle interaction, etc. all result in field data that are more erratic than are simulated by VISSIM. For example, even under the 100% gap-seeking case there are no pedestrian crossings between 20 and 50 second. In the field data there are a few crossings during this time period. This is likely of a result of VISSIM not reflecting the high short term vehicle gap variability that exists, particularly in the urban environment.

Finally, it is noted that providing a field measured percentage of gap-seeking pedestrians for use in a simulation model is a challenging endeavor. If a pedestrian chooses to cross during a DON'T WALK indication that pedestrian may be clearly identified as gap-seeking. However, if a pedestrian arrives during a DON'T WALK indication and does not cross, the pedestrian's decision to gap-seek or not can't be readily field measured (except in obvious cases) as that pedestrian may have been gap-seeking but simply unable to find a sufficient gap. Additionally, it is not possible to make any definitive gap-seeking or complying statements about pedestrians that arrive and cross during the WALK interval. An area of future research will be methods to field measure the variability in gap-acceptance criteria as part of the pedestrian attributes.

7.4.2 Experiment Replication

Finally, in an effort to build confidence in the discussed approach to pedestrian simulation modeling the study was repeated for the same intersection, over the same time period, on September 9th, 2010. With a 100% pedestrian gap-seeking rate and VISSIM generated vehicles the simulated pedestrian waiting time was 21.0 seconds versus a field measured waiting time of 18.6 seconds per pedestrian. Plotted pedestrian departures were also similar between the field and simulated data. While a single successful replication presented pedestrian simulation methodology does not fully validate the approach, it continues to support the method and need for accurately reflecting pedestrian behavior.

7.5 Concluding Remarks

Pedestrian movements are inherently more complex than vehicular movements, and it is because of this complexity that pedestrian behavior has not always been appropriately accounted for in traffic simulation packages. Accounting for such behavior will lead to a greater understanding of pedestrian-vehicle interactions and will help improve multi-modal transportation planning and simulation. As a result, more informed decisions may be made regarding pedestrian and vehicle activity in the urban environment.

In looking to bring about a greater understanding in pedestrian-vehicle interactions, the presented research attempted to represent realistic pedestrian behavior in VISSIM, a microscopic traffic simulation program. The modeling yielded comparable observed and simulated distributions of when pedestrians choose to use the crosswalk during the signal cycle and estimates of average pedestrian waiting time. When these sets of information were compared for the observed behavior and simulated behavior it was seen that the pedestrian behavior is strongly related to the cross street traffic queue clearance time and subsequent traffic flow, not the pedestrian signal indication. Capturing this interaction significantly enhances the models' ability to reflect observed field performance.

Despite the success of this modeling effort a number of challenges were identified. For instance, the VISSIM model's output appeared to be highly sensitive to the pedestrian related parameters, such as pedestrian gap acceptance criteria, priority rule configurations, and effective crosswalk width. Also, the field variability in pedestrian and vehicle arrival and discharge process, pedestrian gap selection, pedestrian to turning-vehicle interaction, etc. result in field be-

havior that is more erratic that the simulated behavior. Ultimately, the modeler's judgment and fine tuning of the model played a strong role in the ability of the simulation to realistically reflect crossing behaviors. Many of the issues raised in this effort merit additional exploration to allow modelers to make more informed choices.

From this research effort, it can be concluded that successful representation of realistic pedestrian behavior is feasible in microscopic traffic simulation. This result is promising as it seeks to be a part of the foundation of efforts geared to capturing pedestrian-vehicle interaction. In capturing this interaction, the ability for the simulated environment to accurately reflect the performance measure has increased. The next step in the test will be a comparative analysis of the vehicle behavior in the simulation and field given that pedestrian behavior is now appropriately reflected. This step is necessary to allow for the incorporation of pedestrians into the real-time platform. However, a final critical issue that will need to be addressed in the implementation of a real-time simulation that incorporates pedestrians will be the ability to implement pedestrian detection in the field.

8 VISUALIZATION OF ARTERIAL PERFORMANCE

One of the final components of this research effort is to present the information, which has been modeled by VISSIM, to the consumers of arterial performance measures. The research team has developed a web-based tool that the consumers may visit to evaluate the current performance of the arterial under study. The following chapter will provide some of the more pertinent details of the web-based tool.

The visualization mechanism has three components: 1) the representation of individual vehicles, 2) the depiction of changes in traffic conditions as a function of time and space, and 3) the historical presentation of key arterial performance measures. Details of these components are presented below with reference to the NGSIM corridor study discussed earlier.

The first component presents traffic on a microscopic scale. Individual vehicle are represented as they travel through the corridor. This animated graphic provides users will an immediate sense of the traffic conditions along the corridor. The animation is powered by (x,y) coordinate data of individual vehicles which are produced by VISSIM. The animated movement of vehicles is layered on top of a Google map image of the study area. This form of representation allows the user to easily relate observed traffic conditions to actual locations at which it is occurring, Figure 52. In Figure 52 the cyan circles represent vehicles traversing the network and the dynamic colored arrows reflect the current indication of each signal head along the corridor.

Figure 52 Real-Time Vehicle Representation along the Peachtree Study Corridor

The second component delivers time-space diagrams (TSD) to users. These diagrams are comprised of individual vehicle trajectories along the corridor. Each point on a trajectory represents a vehicle's place in time, distance traveled along the corridor and instantaneous speed. Time space

diagrams provide a comprehensive view of corridor performance. They present information regarding platoon movement and the effectiveness of a corridor's current signal timing plan. In addition they provide immediate approximations for the number of vehicles on the corridor, queue lengths, and travel speed and travel time along the corridor. Figure 53 is a sample time-space diagram.

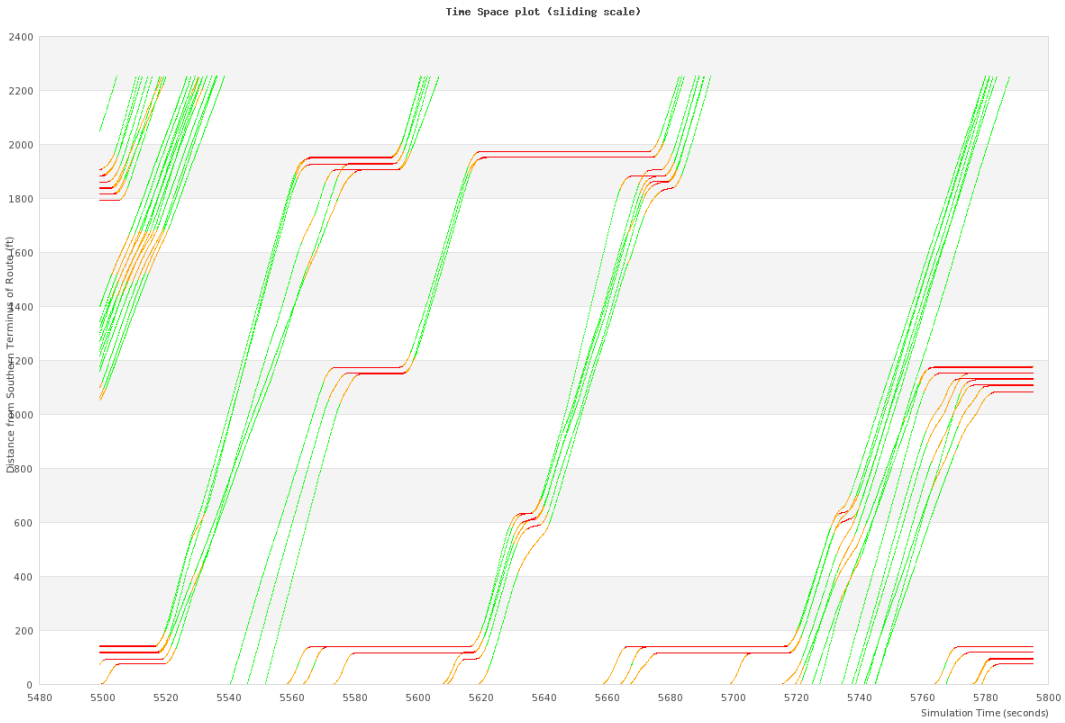

Figure 53 Sample Time-Space Diagram for Northbound Travels

The third component of the visualization mechanism present users with additional performance measure estimates. For each link of the corridor, graphs of historical and current values of flow (number of vehicles), queue length, and average speed are provided. In addition average travel times for the entire length of the corridor, both directions, is illustrated. Figure 54 illustrates a composite of the speed, queue length and flow graphics.

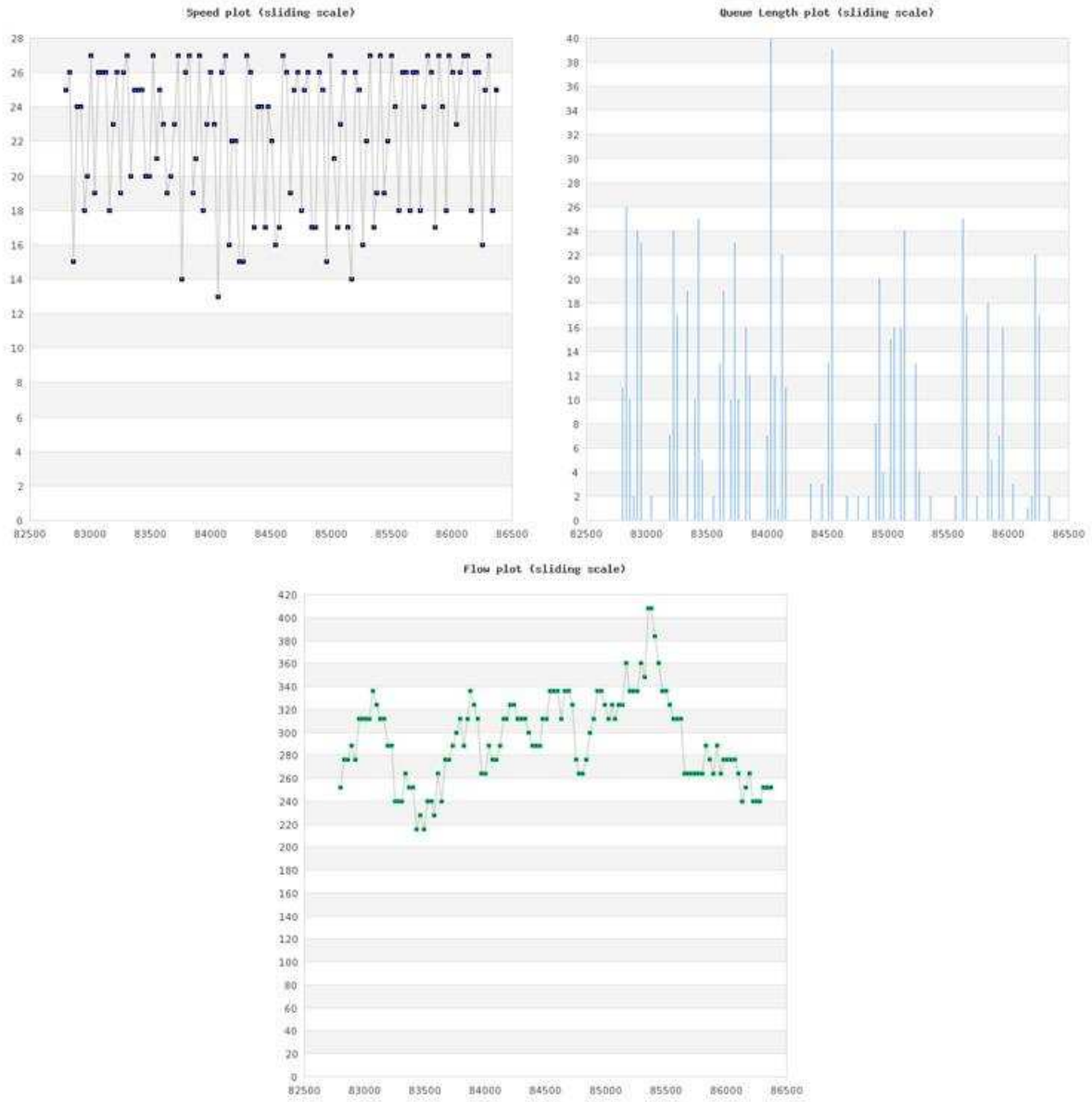

Figure 54 Composite Graphic of Speed, Queue Length and Flow Plot

The above graphics provide travelers and facility managers with comprehensive knowledge regarding the operation of the study corridor. It is hoped that with this information at hand, such consumers will be better equipped to make decisions to aid in increasing the efficiency with which the facility is being used and managed.

A demonstration website has been created to present arterial performance measures. This website is being driven in real-time by a simulation model. Data to the simulation model is being provided from the NGSIM data utilized in Experiment #4, discussed in Chapter 5. The site is still in the alpha testing stage. The website may be accessed through http://realtime.ce.gatech.edu.

9 FUTURE RESEARCH AND IMPLEMENTATION PLAN

The preceding chapters demonstrate the feasibility an online, data-driven, simulation tool to estimate arterial performance measures in real-time. However, five primary opportunities have been identified as needing further effort: 1) improved accuracy of vehicular volumes entering the study network, 2) real-time estimations of turning movement distributions, 3) synchronize field and model traffic signal control, 4) calibration, and 5) reflecting congestion resulting from factors outside the simulated area. The team anticipates that effort in these areas will lead to more accurate and reliable performance measure estimates.

9.1 Vehicular-Volume Accuracy

Errors associated with vehicular volumes at the study zone boundary were prevalent in the third field experiment. When observing vehicles entering a camera's detection zone the two most comment error types were: 1) a single vehicle (usually a larger vehicle) triggered detections in adjacent lanes or 2) a vehicle failed to trigger a detection zone.

9.2 Turning Movement Distribution

In the current effort turning movement proportions are based on historical data and the path of a vehicle through an intersection is randomly assigned based on these proportions. As noted in the chapter 5 experiments this inability to determine turning movements in real-time is a potential

source of error. Estimating turning movement proportions has aspects in common with the development of models that estimate dynamic origin-to-destination flows in a small network [35]. Liu et al. [35] and Chang and Tao [75] present a summary of some the more notable works in turning movement proportion estimation. Future efforts will attempt to build on these and other resources in the development of a real-time turning movement estimation procedure.

9.3 Field and Simulated Signal Synchronization

In the third field experiment it was noted that the simulated signal indications could differ from field. Given the strong correlation between signal operations and arterial performance measures, it is critical that the field and simulated signal state is synchronous. To establish synchronization between traffic signals in the two environments, the team will again seek to understand prior efforts and possibly employ or build up their contributions. One of the works that will be closely examined is presented in Ban et al.[76]. The authors of this article estimated signal timing plans using piecewise linear intersection delay curves and a two-step least square estimation algorithm. Although this method may not be suited for the current real-time approach, the details of this method will provide insights as to how to achieve and automate signal synchronization. To develop a robust signal synchronization plan the team will also investigate means to stream signal states into the simulation.

9.4 Calibration

In this effort extensive effort was expended on off-line calibration of simulation models. Future efforts should explore expansion of this calibration to an online calibration, continually adjusting the model parameters in real time. In addition, the pedestrian modeling efforts should be expanded to allow for incorporating the influence of pedestrians on simulated traffic, particularly in urban areas with high pedestrians demands.

9.5 Boundary Conditions

A final issues that was noted as part of this effort is related specifically to the capabilities of the simulation model. The challenge of real-time simulation is to mirror dynamic traffic conditions in real time. As part of these efforts it was observed that the simulation model was capable of reflecting congested conditions when the cause of the congestion (i.e. bottleneck) resided within the simulation boundaries. However, if the source of congestion was outside the simulation boundaries and spilled back into the simulation region this was not captured. For example, if an intersection outside of simulated region resulted in queues blocking an upstream intersection within the simulation boundary this would not be reflected. The underlying challenge is the development of an ability to restrict flow on simulation exit links such that the blockage due to downstream congestion is reflected. Future efforts will be aimed at dynamically controlling the flow rate at nominally unrestricted exit points in real time.

9.6 Next Steps

This effort has utilized detectorization and equipment specifically installed for this project. This installation allowed for highly detailed information to be streamed real time. The next test should seek to implement a real-time simulation on an arterial corridor utilizing data streams with a potentially lower fidelity. For instance, the current test bed streams per vehicle detections from the VDS. Where this data accuracy is not available the level and impact of data aggregation should be determined. For instance, a field test could be developed on a TACTICS based system, determining what data is available, how it could be streamed, what are the aggregation levels, etc.

The real time research effort should also continue to explore the issues discussed in sections 9.1 through 9.5, i.e. entering vehicle volume accuracy, determination of real time turning movements, synchronization of field and simulated signals, online calibration, and downstream congestion influencing boundary conditions. Improvements in each of these areas will improve the performance of overall real time simulation system. However, the next phase of the project could eliminate several of these issues (pedestrian impacts and downstream congestion influencing boundary conditions) through targeted selection of the next site, allowing for a more focused effort.

In addition a broader field test would also need to explore potential communication challenges. The current test bed had the benefit of utilization of the campus fiber network. To be successful the next implementation should investigate the communications between the detectors and the data processing center and communication between the processed data node and the simulation in a location without this benefit.

Finally, with the rich data streams being leveraged as part of the real time simulation effort the next implementation should incorporate an analytical model based directly on the available detector and signal data to compliment and support the simulated results. A combined simulated and analytic approach has the potential to address the challenges unique to both approaches.

10 CONCLUSION

As seen a wide variety of advanced technological tools have been implemented throughout Georgia's transportation network to increase its efficiency. This research project explored the feasibility of integrating real-time data streams with an arterial simulation to support an arterial performance monitoring system. Such information will facilitate increased efficiency in facility utilization by enabling more informed decisions in the use and management of Georgia's transportation facilities.

In the initial stage of this effort a federation (i.e. integration) of two simulation instances to be used as a conceptual test bed was developed. It was seen using this test bed that the underlying real time approach could be successful in a simulated environment. Next a "hardware-in-the-loop" framework was developed that directly inputs detector data into a simulation model during runtime. Successful integration of the data stream with VISSIM enabled a field evaluation of the framework on an arterial using streaming point sensor data. A key attribute of the federation is the ability for the simulation to receive a PVR (per vehicle record) detector data stream in a real-time, allowing for the use of multiple detector technologies.

Using this ability to stream real time detection into the simulation an in-field test bed with detectors that are capable of streaming traffic data in real time to a central server was created. Utilizing this test bed several real time simulation experiments were undertaken. These experiments demonstrated the ability of the real time simulation, for the given system, to provide

reasonable estimates of travel time. However, in several instances difference were noted. These difference where attributed to several causes: detector errors at simulation boundary detectors resulting in volume discrepancies between the simulation and field, differences between individual vehicle turning movements in the field and simulated environment, challenges in the synchronization of field and simulated signal indications, model calibration, and downstream congestion influencing simulations boundary conditions. Future efforts will seek to continue to improve the real time environment in each of these areas.

To test the proposed real time approach in an environment that allowed for eliminating or significantly reducing the errors resulting from the proceeding issues a “pseudo” real time field test was undertaking using the FHWA Next Generation Simulation (NGSIM) program. Utilizing this data set to create a pseudo real time data stream it is seen that the real time approach is capable of providing accurate performance measures given high quality data inputs. Future efforts will seek to explore the relationship between degradations in data accuracy and performance measure estimates.

In addition, a web-based interface was developed presenting the arterial performance measures in real time. The data generated by the simulation is polled in real-time to generate time space diagrams and summary charts and statistics of the various performance measures. An animated representation of traffic moving through the study corridor is also provided

In summary, it has been seen through this research effort that real time simulation provides a potential opportunity to determine high fidelity arterial performance metrics in real time. As stated challenges still exist to a wide spread implementation however this initial effort devel-

oped techniques for addressing many of the challenges of real time simulation, identified future challenges that remain to be addressed, and created a foundation upon which future implementations of real time arterial simulation may be based.

11 REFERENCES

[1] D. Schrank and T. Lomax, "Urban Mobility Report 2009," *Report for the Texas Transportation Institute*, no. July, 2009.

[2] R. A. I. T. A. RITA, "Intelligent Transportation Systems Benefits, Costs, Deployment, and Lessons Learned 2008 Update," Washinton DC, 2008.

[3] R. and I. T. A. RITA, "Intelligent Transportation Systems," *Web Page*, 2009. [Online]. Available: http://www.its.dot.gov/index.htm. [Accessed: 03-Jan-2010].

[4] Google, "Google Maps," *Web Page*, 2011. [Online]. Available: http://maps.google.com/. [Accessed: 03-Jan-2010].

[5] NAVTEQ, "NAVTEQ Traffic," *Web Page*, 2011. [Online]. Available: http://www.navteq.com/. [Accessed: 03-Jan-2009].

[6] Inrix, "INRIX," 2011. [Online]. Available: http://www.inrix.com/.

[7] P. G. Gipps, "The Estimation of a Measure of Vehicle Delay from Detector Output," Newcastle, 1977.

[8] V. Sisiopiku and N. Rouphail, "Toward the use of Detector Output for Arterial Link Travel Time Estimation: A Literature Review," *Transportation Research Record*, vol. 2, no. 1457, pp. 158-165, 1994.

[9] H. E. Gault and I. G. Taylor, "The Use of Vehicle Detector to Assess Delay in Computer-Controlled Area Traffic Control," Newcastle, 1977.

[10] H. Zhang and E. Kwon, "Travel Time Estimation on Urban Arterials Using Loop Detector

Data," Iowa City, 1997.

[11] H. Strobel, "Traffic Control Systems Analysis by Means of Dynamic State and Input-Output Models," Laxenburg, Austria., 1977.

[12] P. Bohnke and E. Pfannerstill, "A system for the automatic surveillance of traffic situations," *ITE Journal*, vol. 56, no. 1, pp. 41 - 45, 1986.

[13] N. Sensys, "Sensys Networks," 2012. [Online]. Available: http://www.sensysnetworks.com/. [Accessed: 18-Feb-2012].

[14] T. Usami, K. Ikenoue, and T. Miyasako, "Travel Time Prediction Algorithm and Signal Operations at Critical Intersection Controlling Travel Time," in *Second International Conference on Road Traffic Control*, p. 1986.

[15] B. O. P. R. BPR, "Traffic Assignment Manual," Washinton DC, 1964.

[16] H. M. Zhang, "Link-Journey-Speed Model for Arterial Traffic," *Transportation Research Record*, vol. 1676, no. 1, pp. 109-115, Jan. 1999.

[17] H. X. Liu and X. W. Wenteng Ma, "Time-dependent travel time estimation model for signalized arterial network," in *86th Transportation Research Board Annual Meeting 2007*, 2007, vol. 1, p. 21.

[18] H. Wang and A. Hobeika, "Travel Time Estimation on Arterial Streets," Blacksburg, VA, 2007.

[19] D. J. Dailey and F. W. Cathey, "AVL-Equipped vehicles as traffic probe sensors," Seattle, 2002.

[20] Y. Li and M. McDonald, "Link travel time estimation using single GPS equipped probe

vehicle," in *The IEEE 5th International Conference on Intelligent Transportation Systems, 2002. Proceedings*, 2002, pp. 932–937.

[21] K. Choi and Y. Chung, "A data fusion algorithm for estimating link travel time," *Intelligent Transport Systems*, vol. 7, no. 3 & 4, pp. 235-260, 2003.

[22] W. Pu, J. (Jane) Lin, and L. Long, "Real-Time Estimation of Urban Street Segment Travel Time Using Buses as Speed Probes," *Transportation Research Record: Journal of the Transportation Research Board*, vol. 2129, pp. 81-89, 2009.

[23] D. E. Lucas, P. B. Mirchandani, and N. Verma, "Online travel time estimation without vehicle identification," *Transportation Research Record: Journal of the Transportation Research Board*, vol. 1867, no. 1, pp. 193–201, 2004.

[24] S. M. Turner, T. J. Lomax, and H. S. Levinson, "Measuring and Estimating Congestion Using Travel Time-Based Procedures," *Transportation Research Record*, vol. 1564, no. 1, pp. 11-19, Jan. 1996.

[25] T. Park and S. Lee, "A bayesian approach for estimating link travel time on urban arterial road network," *Lecture notes in computer science*, pp. 1017–1025, 2004.

[26] R. L. Cheu, D.-h D.-H. Lee, and C. Xie, "An arterial speed estimation model fusing data from stationary and mobile sensors," *ITSC 2001. 2001 IEEE Intelligent Transportation Systems. Proceedings (Cat. No.01TH8585)*, vol. pp, pp. 573-578, 2001.

[27] P. V. Palacharla and P. C. Nelson, "Application of fuzzy logic and neural networks for dynamic travel time estimation," *International Transactions in Operational Research*, vol. 6, no. 1, pp. 145-160, Jan. 1999.

[28] S. Robinson and J. Polak, “Modeling Urban Link Travel Time with Inductive Loop Detector Data by Using the k-NN Method,” *Transportation Research Record*, vol. 1935, no. 1, pp. 47-56, Jan. 2005.

[29] N. Geroliminis and A. Skabardonis, “Prediction of Arrival Profiles and Queue Lengths Along Signalized Arterials by Using a Markov Decision Process,” *Transportation Research Record*, vol. 1934, no. 1, pp. 116-124, Jan. 2005.

[30] A. Skabardonis and N. Geroliminis, “Developement of Performance Measures on Signalized Arterials,” Berkeley, 2008.

[31] T. Tsekeris and A. Skabardonis, “On-line performance measurement models for urban arterial networks,” in *Transportation Research Board Annual Meeting*, 2004, vol. 935, p. 24.

[32] K. Kwong, R. Kavaler, R. Rajagopal, S. Networks, P. Varaiya, and C. Sciences, “A practical scheme for arterial travel time estimation based on vehicle re-identification using wireless sensors,” in *TRB 2009 Annual Meeting (CD-ROM)*, 2009, no. 1750, p. 15.

[33] J. Luk, C. Karl, M. Su, and P. Bennett, “Real-time estimation of travel times on arterial roads in melbourne,” in *22nd ARRB Conference – Research into Practice*, 2006, p. 14.

[34] J. Wahle, “A cellular automaton traffic flow model for online simulation of traffic,” *Parallel Computing*, vol. 27, no. 5, pp. 719-735, Apr. 2001.

[35] H. H. Henry X. Liu, Wenteng Ma, Xinkai Wu, “Development of a Real-Time Arterial Performance Monitoring System Using Traffic Data Available from Existing Signal Systems,” Minneapolis, 2009.

[36] INRIX Inc., “INRIX - Go Anywhere,” 2011. [Online]. Available: http://www.inrix.com/. [Accessed: 01-Sep-2011].

[37] Clear Channel Radio, “Total Traffic Network - Navigating the Future,” 2011. [Online]. Available: http://totaltraffic.com/. [Accessed: 01-Sep-2011].

[38] SpeedInfo, “SpeedInfo - Delivering Data that Knows the Flow,” 2007. [Online]. Available: http://www.speedinfo.com/. [Accessed: 01-Sep-2011].

[39] PTV, “VISSIM User Manual,” Karlsruhe, Germany, 2010.

[40] PTV, “VISSIM 5.10-06 COM Interface Manual,” Karlsruhe, Germany, 2009.

[41] T. McLean and R. Fujimoto, “The Federated-simulation Development Kit: A Source-Available RTI,” 2000. [Online]. Available: http://www.cc.gatech.edu/computing/pads/fdk.html.

[42] F. Darema, “Dynamic data driven applications systems: New capabilities for application simulations and measurements,” *Computational Science–ICCS 2005*, vol. 3515/2005, pp. 610-615, 2005.

[43] B. Plale et al., “Analysis and Forecasting in LEAD,” *Computational Science–ICCS 2005*, vol. 3515/2005, pp. 624-631, 2005.

[44] J. Mandel et al., “Towards a Dynamic Data Driven Application System for Wildfire Simulation,” *Computational Science -- ICCS 2005*, vol. 3515/2005, pp. 632-639, 2005.

[45] L. Golubchik et al., “A Generic Multi-scale Modeling Framework for Reactive Observing Systems: An Overview,” *Computational Science–ICCS 2006*, vol. 3993/2006, pp. 514-521, 2006.

[46] C. Kennedy and G. Theodoropoulos, “Intelligent Management of Data Driven Simulations to Support Model Building in the Social Sciences,” *Computational Science–ICCS 2006*, vol. 3993/2006, pp. 562-569, 2006.

[47] D. Brogan, P. Reynolds, R. Bartholet, J. Carnahan, and Y. Loitiere, “Semi-automated simulation transformation for DDDAS,” *Computational Science–ICCS 2005*, vol. 3515/2005, pp. 721-728, 2005.

[48] P. Lendermann, M. Y. H. Low, B. P. Gan, N. Julka, and L. P. Chan, “An Integrated and Adaptive Decision-Support Framework for High-Tech Manufacturing and Service Networks,” in *Winter Simulation Conference*, 2005, pp. 2052-2062.

[49] Microsoft, “Microsoft Developer Network,” 2011. [Online]. Available: http://msdn.microsoft.com/en-us/.

[50] NGSIM, “The NGSIM Community Website,” 2011. [Online]. Available: http://ngsim-community.org/. [Accessed: Jan-2011].

[51] C. Systematics, “NGSIM Peachtree Street (Atlanta) Data Analysis (12:45 p.m. to 1:00 p.m.),” Oakland, 2007.

[52] C. Systematics, “NGSIM Peachtree Street (Atlanta) Data Analysis (4:00 p.m. to 4:15 p.m.),” Oakland, 2007.

[53] D. Miller, “Developing a Procedure to Indentify Parameters for Calibratoin of a VISSIM Model,” Georgia Institute of Technology, 2009.

[54] H. Park, Byungkyu Brian, Qi, “Development and Evaluation of a Calibration and Validation Procedure for Microscopic Simulation Models,” Charlottesville, VA, 2004.

[55] B. B. Park, P. D, and J. Won, “Simulation Model Calibration and Validation: Phase II: Developmen of Implementation Handbook and Short Course,” Charlottesville, VA, 2006.

[56] B. (Brian) Park, J. Won, and I. Yun, “Application of Microscopic Simulation Model Calibration and Validation Procedure: Case Study of Coordinated Actuated Signal System,” *Transportation Research Record*, vol. 1978, no. 1, pp. 113-122, Jan. 2006.

[57] S. S. Pulugurtha, S. S. Nambisan, M. Dangeti, and M. Kaseki, “Evaluation of the Default Parameters of CORSIM and VISSIM Traffic Simulation Software on Basic Freeway Segments Using Field Data,” in *Proceedings of the International Conference on Applications of Advanced Technologies in Transportation Engineering*, 2002, pp. 803-810.

[58] Legion, “Legion Pedestrian Simulation,” 2011. [Online]. Available: www.legion.com. [Accessed: 31-Jul-2011].

[59] SimWalk, “SimWalk: The Human Movement Simulator,” 2011. [Online]. Available: www.simwalk.com. [Accessed: 31-Jul-2011].

[60] PedGo, “PedGo: Pedestrian Evacuation Simulation,” 2011. [Online]. Available: http://www.traffgo-ht.de/en/pedestrians/products/ pedgo/index.html. [Accessed: 31-Jul-2011].

[61] Z. Fang, Q. Li, Q. Li, L. D. Han, and D. Wang, “A proposed pedestrian waiting-time model for improving space–time use efficiency in stadium evacuation scenarios,” *Building and Environment*, vol. 46, no. 9, pp. 1774-1784, Sep. 2011.

[62] C. . Castle, “Agent-Based Modelling of Pedestrian Evacuation: A Study of London’s King’s 10 Cross Underground Station,” University College London, 2007.

[63] M. Virkler, “Pedestrian Compliance Effects on Signal Delay,” *Transportation Research Record*, vol. 1636, no. 1, pp. 88-91, Jan. 1998.

[64] M. M. Ishaque and R. B. Noland, “Pedestrian and Vehicle Flow Calibration in Multimodal Traffic Microsimulation,” *Journal of Transportation Engineering*, vol. 135, no. 6, p. 338, 2009.

[65] J. Yang, W. Deng, J. Wang, Q. Li, and Z. Wang, “Modeling pedestrians’ road crossing behavior in traffic system micro-simulation in China,” *Transportation Research Part A: Policy and Practice*, vol. 40, no. 3, pp. 280-290, Mar. 2006.

[66] N. Rouphail and B. Eads, “Pedestrian Impedance of Turning-Movement Saturation Flow Rates: Comparison of Simulation, Analytical, and Field Observations,” *Transportation Research Record*, vol. 1578, no. 1, pp. 56-63, Jan. 1997.

[67] B. Wan and N. Rouphail, “Using Arena for Simulation of Pedestrian Crossing in Roundabout Areas,” *Transportation Research Record*, vol. 1878, no. 1, pp. 58-65, Jan. 2004.

[68] B. and N. R. Schroeder, “Adapting VISSIM for Variant Pedestrian Behavior and Facility Modeling in a Mixed-Priority Environment.” Seattle, 2010.

[69] J. Milazzo, N. Rouphail, J. Hummer, and D. Allen, “Effect of Pedestrians on Capacity of Signalized Intersections,” *Transportation Research Record*, vol. 1646, no. 1, pp. 37-46, Jan. 1998.

[70] J. Coeymans A and J. Herrera M, “Estimating Values for Traffic Parameters in Turning Lanes,” *Transportation Research Record*, vol. 1852, no. 1, pp. 47-54, Jan. 2003.

[71] S. M. L. Hubbard, R. J. Awwad, and D. M. Bullock, “Assessing the Impact of Turning

Vehicles on Pedestrian Level of Service at Signalized Intersections: A New Perspective," *Transportation Research Record*, vol. 2027, no. 1, pp. 27-36, Dec. 2007.

[72] M. Virkler, "Prediction and Measurement of Travel Time Along Pedestrian Routes," *Transportation Research Record*, vol. 1636, no. 1, pp. 37-42, Jan. 1998.

[73] TRB, "HIGHWAY CAPACITY MANUAL 2000," Washinton DC, 1997.

[74] D. Helbing and P. Molnár, "Social force model for pedestrian dynamics," *Physical Review E*, vol. 51, no. 5, p. 4282, May 1995.

[75] G.-L. Chang and X. Tao, "Estimation of Time-Dependent Turning Fractions at Signalized Intersections," *Transportation Research Record*, vol. 1644, no. 1, pp. 142-149, Jan. 1998.

[76] X. Ban, R. Herring, P. Hao, and A. Bayen, "Delay pattern estimation for signalized intersections using sampled travel times," in *2009 Transportation Research Board Annual Meeting,(Washington, DC)*, 2009, p. 21.